**EUROPEAN COMMISSION**
**DG RESEARCH**
**SEVENTH FRAMEWORK PROGRAMME**
**THEME 5 - Energy**

ENERGY.2010.5.2-1: CCS - storage site characterisation

Collaborative Project– GA No. 256705

# SiteChar

## Characterisation of European $CO_2$ storage

## Deliverable N° D3.1

Geological report of the integrated UK multi-store site

| | | |
|---|---|---|
| **Deliverable No.** | SiteChar D3.1 | |
| **Deliverable Title** | Geological report of the integrated UK multi-store site V2 | |
| **Nature** | Report | |
| **Dissemination level** | Restricted | |
| **Lead Beneficiary** | NERC (British Geological Survey) | |
| **Written By** | M F Quinn, M C Akhurst, P Frykman, S Hannis, J Hovikoski, T Kearsey, J-C Lecomte and M McCormac | 31st July 2012 |
| **Due date** | 31 December 2011 | |

# Geological report of the integrated Blake Oil Field and Captain Sandstone aquifer, UK multi-store site, SiteChar

M.F. Quinn[1], M.C. Akhurst[1], P. Frykman[2], S. Hannis[1], J. Hovikoski[2], T. Kearsey[1], J-C. Lecomte[3] and M. McCormac[1]

1 – NERC British Geological Survey (BGS)
2 – Geological Survey of Denmark and Greenland (GEUS)
3 – IFP Energies nouvelles (IFPEN)

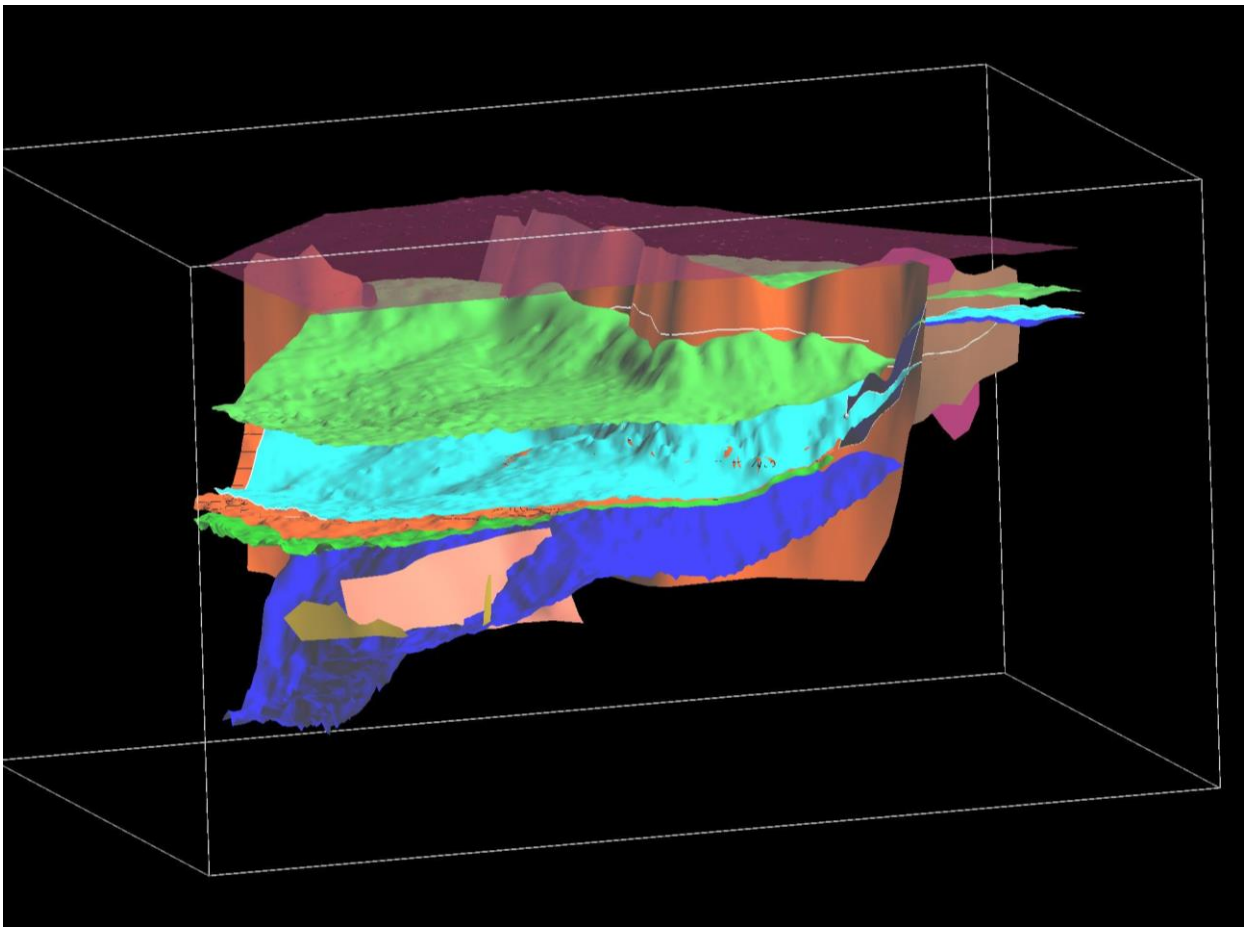

**CONTENTS** **Page number**

## FOREWORD

This report is a deliverable (D3.1) from the Framework 7 European Union-funded SiteChar project (Work Package 3, Task 3.1) to facilitate implementation of geological storage of carbon dioxide in Europe. The SiteChar project has presented a draft workflow for the implementation of the EU Carbon Capture and Storage (CCS) Directive in member states. The draft workflow is tested by the characterisation of storage sites, assessment of risks and development of site monitoring plans needed for storage site licensing in five EU member states and affiliated countries (Denmark, Italy, Norway Poland, and UK). Two of the sites, an offshore site in the UK and an onshore site in Denmark, will develop 'dry-run' licence applications to be reviewed by relevant regulatory authorities. Learning from investigations at the five sites will feedback into the final workflow and inform recommendations to the European Commission on the implementation of the CCS Directive.

A storage licence application is undertaken in two parts, an application for an Exploration Permit and an application for a Storage Permit. The objective of Work Package 3 in SiteChar is to carry out geological characterisation and assess long-term storage complex behaviour required to gain a storage licence addressed through a 'dry run' Storage Permit application.

This report details the geological characterisation of the chosen North Sea Storage Site. It acts as a reference document to the Storage Permit application (preliminary version, MS7) and as such may not be fully up–to-date with the final Storage Permit application, MS8, due to be submitted in December 2012. Appropriate injection schemes, site boundaries and dynamic capacity of the site will be investigated in subsequent tasks in WP3 SiteChar that build on results presented in this report and will update the final Storage Permit application.

The report has been written by researchers at the Natural Environment Research Council, British Geological Survey (BGS), in Edinburgh and Nottingham, IFP Energies nouvelles (IFPEN), Paris, and the Geological Survey of Denmark and Greenland (GEUS), Copenhagen. Task 3.1 was led by BGS who undertook selection, acquisition and interpretation of seismic and well data, assessment of the geological character of the site, construction of gridded model surfaces, identification and generation of facies logs and advised of the presentation of results suitable for the dry-run Storage Permit licence application. GEUS proposed and advised on the method of facies log generation, trialling and outcome of the implemented method and sedimentological context of the storage site strata. IFPEN advised on the construction of the gridded surface model, constructed the geocellular model, proposed and implemented the method for model population of appropriate petrophysical parameters. We gratefully acknowledge the collaborative working, informative discussion and innovative contribution from all Task 3.1 colleagues.

Results and interpretations that were used in the geological characterisation of the Storage Complex utilised data initially acquired by the hydrocarbon industry. The data was generally of good quality and interpretation of this has informed the 'dry-run' licence application. However, due to confidentiality issues in this active hydrocarbon province, there were gaps

in the data that resulted in uncertainties that would hopefully be resolved in a 'real' application where greater resources would be available and crucially, the current operator of the hydrocarbon field, that forms a key part of the Storage Complex, would be a key partner.

Seismic data for the characterisation of the UK northern North Sea site in the Moray Firth, Scotland has been provided under licence from PGS Exploration Ltd. Well data to attribute the geology of the site was made available to BGS under agreement with Common Data Access (CDA) and to other partners under a licensing agreement with IHS Limited.

**ACKNOWLEDGEMENTS**

We would like to thank all SiteChar Work Package 3 partners for their contributions to this report. In particular, thanks are due to the following individuals:

Florence Delprat-Jannaud IFPEN

Jean-Marc Daniel IFPEN

Anna Korre IMPERIAL COLLEGE

We would also like to thank PGS for supplying a portion of the 3D MegaSurvey, Amerada Hess for sourcing the original raw stack data of this survey as well as Fugro and Western Geco for use of their 2D seismic datasets. For BGS, well data was viewed from the CDA under the BGS academic licence. A licensing agreement with IHS allowed project partners access to this data.

Finally, for the British Geological Survey, thanks are due to Joe Bulat (Data loading and velocity model), Eileen Callaghan (well data review), Kirstin Crombie (seismic interpretation), Sandy Henderson (figure production and data downloads), James Thompson (production data graphs), Gary Kirby and Jonathan Pearce (peer review for Task 3.7 SiteChar) for their contributions to this report.

## EXECUTIVE SUMMARY

SiteChar research will inform implementation of the European Union Carbon Capture and Storage (CCS) Directive by presentation of a standard site characterisation workflow based on the investigation of five representative potential carbon dioxide ($CO_2$) storage sites. One of the sites investigated, in Work Package 3 (WP3) of the SiteChar project, lies offshore in the Outer Moray Firth within the UK sector of the North Sea. The ultimate aim of Work Package 3 is to submit a dry-run licence application to the competent authorities in Scotland. This (D3.1) report acts as one of the reference documents used to inform the application.

### Work Package 3 project concept

The project concept at this stage is of a multi-store $CO_2$ storage site that demonstrates $CO_2$ storage in the Blake depleted hydrocarbon field, followed by further storage in the surrounding saline aquifer, principally the Captain Sandstone Member of the Wick Sandstone Formation.

It is envisaged that $CO_2$ will be injected into the saline aquifer, down-dip and beyond the extent of the field. Residual trapping and dissolution will occur as it migrates up-dip through the aquifer into the hydrocarbon field where it will also be structurally and stratigraphically contained by the sealing formation. Injection will continue to fill beyond the field to allow the $CO_2$ to migrate beyond the field boundaries and storage in the wider saline aquifer. Here it will be trapped structurally beneath the regional seal and retained along the migration route by residual trapping and dissolution within pore spaces of the sandstone.

### The Storage Site and Complex

The proposed Storage Site is located principally in the Captain Sandstone Member of the Lower Cretaceous Wick Sandstone Formation. It is defined as the entire Wick Sandstone Formation because it is known that the Captain, Coracle and Punt sandstone members may be connected in the area. The Storage Complex is a defined volume that extends beyond the Storage Site and is defined by the envelope of the maximum extent of the $CO_2$ plume suggested by dynamic modelling. The Storage Complex includes the following:

- The primary seal to the Storage Site are mudstones of the Valhall, Carrack and Rodby formations. Rocks of the overlying Chalk Group may also act as seal if they are of sufficiently low permeability;
- Secondary reservoirs for $CO_2$ are provided by strata overlying and laterally continuous with the Storage Site that may be hydraulically connected. These include possible lateral continuation of the Storage Site reservoir within the Coracle or Punt sandstone members of the Wick Sandstone Formation and any rocks with available pore volume that overlie the primary seal; for example the rocks of the Chalk and Montrose Groups.
- Secondary seals (to the secondary reservoirs) are mudstone within the Lista Formation of the Montrose Group and the mud-prone Moray Group.

The Captain Sandstone Member of the Wick Sandstone Formation is both highly porous and permeable and extends across an area of at least 3,400 km$^2$ in the Moray Firth region of the UK Northern North Sea. Characterisation and calculation of storage capacity by a previous dynamic modelling study of $CO_2$ injection suggests a potential capacity of more than 360 Mt for the Captain Sandstone saline aquifer (Scottish Carbon Capture & Storage, 2011). It is overlain by and contained within the regional seals of the Rodby, Carrack and Valhall formations. It also hosts several hydrocarbon fields (Captain, Blake, Atlantic and Cromarty are the four closest to the area of interest). Initial research in Task 3.1 reviewed and selected the Blake Oil Field as a suitable hydrocarbon field store and data sets were acquired and interpreted for the characterisation and static modelling of the area of the proposed Storage Site and Storage Complex.

**Task 3.1 outcomes**

1. The Blake Oil Field has been selected as part of the multi-store for the initial demonstration (prior to storage in the wider Captain Sandstone saline aquifer) for the following reasons:
   - It is estimated to have ceased production by 2016 to allow site handover for change of use of the site for the geological storage of $CO_2$.
   - It is at depths greater than 800 m TVDSS (True-Vertical Depth Sub Sea) that will allow $CO_2$ to be stored in its supercritical state. This is necessary to maximise the storage capacity of the reservoir. The depth to the top of the sandstone ranges from 1350 m TVDSS in the north-east of the field to a maximum of 1650 m TVDSS in the south-western part of the field.
   - Initial static capacity calculations suggest that the field will be able to store up to ~28 Mt of $CO_2$. It therefore has sufficient potential storage to contribute a significant proportion of the total multi-store capacity.
   - At 74 km north-east of the St Fergus gas terminal, it is relatively close to $CO_2$ sources and infrastructure.
   - Blake, lying near the top of the ‘pan handle’ of the Captain sandstone distribution, is in the best position, compared to the Cromarty (gas) and Atlantic (condensate) fields, in terms of the potentially adverse pressure build-ups modelled by an earlier study.
   - For the purposes of SiteChar the field is also available for study with sufficient data, in the form of seismic profiles, well information and associated reports, of the necessary quality to carry out an interpretation at a data cost within project budget.

2. Two static 3D geological models, a regional ‘Basin-scale’ static model and, lying within it, a local ‘Detailed’ model provide the means by which the $CO_2$ multi-store concept can be explored and assessed and results inform the ‘dry-run’ licence application. The ‘Basin-scale’ model covers a large part of the Captain Sandstone

saline aquifer and was built in an earlier study; it has been modified slightly for this project. The 'Detailed' model has been built using mapped geological surfaces and faults interpreted from a comprehensive seismic and well dataset.

3. The Blake Oil Field forms a significant part of the 'Detailed' 3D geological model and the large amount of data associated with its appraisal and development as a hydrocarbon field was examined to identify the different facies associations and characterise the reservoir. This information was also used to help characterise the 'Basin-scale' model where less detailed information was available.

4. Porosity and permeability measurements taken from cores through the Captain Sandstone reservoir were collated and well logs from selected wells over both basin-scale and detailed areas where interpreted. Curves representing the different facies associations were generated through analysis of this data and relationships between porosity and permeability for the different associations was established. These relationships enabled population of the static 3D models in readiness for flow simulation modelling in Task 3.2.

This technical report informs the 'dry-run' licence application document (MS7) and provides information to the other tasks in Work Package 3 that will in turn provide the necessary information to the final licence application (MS8).

## INTRODUCTION

### Carbon Capture and Storage (CCS) Project context

Deeply buried strata beneath the North Sea are well known from the exploration and production of oil and gas. Countries around the North Sea have assessed the suitability and feasibility of depleted oil and gas fields and sandstones containing salt water (saline aquifers) for the geological storage of carbon dioxide ($CO_2$) captured from industrial sources. These assessments are based on data and knowledge gained from more than three decades of offshore hydrocarbon production. The first demonstrator CCS storage projects for the UK are planned to exploit depleted oil and gas fields. In the longer term large, commercial-scale storage sites are anticipated to be hosted in sandstone containing salt water (Saline Aquifers) rather than oil or gas taking advantage of their likely much larger storage capacity. The UK projects would complement active pilot and demonstrator CCS projects in saline aquifers at Sleipner and Snøhvit in the Norwegian sector of the North Sea.

Exploration and production of oil and gas from the North Sea continues alongside planned development of depleted fields, and the saline aquifer sandstones that host them, for CCS. In a wider context the very extensive sandstones, with potential $CO_2$ storage capacities that are orders of magnitude larger than hydrocarbon fields, are being considered as 'storage assets' by EU member states. It is a logical step to continue use of $CO_2$ capture, transport and injection infrastructure established at a demonstrator hydrocarbon field site for commercial-scale $CO_2$ storage in the adjacent saline aquifer sandstone.

The potential storage site investigated in the UK northern North Sea in Work Package 3 (WP3) of the SiteChar research project anticipates the development of *multi-store* hydrocarbon field and saline aquifer sandstone $CO_2$ storage sites. The SiteChar case study of a *multi-store site* in the Outer Moray Firth offshore Scotland (Figure 1) examines storage in a hydrocarbon field, the Blake Oil Field, and the host Captain Sandstone saline aquifer. The research will also inform the interaction between $CO_2$ storage in hydrocarbon fields (producing and depleted) and sandstone in which they are hosted.

The Work Package comprises a series of tasks that will chart the development of the *multi-store site* culminating in identification and definition of a *Storage Complex* and specific *Storage Site* that will form the subject of a dry-run storage licence application to regulators. Text presented in italics is defined in Appendix 1.

### Aims of this report

This report summarises the geological setting and selection of a hydrocarbon field for the *multi-store site*. It describes the geology of a 'Basin-scale' static geological 3D model and the characterisation a 'Detailed' static geological 3D model that sits within it. These combined models will contain the *multi-store site* within which the *Storage Site* and the *Storage Complex* will be defined for the licence application. Activities to interpret and construct a static geological 3D model are described and uncertainties and risks are highlighted that are

to be addressed by research in WP3. Scenarios for $CO_2$ injection are proposed, potential *leakage* points (e.g. abandoned wells and cross-cutting faults) are identified and risks to be assessed and managed are tabulated.

The report details the results of Task 3.1 of Work Package 3 of the SiteChar project. Work Package 3 investigates the concept of injection of $CO_2$ in a *multi-store site*, namely maximising storage space by utilising both a depleted hydrocarbon reservoir and a saline aquifer sandstone, in the Outer Moray Firth, offshore north-east Scotland (Figure 1).

Investigations of the UK site in WP3 are presented in a format suitable to inform a 'dry-run' application for a storage site licence to be submitted for review to the relevant competent regulatory authorities. The report structure reflects the information required for the licence application: site location; model construction, data sources and uncertainties; development history; possible scenarios for $CO_2$ injection and storage; site capacity; and containment of $CO_2$ within the site. At this interim stage in the progress of the research, results of Task 3.1 identify uncertainties and risks to the site that will be further investigated by other tasks in WP3 (Appendix 4). The results presented here will inform a preliminary licence application to be prepared for consideration by the UK CCS Regulatory Group co-ordinated by the Scottish Government. Results from other WP3 activities will inform the final licence application, including the injection scenario selected from those proposed in this report and the final definition of the *Storage Site* and *Storage Complex*.

The results of the investigations in SiteChar, including methods used, will inform the workflow for implementation of the EU CCS Directive in WP1, regulatory licensing and recommendations to the European Commission in WP2. The offshore setting, hydrocarbon field and saline aquifer sandstone stores in the UK North Sea site complements the investigation of sites in Denmark, Italy, Norway and Poland for SiteChar.

The key part of the application from this report is to provide an attributed 3D model of the *multi-store site* to enable these assessments to take place.

This report:

- Puts the *multi-store site* in its geological setting;
- Describes the process carried out for selection of the hydrocarbon field;
- Describes interpretation, mapping and construction of the 'Detailed' 3D static geological model of the Blake Oil Field and adjacent area;
- Describes the development of the Blake Oil Field;
- Details the methodology used to calculate static storage capacity of the store;
- Assesses the injectivity of the Captain Sandstone at two potential injection sites;
- Details the geological parameters that define the containment of the *multi-store site* and assesses our understanding of them and consequent risks;

- Presents and implements a method for the population of the static model with petrophysical parameters, by using a stochastic method that honours measurements of core samples;
- Where necessary, sections of the report are supported by an appendix that contains the background data and detailed methodologies utilised to inform the findings set out above and tabulates uncertainties identified during static model construction relevant to a dry-run Storage Permit licence application.

**Site project concept and geology**

The concept for the UK northern North Sea site within the SiteChar research is of a feasible but hypothetical CCS project which demonstrates $CO_2$ storage in the Blake Oil Field and surrounding saline aquifer as a multi-store site. The storage reservoir within the multi-store site will be the highly porous and permeable Lower Cretaceous sandstone of the Wick Sandstone Formation, principally the Captain Sandstone Member, but may include the older Coracle Sandstone Member which directly underlies the Captain Sandstone at some locations.

The Captain Sandstone covers an area of at least 3,400 $km^2$ in the Moray Firth region of the UK Northern North Sea. The Captain Sandstone saline aquifer was delineated by Johnson and Lott (1993), remapped and a 'Basin-scale' static geological 3D model built and the aquifer assessed for $CO_2$ storage potential (Scottish Carbon Capture & Storage, 2011). The Captain Sandstone has a static $CO_2$ storage capacity ranging from 36 Mt (applying a storage efficiency of 0.2%) to 363 Mt (applying a storage efficiency of 2%) (Scottish Centre for Carbon Storage, 2009). Characterisation and calculation of storage capacity by dynamic modelling of $CO_2$ injection endorses a potential capacity of more than 360 Mt for the Captain Sandstone saline aquifer (Scottish Carbon Capture & Storage, 2011). Further assessment and appraisal of the Captain Sandstone as a $CO_2$ store is justified from the results of the previous research (Scottish Carbon Capture & Storage, 2011).

The 'Basin-scale' static geological 3D model of the Captain Sandstone saline aquifer in the Moray Firth has been made available for further research within the SiteChar project. Detailed investigation and modelling of a hydrocarbon field, a 'Detailed' static geological 3D model, will be integrated with the 'Basin-scale' 3D model to form a *multi-store site*. The top and base of both of these models is defined by the Sea bed and Base of the Cretaceous, respectively.

The area selected for definition and assessment of the *multi-store site* lies within the 'Basin Scale' model and includes the Blake Oil Field that it is estimated will have ceased production by 2016. The Blake Oil Field forms a key element of the *multi-store site* and was selected at the beginning of Task 3.1 from four hydrocarbon fields that produce from the Captain Sandstone reservoir within the limits of the 'Basin-scale' 3D model namely Captain, Blake, Atlantic and Cromarty (Figure 1). The Captain Oil Field was eliminated as parts of this field lie above 800 m and therefore too shallow to store $CO_2$ in the supercritical state necessary to maximise storage capacity of the reservoir. Of the remaining three fields, the key factors

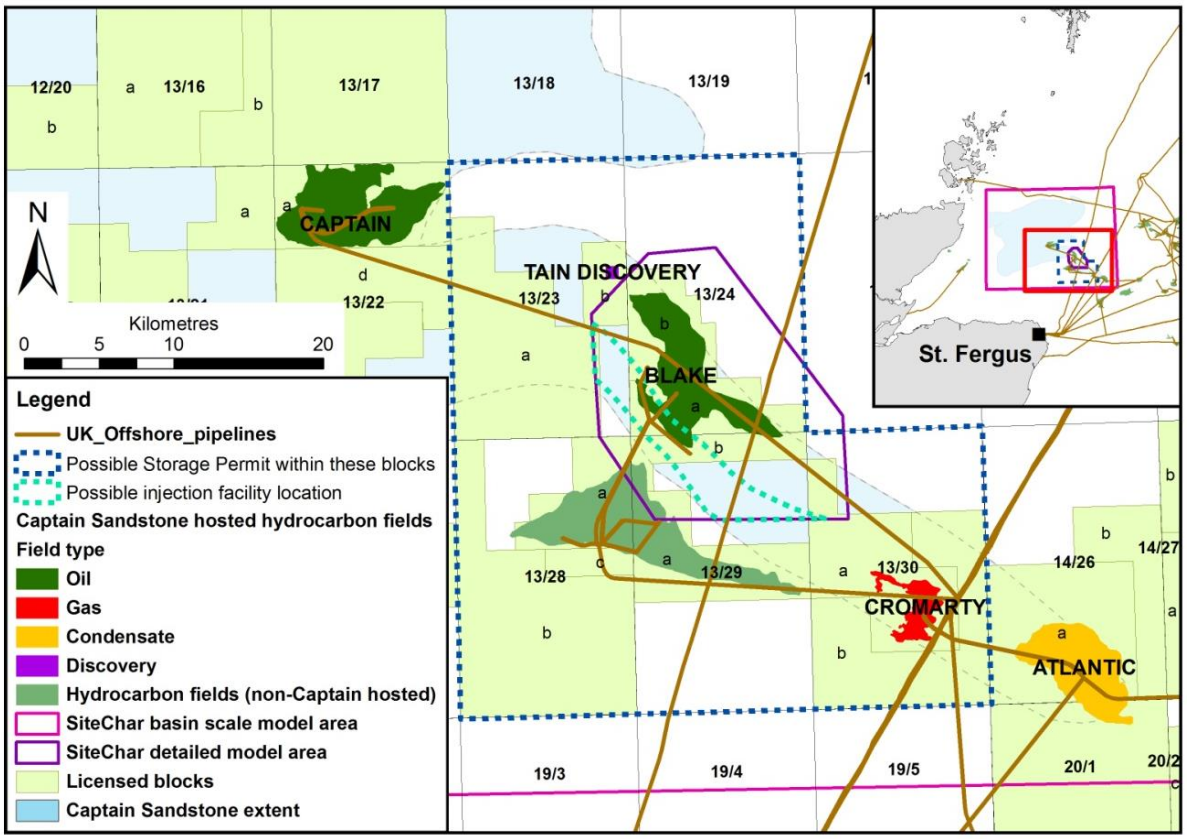


**Figure 1: Proposed Storage Permit location map.**
**Captain Sandstone extent from Scottish Carbon Capture & Storage (2011).**
**Contains public sector information licensed under the Open Government Licence V.1.0. Field outlines and wells from DECC 2011' Data available from:**
**https://www.og.decc.gov.uk/pprs/full_production.htm**

that drove selection of the Blake Oil Field were size, position, access to hydrocarbon transport infrastructure and availability of data.

In summary, the criteria for selection of the hydrocarbon field that can form part of the multistore are:

- Production is, at least in part, from the Captain Sandstone Member;
- Field is at depths greater than 800m TVDSS. In order to utilise the available pore space in the reservoir most efficiently, the injected $CO_2$ must be in its supercritical phase that occurs at a temperature of 31.1°C and pressure of 73.8 bar (likely to be at a depth of > 800 m TVDSS). $CO_2$ is most dense when in its supercritical phase and the storage space utilised will be at least two orders of magnitude greater; the Blake Oil Field reservoir lies at a minimum depth of approximately 1350 m TVDSS (True-Vertical Depth Sub Sea);
- Field has sufficient potential storage to contribute a significant proportion of the total *multi-store* capacity;

  - The Blake Oil Field, has the greatest potential storage capacity of the remaining three hydrocarbon fields.
- Location of the field in the Captain Sandstone saline aquifer is as optimal as possible with regard to pressure effects during injection (see below);
  - The Blake Field is located in the north-western end of the 'pan-handle' where the sandstone begins to widen out into the main Captain Sandstone aquifer (Figure 4). Dynamic simulation of $CO_2$ *migration* in this area for the Scottish CCTS Development Study (Scottish Carbon Capture & Storage, 2011) showed that pressure increase due to $CO_2$ injection was greater in the south-eastern part of the 'pan handle' where the width of the Captain sandstone reservoir is thought to be at its narrowest. Thus the Blake Oil Field is in the best position, compared to the Cromarty (Gas) and Atlantic (Condensate) fields, in terms of the pressure effects modelled by Scottish Carbon Capture & Storage (2011).
- Sufficient data, in the form of seismic profiles, well information and associated reports, is available (Figure 2; Appendix 2);
  - Data is of necessary quality to carry out an interpretation;
  - Cost of data is within project limits.
- Field is available for study (when the field is estimated to cease production and thus be available for utilisation as a $CO_2$ store will be a factor in its selection for the licence application);
- Field is relatively close to $CO_2$ sources and infrastructure.

The study area is located 74 km north-east of the St Fergus gas terminal in approximately 104 m water depth. The site is located within currently (2012) licensed *UKCS* blocks 13/23b (Talisman), 13/24a (BG Group), 13/24b (BG Group), 13/28a (Talisman) 13/29b (Talisman) and 13/30a (Hess), as well as small, presently unlicensed areas, adjacent to the licensed blocks (Figure 1). The extent of the 'Detailed' geological 3D model is shown an outlined polygon in Figure 1. The *Storage Complex* will be specifically defined following dynamic modelling of $CO_2$ injection and other tasks to be carried out in Work Package 3.

In order to fully test the multi-store concept the total quantity of $CO_2$ to be stored is assumed to be >100 Mt. It is also assumed that injection of $CO_2$ will commence in 2016 and that containment will initially be demonstrated in the depleted hydrocarbon field followed by continuing injection into the saline aquifer until the dynamic capacity applied for, has been reached. A single gas-fired power station source may be able to supply up to one million tonnes (Mt) per year. To fully utilise the multi-store site the annual rate and composition of supply is assumed to be from a number of industrial sources transported to St Fergus via a

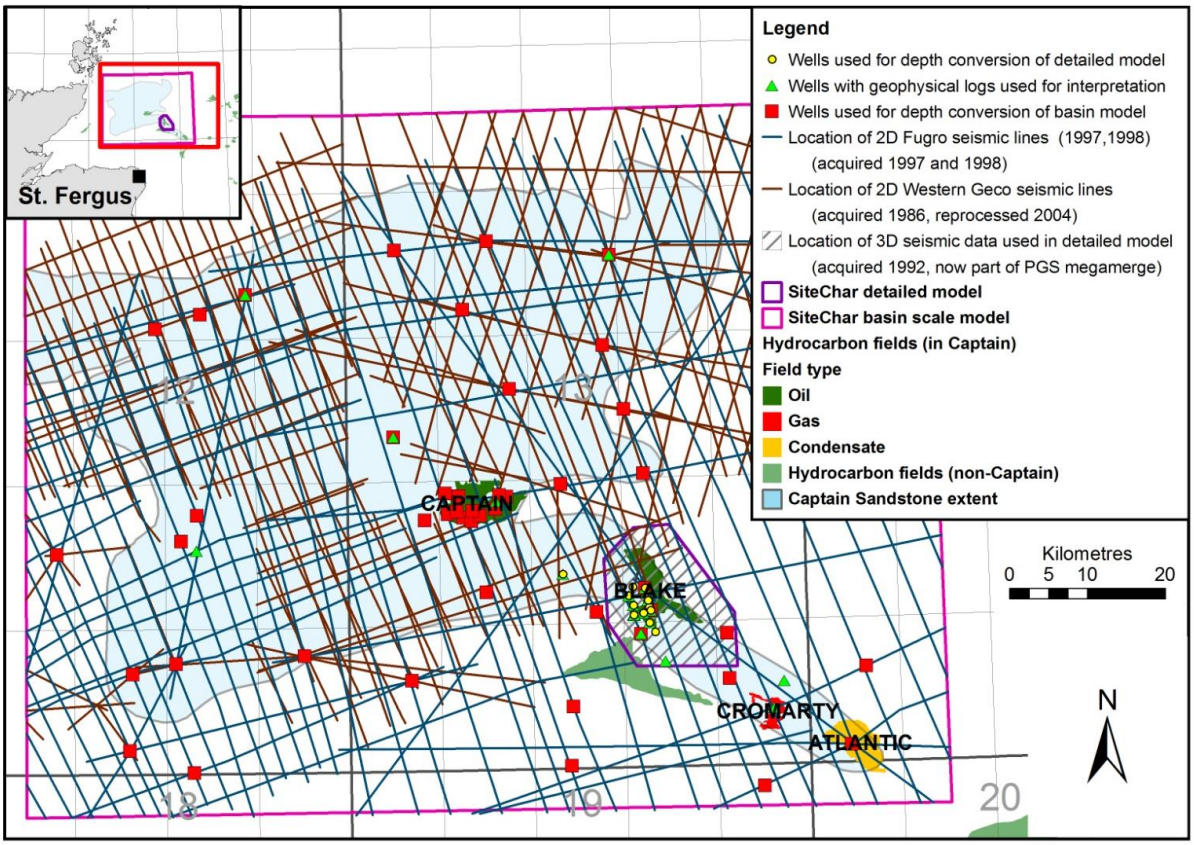


**Figure 2. Distribution of data sources used. Interpretation of 2D seismic surveys and well data for the basin-scale model by Scottish Carbon Capture & Storage (2011). Interpretation of geophysical logs and other data by this study.**

pipeline network as within the $CO_2$ transport options for Scotland presented by Scottish Carbon Capture & Storage (2009).

The $CO_2$ would be industrially sourced from onshore eastern coastal Scotland where there are around 20 sources that emitted more than 100 000 tonnes of $CO_2$ in 2006 (Scottish Centre for Carbon Storage, 2009). Transport of the $CO_2$ from the source to the storage site is envisaged to be by pipeline, such as those that have landfall at the St Fergus gas terminal (inset on Figure 1). The $CO_2$ is anticipated to be compressed to dense phase, with a gauge pressure of around 130 bar, for transport offshore. The composition of the gas supply will be overwhelmingly of $CO_2$ (greater than 99%). Where supply is from a number of sources, a supply rate of up to 10 Mt per year is envisaged and with an assumed composition of more than 99% $CO_2$.

In order to define the *Storage Complex* and *Storage Site* that have the capacity and security of containment for the expected quantities of $CO_2$ to be delivered, modelling of injection of $CO_2$ into the *multi-store* site will be carried out (Task 3.2 (IFPEN)). As the $CO_2$ moves through the Captain Sandstone, a significant portion of it will be retained within the pore

space or dissolved within the saline pore water of the sandstone along the *migration* route. These storage mechanisms will also apply within the depleted hydrocarbon field where structural and stratigraphic trapping will provide additional security of containment of the migrating $CO_2$ supercritical fluid (Section 4).

## 1. GEOLOGICAL OVERVIEW OF PROPOSED STORAGE SITE AND COMPLEX

The proposed *Storage Site* is located within the Lower Cretaceous Wick Sandstone Formation, principally the Captain Sandstone Member (Figure 3). Its boundaries will be defined by the dynamic modelling carried out by IFPEN for Task 3.2 but will likely be constrained by a combination of *structural* and *stratigraphic trapping*. The Captain Sandstone is both highly porous and permeable and extends across an area of at least 3,400 km$^2$ in the Outer Moray Firth region of the UK Northern North Sea. Mean porosity, interpreted from selected wells within the 'Basin-scale' and 'Detailed' 3D model areas, is 23% with a maximum value of 28%; permeability ranges from less than 1 mD to several Darcies (Tables 1 and A3.3). The Captain Sandstone forms the principal reservoir for four producing hydrocarbon fields within the area of study (Captain, Blake, Atlantic and Cromarty) as well as other discoveries outside the study area (Law *et al*., 2000; Rose, 1999; Pinnock and Clitheroe, 1997; Figure 4). The Captain and other Lower Cretaceous sandstones are overlain and contained within very efficient regional seals.

The *Storage Complex* will sit within a defined (extents will be defined after dynamic modelling by Task 3.2 SiteChar) rock and sediment volume (within the 'Detailed' and 'Basin-scale' 3D models) comprising a geological succession deposited from latest Jurassic time to the present day (Figure 3). The *Storage Complex* will include:

- Top, base and lateral seal rocks of the *Storage Site*;
- Strata overlying and laterally continuous with the *Storage Site* providing secondary containment for $CO_2$ that;
  - are hydraulically connected (lateral continuation of the *Storage Site* reservoir);
  - have available pore volume overlying the seal into which $CO_2$ may migrate and be stored;
- The *Storage Complex* will also include sealing rocks to the secondary containment reservoirs.

The succession of rocks within the *Storage Complex* accumulated during the Cretaceous Period and Early Palaeogene, with a combined time span of 150 million years, in a deep marine setting (Figure 3). From Late Jurassic until late Cretaceous times, the sedimentary environment in this area was set against a background of rising sea-level that culminated in a maximum sea-level/flooding surface. However, during the Lower Cretaceous this general increase in sea-level was punctuated by sea-level falls during the Hauterivian-Valanginian and later during the Aptian times (Figure 3), related to far-field tectonic events (Oakman, 2005). These periods of lowered sea-level caused sand to bypass the exposed shelf areas and be deposited in deeper water by gravity flow processes that fed submarine fans and led to the accumulation of three sandstone intervals, the Punt (oldest), Coracle and Captain (youngest) sandstone members. These sandstone members form part of the Wick Sandstone Formation (Figure 3; Johnson and Lott, 1993). Sediment sources for these three members were north and west of the Wick Fault Zone (Figure 4).

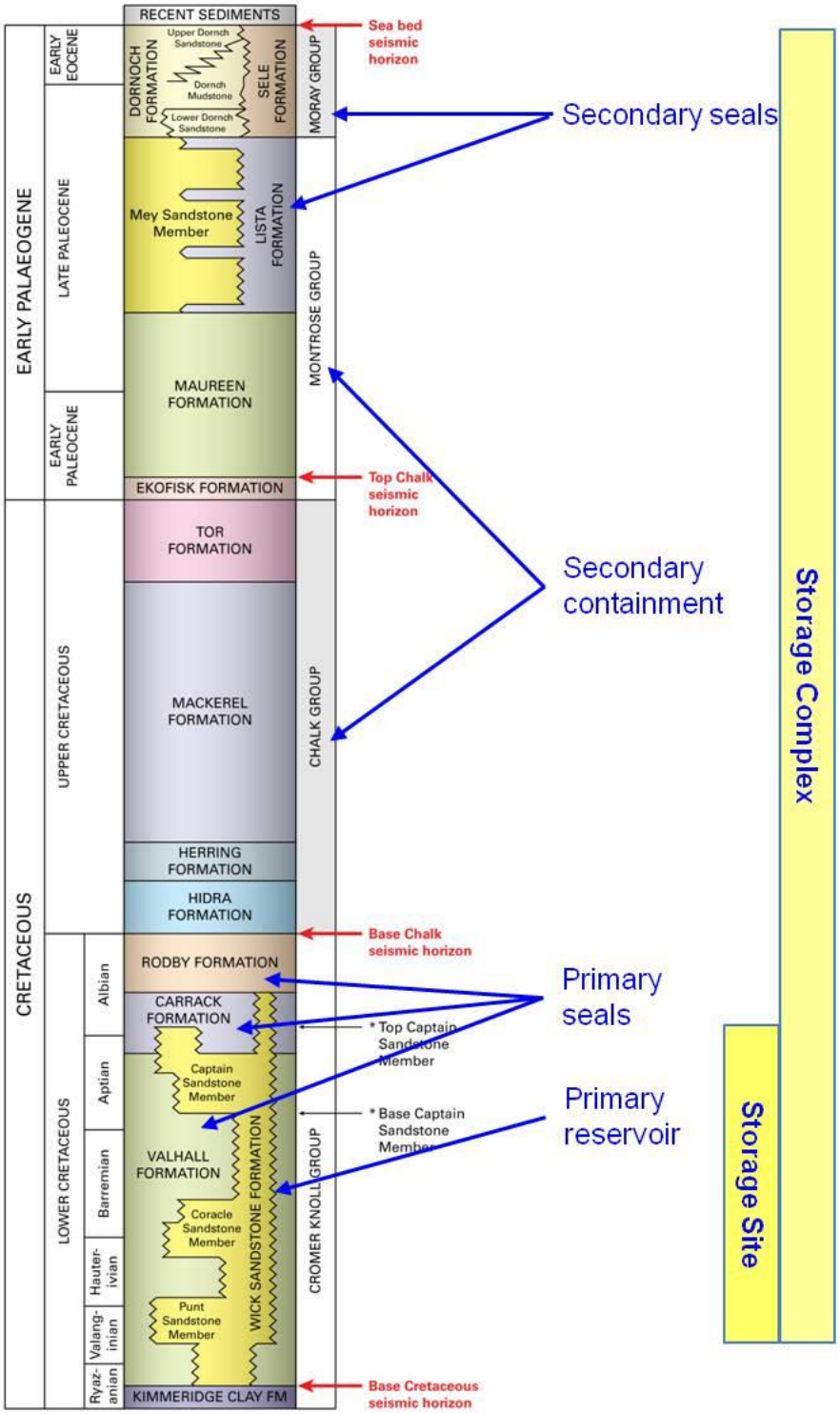


**Figure 3. Lithostratigraphy of the geological succession in the Storage Permit area indicating proposed/expected Storage Site & Complex*(after Johnson & Lott, 1993 and Knox & Holloway, 1992).***

The lithologies of the Upper Cretaceous Chalk reflect continuing sea level rise and consequent landward migration of facies belts with diminishing sediment input from sub-aerial sources and extensive deposition of calcareous strata. The Early Paleocene marks a change to siliciclastic deposition over the area as sediment sourced from uplifted areas to the west and north were shed into the area.

An extensive Upper Jurassic organic-rich mature source rock in the West Halibut Basin (Figure 4), located down-dip and beneath the Lower Cretaceous reservoir sandstones, has generated the hydrocarbons that have charged the hydrocarbon fields present in the area. The Lower Cretaceous sandstone hydrocarbon play is challenging but also productive and continues to be actively explored to the present day.

## 1.1 Regional geology

### 1.1.1 Structure

The geological structure of the Moray Firth region is characterised by a number of fault-defined structural highs, basins and sub-basins (Figure 4). These structures were formed

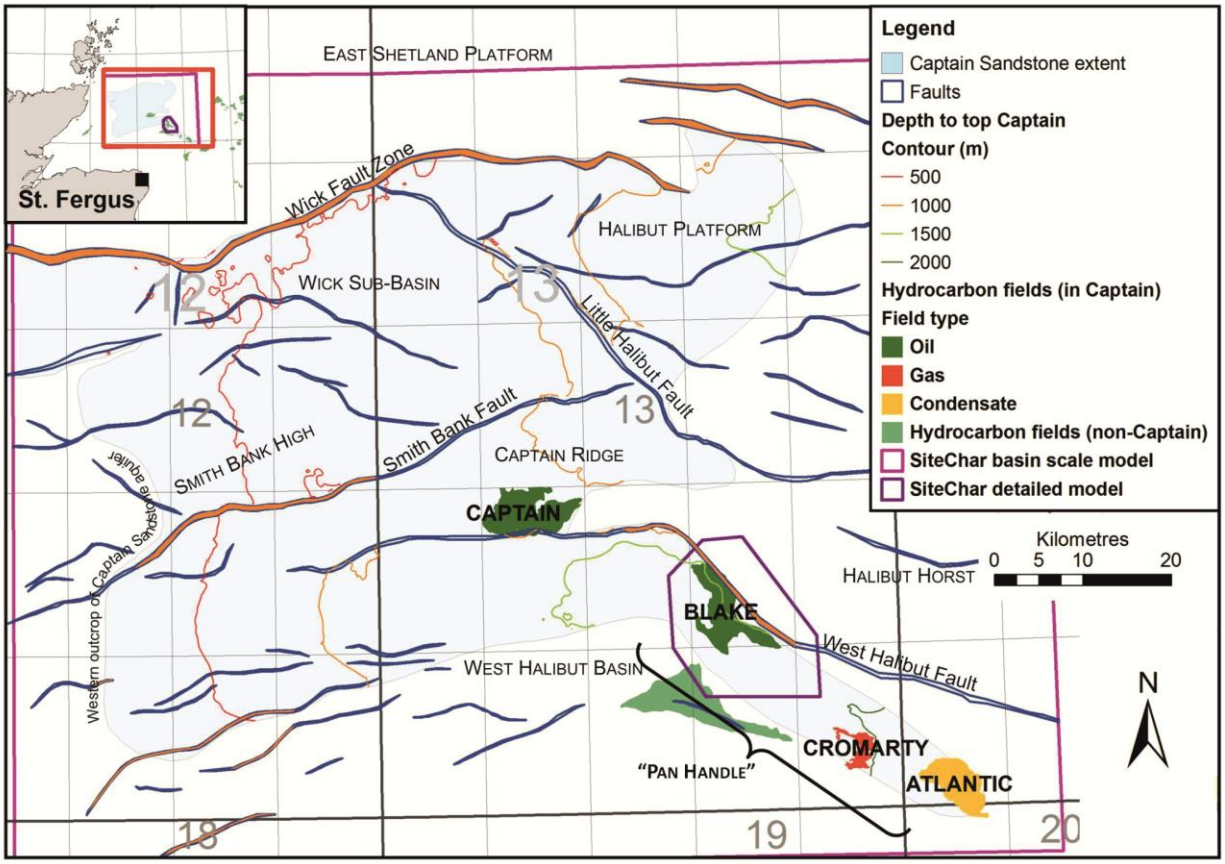


**Figure 4. Map of the extent and depth to top of the Captain Sandstone, faults, basins, ridges and platforms at base Cretaceous surface (from Scottish Carbon Capture & Storage, 2011) and hydrocarbon fields *(the parts of the faults coloured orange extend up to the sea bed).***

from a series of Mesozoic displacements (post-Triassic, post-Jurassic) on major ENE-WSW-trending faults. Major faults within the area include the ENE-trending Wick Fault Zone and Smith Bank Fault. The West Halibut and the Little Halibut faults mark the approximate southern and northern boundaries of a key fault-bounded structural high, the Halibut Horst (Figure 4).

### 1.1.2 Stratigraphy

The Halibut Horst, a major Jurassic structural high (Ahmadi *et al*., 2003), influenced sedimentation patterns for a long period of time until it was eventually drowned during the Late Cretaceous. Crucially, it was present throughout the Lower Cretaceous when deep submarine fans, represented by the Captain, Coracle and Punt sandstones that form the reservoir rocks of the proposed $CO_2$ *Storage Site*, were deposited. The 'Detailed' geological 3D model built for this study includes the southern bounding fault of the Halibut Horst, the West Halibut Fault (Figure 4).

Over the 'Basin-scale' 3D model, the Lower Cretaceous succession varies in thickness from very thin or absent over the Halibut Horst to more than 2000 m thick just south of the Wick Fault, close to its intersection with the Little Halibut Fault (Figure 4), and nearly 1550 m thick within the 'Detailed' 3D model area. The Halibut Horst appears to have been a control in Captain Sandstone deposition, especially along its southern margin. The Captain Sandstone has a confined distribution south of the West Halibut Fault, having entered the South Halibut Basin in the vicinity of the Captain Field (Rose, 1999) and other possible point sources along the Halibut Horst (Law *et al*., 2000).

The Upper Cretaceous Chalk Group comprises five formations, the oldest is the Hidra Formation which rests directly on the Lower Cretaceous Rodby Formation (Figure 3). The Hidra Formation is succeeded by the Herring, Mackerel, Tor and Ekofisk formations. In the 'Detailed' 3D model area, the Chalk Group comprises thick successions of limestone and chalky limestone with occasional mudstone units. One such mudstone unit is the Black Band bed formerly the Plenus Marl Formation (Deegan and Scull, 1977) forming a unit at the base of the Herring Formation. The Black Band bed comprises non-calcareous, pyritic mudstone characterised by high gamma values and low velocity that is commonly a marked event on seismic survey profiles; in Well 13/24a- 4, the Black Band Bed comprises 6 m of claystone (Figure 5). The Chalk Group reaches a maximum thickness of 500 m in the West Halibut Basin.

Over the regional 'Basin-scale' 3D model of the Captain Sandstone, the majority of the Palaeogene succession overlying the Chalk Group comprises Paleocene sedimentary rocks. These strata thin westwards and are absent in the west of the 'Basin-scale' 3D model area due to uplift and erosion (Ahmadi *et al*., 2003; Argent *et al*., 2002; Scottish Carbon Capture & Storage, 2011). The Paleocene succession in the 'Detailed' 3D model area comprises the very sand-prone Montrose Group, Maureen and Lista formations. The group reaches a maximum thickness of about 1700 m in the West Halibut Basin. The Maureen Formation, where present in the *Storage Complex*, is composed of heterolithic sandstone interbedded

with siltstone and basinal carbonate rocks derived from amalgamated high- and low-density sediment gravity flows (Ahmadi *et al.*, 2003). The Lista Formation is mostly of non-calcareous mudstone interbedded with sandy, high-density gravity flow deposits and includes some volcaniclastic sedimentary rocks (Ahmadi *et al.*, 2003). In general, the Palaeogene succession within the *Storage Complex* will provide substantial secondary storage capacity for any $CO_2$ migrating out of the *Storage Site*.

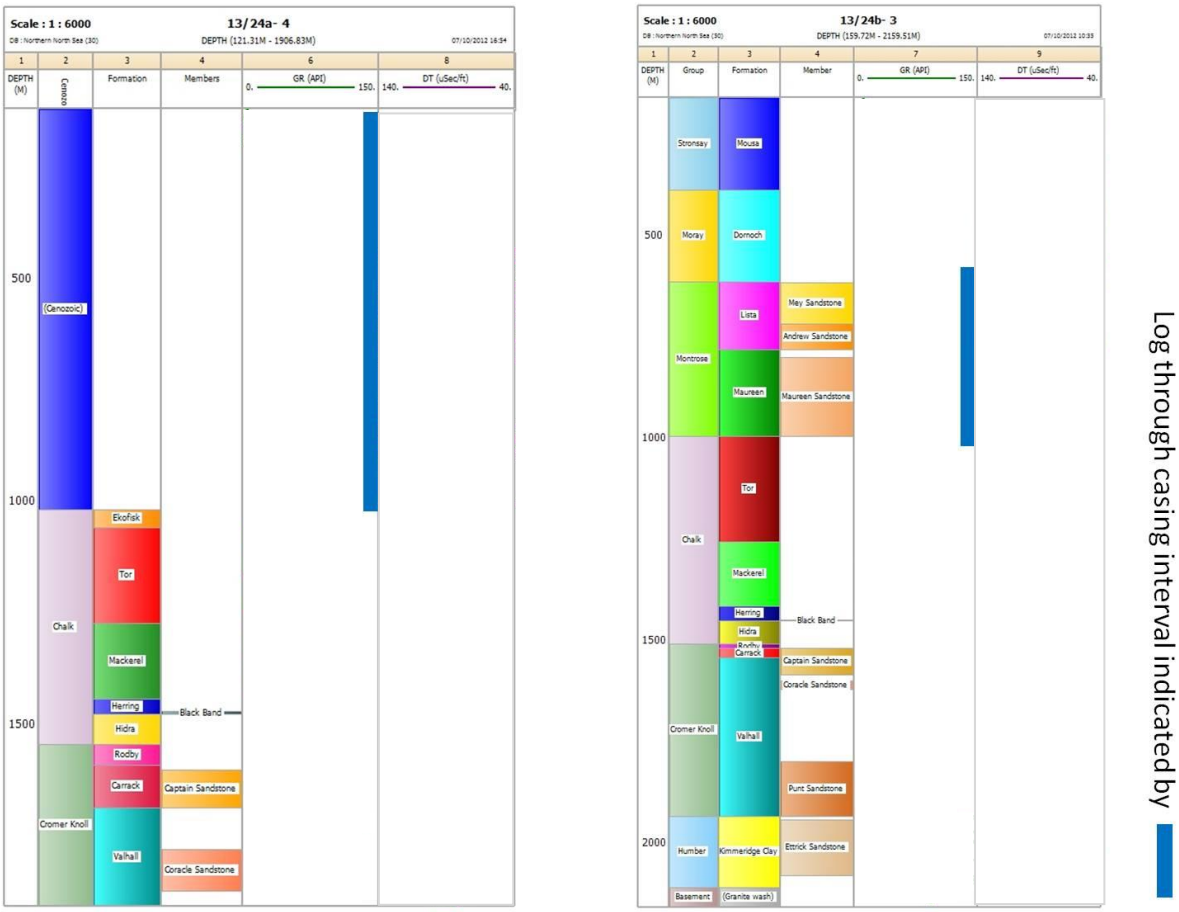


**Figure 5. Examples Gamma Ray and Sonic log displays over the Storage Site and Storage Complex rock succession. Original data used in this interpretation (not shown) provided under agreement from IHS Global Limited.**

### 1.2 Structure within the 'Detailed' geological 3D model area

The area covered by the 'Detailed' static geological 3D model is located within parts of UK Blocks 13/23, 13/24, 13/28 and 13/29 and includes part of the southern boundary of the Halibut Horst marked by the West Halibut Fault and northern margin of West Halibut Basin (Figure 4). All mapped surfaces have a general dip ranging from the SW to SE and they shallow towards the NE onto the Halibut Horst (e.g. Figures A3.7 to A3.10). Within the West

Halibut Basin, faults have been mapped at the Base Cretaceous surface but were not interpreted to pass up into the Captain Sandstone reservoir. No significant faulting was

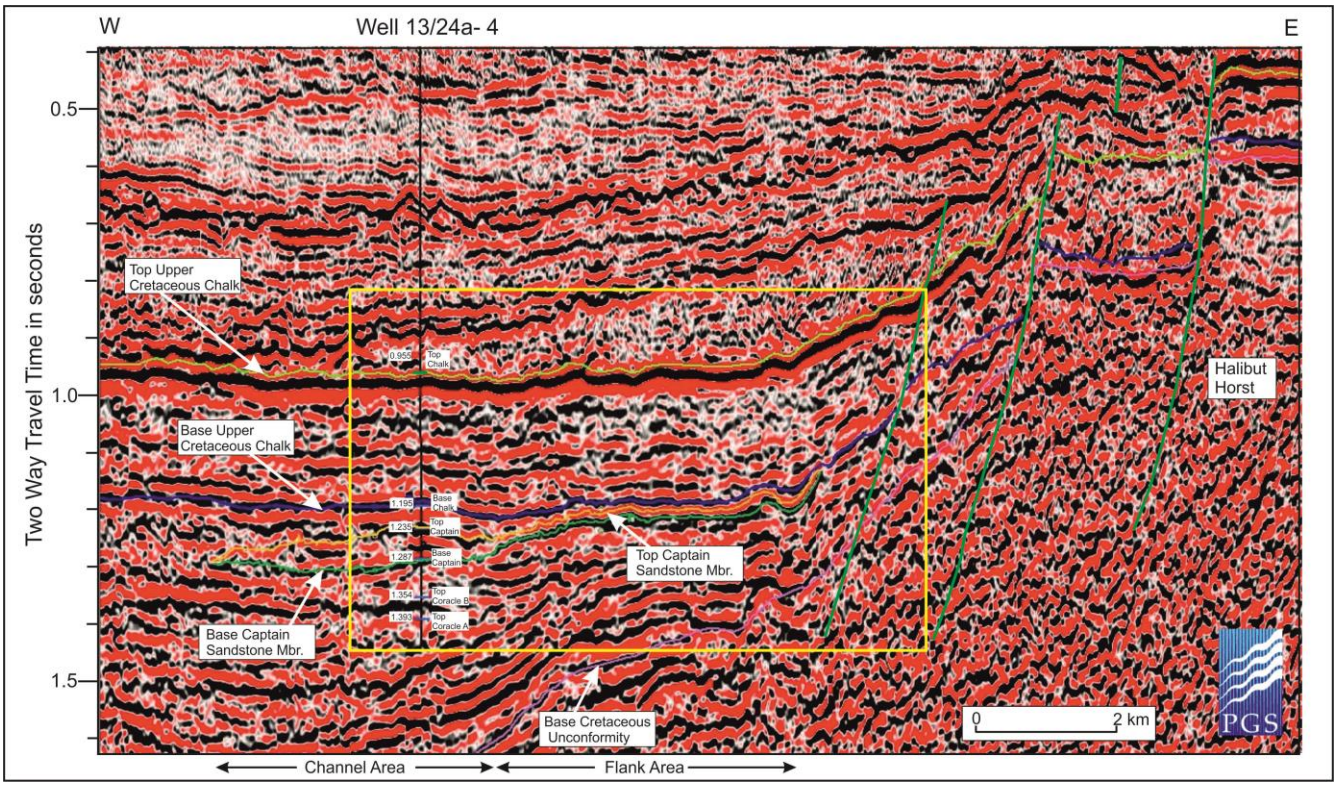


**Figure 6a. Seismic section showing pinch out of sands before fault.**

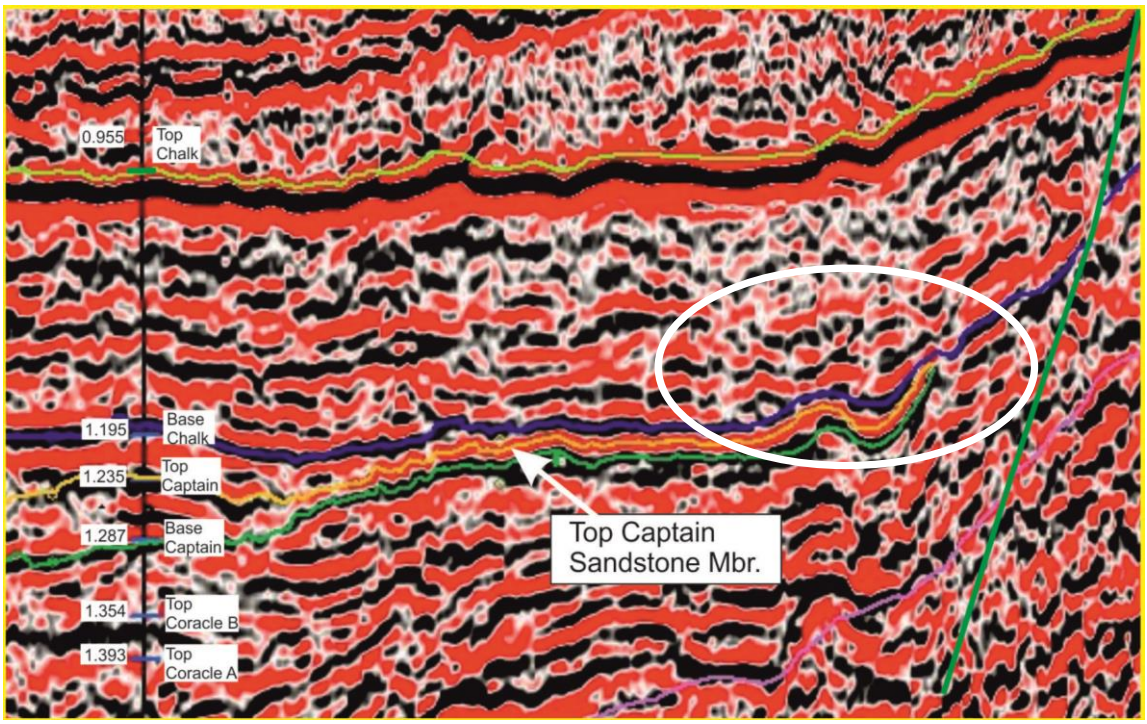


**Figure 6b. Detail (within yellow rectangle on Figure 6a) of interpretation showing pinch out of sands before fault.**

observed in the Captain Sandstone reservoir and it is interpreted to pinch-out close to, and not to reach the bounding West Halibut Fault (Figure 6a,b); Figure A3.4a,b; Figure A3.5a,b). Nevertheless, *migration* of $CO_2$ along the fault-plane of the West Halibut Fault is a risk to the integrity of the *Storage Site*.

The faulted southern boundary of the Halibut Horst (the West Halibut Fault) has a general NW-trend. However, in the area mapped for this study, the disposition of the fault is complex with changes in orientation and a major offset. The fault line interpreted within the 'Detailed' 3D model is approximately 20 km long and exhibits a steeply dipping fault plane with displacement of strata across the fault ranging from about 100 m to 550 m at Base Chalk level (Figure A3.9). Assessment of faults in an earlier study (Scottish Carbon Capture & Storage, 2011) interpreted parts of their lengths to reach rock head and therefore be potential *migration* routes for injected $CO_2$ (highlighted orange in Figure 4).

### 1.3 Stratigraphy within the 'Detailed' geological 3D model area

The top of the 'Detailed' 3D geological model is defined by mean sea-level and the sea bed that marks the top of the rock section (Figure 7; Figure A3.11) while the mapped Base Cretaceous surface defines its base (Figure A3.7). The geological succession comprises Lower and Upper Cretaceous and Early Palaeogene sedimentary rocks that reach a maximum thickness of approximately 3300 m within the model area.

Over the 'Detailed' 3D geological model area, the Base Cretaceous surface generally rests conformably upon the Kimmeridge Clay Formation of earliest Cretaceous (Early Ryazanian) to Upper Jurassic age (Figure 3; Thomson and Underhill, 1993). It should be noted that the Kimmeridge Clay Formation contains several sandstone members of Upper Jurassic age, which may, at some locations, occur directly beneath the Lower Cretaceous (e.g. the Burns Sandstone Member, see Richards *et al*., 1993). To the north-east, the Lower Cretaceous succession thins and onlaps the Halibut Horst (Figure A3.4). In well 13/24a- 2A (Figure A3.1), drilled on the Halibut Horst, 257m of Palaeogene sediments, thin Upper Cretaceous Chalk (26 m) and a Lower Cretaceous succession (9 m) rest directly on granite basement rock of probable Silurian-Devonian age.

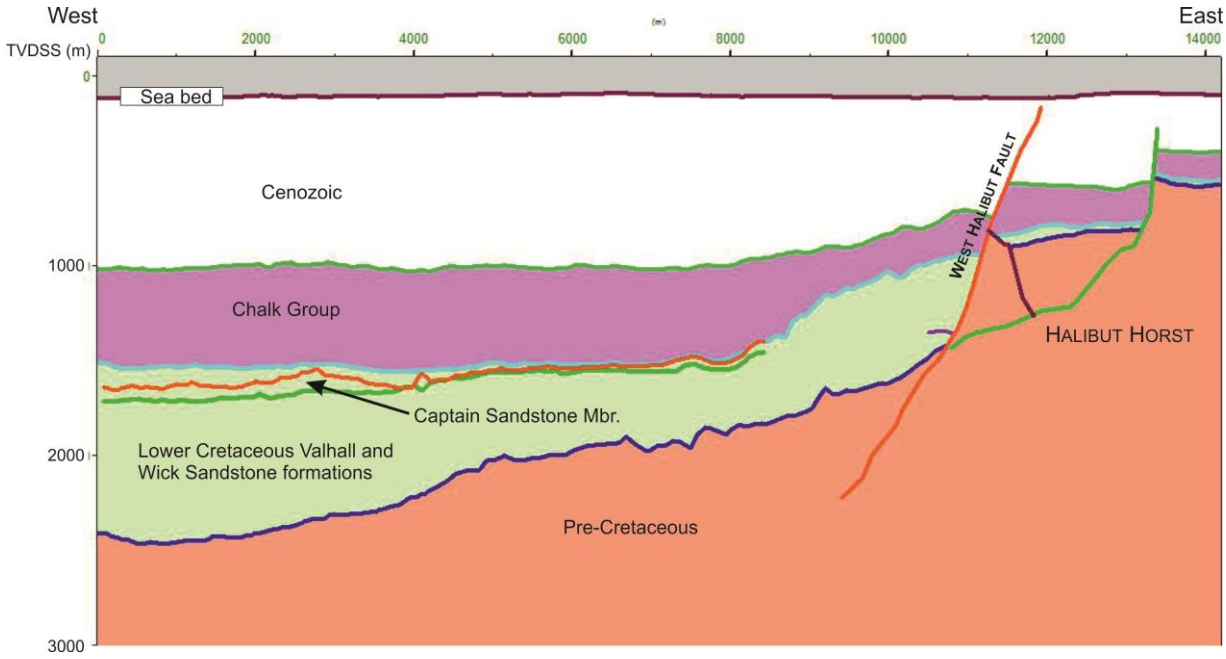


**Figure 7. Geological cross-section across the SiteChar 'Detailed' 3D model.**

### 1.3.1 Lower Cretaceous succession

In the 'Detailed' geological 3D model area, the complete Lower Cretaceous succession comprises the Cromer Knoll Group which is made up of four formations, the dominantly mud-prone Rodby, Carrack and Valhall formations and dominantly sand-prone Wick Sandstone Formation (Figure 3; Johnson and Lott, 1993**)**. The *Storage Site* will sit within the Wick Sandstone Formation.

**Lower Cretaceous succession- *the Storage Site***

Three sandstone members, Captain, Coracle and Punt, interpreted as laterally extensive turbiditic strata deposited by a range of mass-flow processes, have been recognised within the Wick Sandstone Formation (Figure 3; Johnson and Lott, 1993). The Wick Sandstone Formation comprises thick units of mass-flow sandstone interbedded with siltstone and mudstone. The *Storage Site* will utilise the pore volume within the Wick Sandstone

Formation focussing on the Captain Sandstone Member that forms the main reservoir within the Blake Oil Field (Figure 8). However, the underlying Coracle Sandstone may form part of the *Storage Site* as it is in places juxtaposed with the Captain Sandstone.

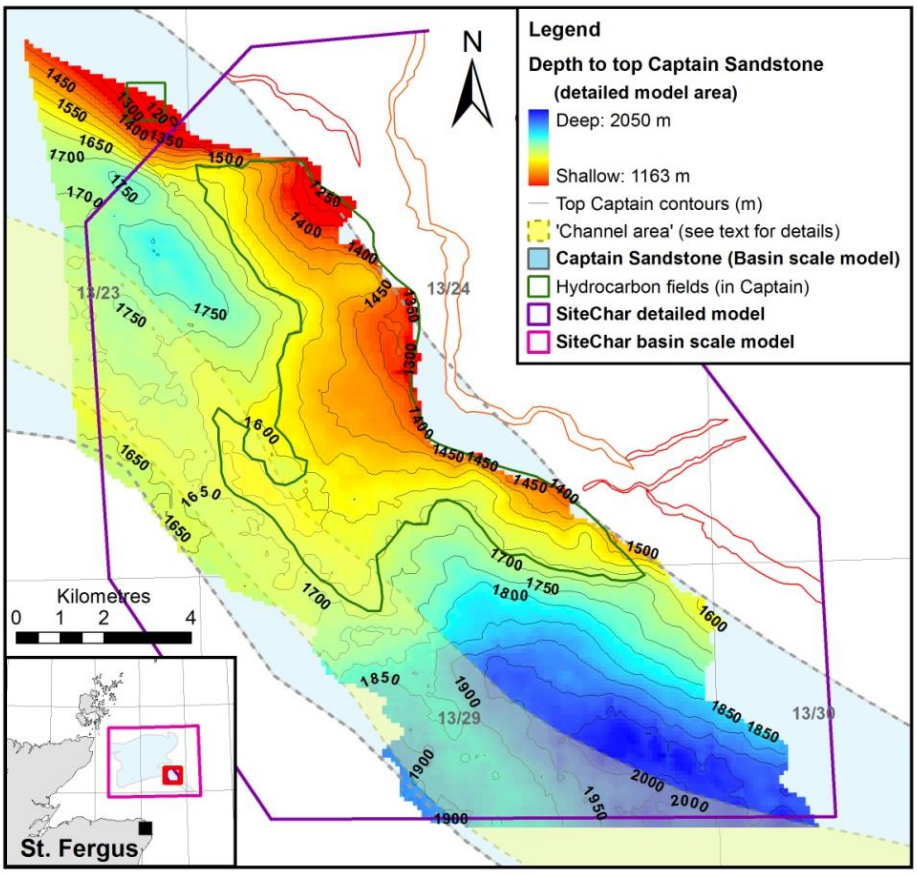


**Figure 8. Map showing depth to top reservoir, in metres (m) below sea level, showing Blake Oil-Water Contact (green line)and Tain discovery (green square).**

The Wick Sandstone Formation passes laterally into the Carrack and Valhall formations which will contribute to the seal to the *Storage Site* (Figure 3). The extent and disposition of the Coracle and Punt sandstones is not well constrained due to fewer well penetrations and its poor resolution in available seismic surveys.

The Blake hydrocarbon field reservoir sandstone principally comprises the Captain Sandstone Member but may also include the Coracle Sandstone Member when it is in communication. These sandstones were deposited in a deep water submarine environment, derived from a sediment source to the north and west of the area and deposited by a range of gravity flow processes including high- and low-density turbidites, mud flows, debris flows, slides and slumps and settling of hemi-pelagic sediment. The Blake Oil Field reservoir has been divided into two distinct areas (e.g. Hilton 1999, p. 43) whose facies associations reflect this range of depositional processes (Figures 9 and 13):

- The 'Channel' area in the down-dip, south-western part of the field;
- The 'Flank' area up-dip to the north-east.

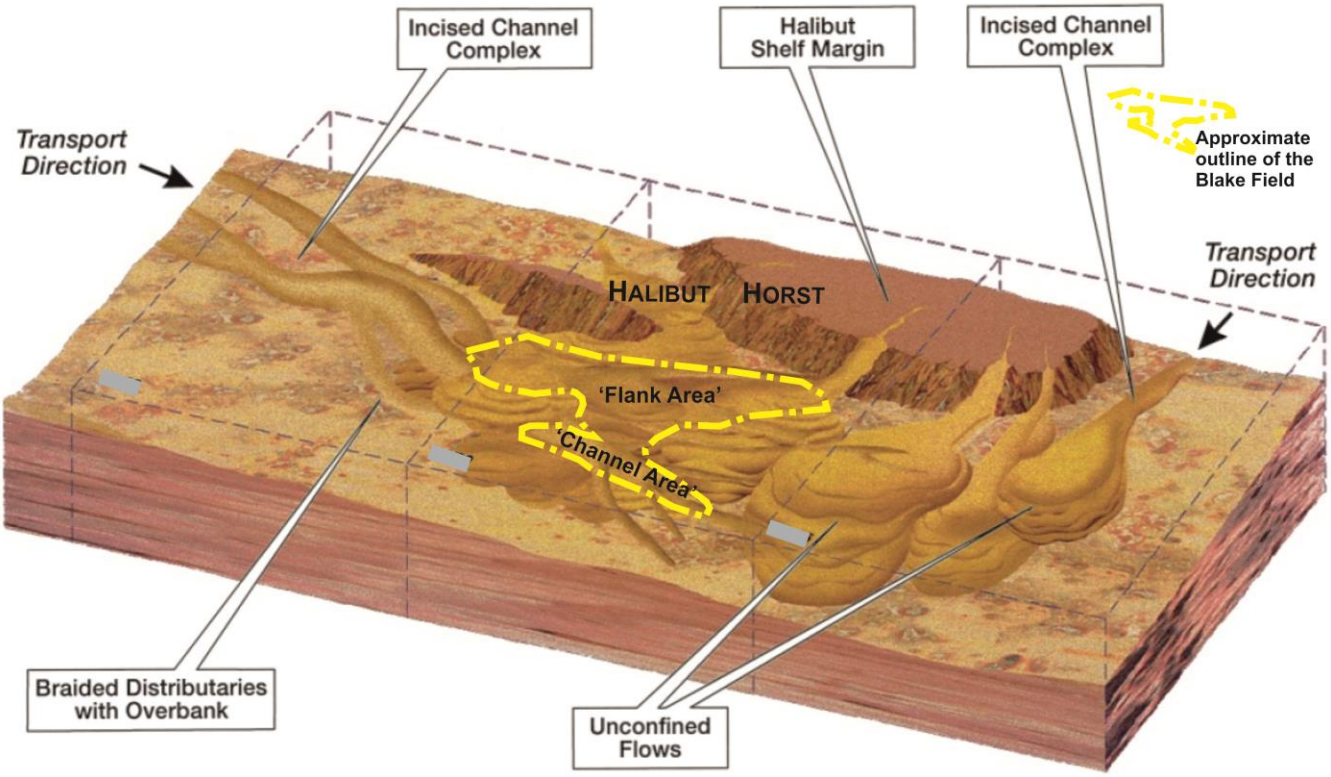


**Figure 9. Diagram showing depositional environment during the Lower Cretaceous in the Blake Oil Field area (modified after Law *et al.*, 2000).**

The nature of the boundary between the two areas, and its precise location, is difficult to define in detail though this is important as it will impact on the dynamic modelling of the $CO_2$ through the reservoir (See Appendix 2, Figures A2.1, A2.2, A2.3 and associated text for further discussion). The juxtaposition of the Channel and Flank area facies associations will result in a wide range of contact relationships. The Channel area is likely to comprise relatively consistent high Net sandstone To Gross Thickness (NTG) sandstone with good permeability and porosity. However, the Flank area will be much more variable with juxtaposition at the Channel/Flank boundary of sand on sand, sand on shale and a high number of variations between these two end members. The Channel and Flank areas have been developed separately with the Flank area exhibiting complex reservoir architecture with possible compartmentalisation of reservoir sands (see below).

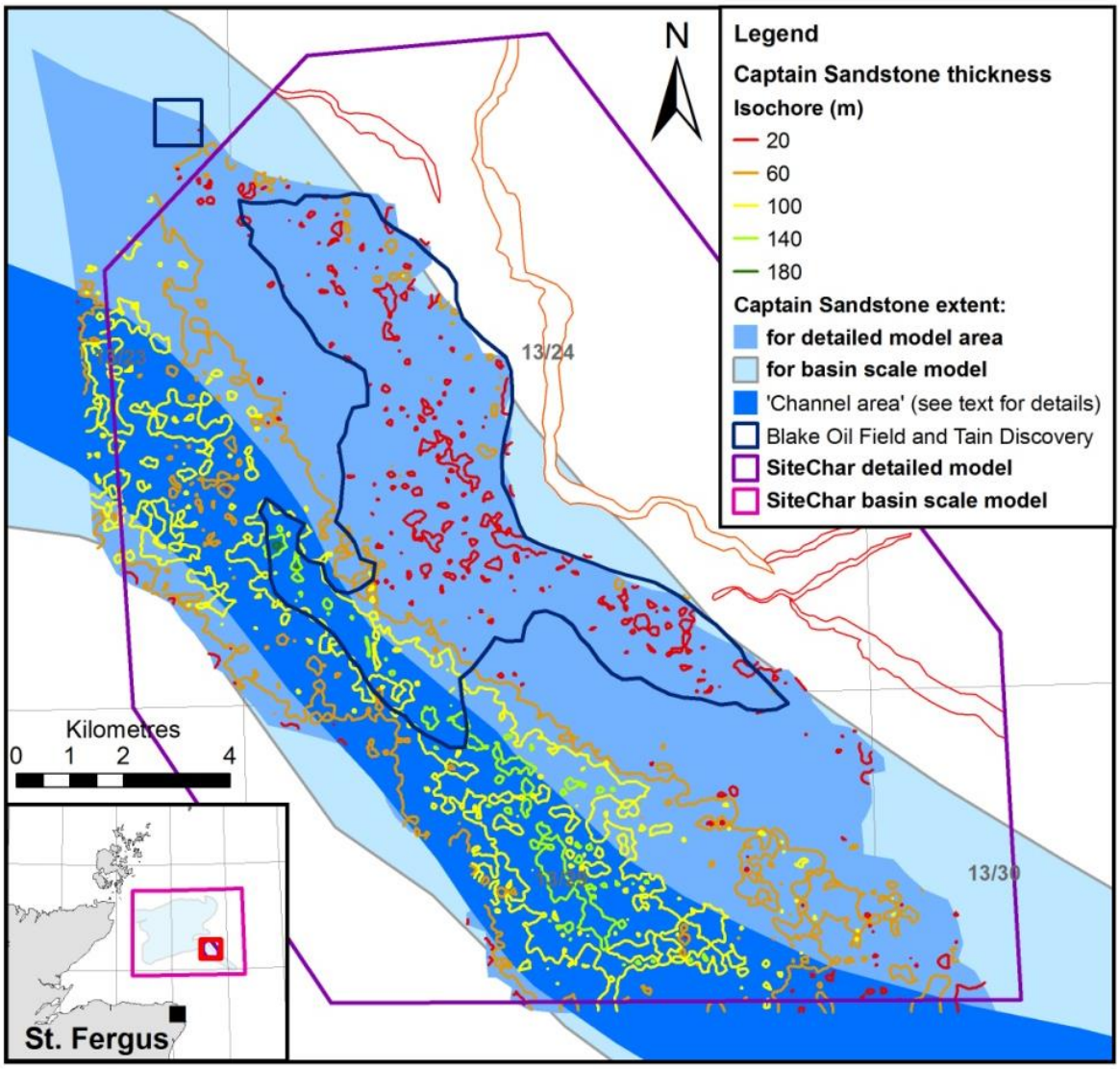


**Figure 10. Map showing Captain Sandstone extent, contours of thickness in metres and approximate location of 'Channel' (dark blue) and 'Flank' areas (remainder) in detailed model area.**

Interpretation of geophysical logs of twenty-three wells (including deviated wells) within the Blake Oil Field enabled porosity, permeability and NTG values to be derived for both Channel and Flank areas (Section 3.4 and Appendix 3). These log interpretations were compared to actual core measurements and are summarised and tabulated in Table 1 and Table A3.3, respectively. Porosity and permeability values taken from core analyses enabled attribution of the model with permeability values (Section 3.4; A3.7; Figure A3.25).

***The Channel area***

The 'Channel area' of the Blake Oil Field is interpreted to comprise a series of stacked and amalgamated channels that together form part of a major submarine channel system approximately 700 m wide and at least 6 km in length, with a NW trend (orientated from mapping of seismic data). The area has been drilled by wells 13/24a- 4, 6, 7, 7z & 13/29b- 6 as well as numerous development wells and the Captain Sandstone Member extensively cored (Figures 15a, b). The sandstone contains very few shale intercalations, which could be either remnant layers that were deposited in shallow depressions at times between the sand deposition episodes, or in addition modified by erosion as indicated by the presence of mud clast-rich sands. Therefore all these layers are assumed to have limited areal extent, and not forming significant baffles to flow. Porosity and NTG of Captain Sandstone in the Channel Area of the Blake Oil Field, derived from log interpretation, and average permeability from core measurement, is shown in Table 1 below.

| BLAKE OIL FIELD | Average NTG | Average effective porosity | Average total porosity | Average permeability |
|---|---|---|---|---|
| Channel area (15 wells) | 0.985 | 24.6% | 29.2% | 2324 mD |
| Flank area (5 wells) | 0.334 | 15.6% | 20.7% | 153.6 mD |

**Table 1. Summary of Net to Gross and porosity from log data and permeability from core measurement in the Channel and Flank areas of the Blake Oil Field. (derived from data in table A3.3).**

***The Flank Area***

The 'Flank Area' of the Blake Oil Field is interpreted to comprise deep-marine slope strata, dominated by mud deposition, but with minor amounts of thin-bedded sand and moderately thick-bedded sand deposited by low-density and high-density turbidity currents, respectively. The area has been drilled by wells 13/24b- 3, 13/24a- 5, 8, 8y and 8z. Evidence of sedimentary slumping, synsedimentary faulting and minor injection of sand have all been observed in core and Formation Micro Imagery (FMI) (Hilton and Morris, 2002). The reservoir architecture in the Flank area is complex. Hilton and Morris (2002) note that sandstone bodies recognised in flank wells are not laterally continuous. This is borne out by Du (2002) whose interpretation of Modular formation Dynamics tester Tool (MDT) analyses suggests that the reservoir is compartmentalised and/or layered, and cites:

- pressure difference both between Coracle Sandstone intervals in wells 13/24a- 8y and 13/24a- 5 and also the Captain Sandstone;
- over the same depth interval in two different wells, one interval oil-bearing, the other water-bearing suggesting faulting or structural heterogeneity;

This compartmentalization is fully in accordance with the depositional interpretation for a mud-rich deep marine environment. The episodic deposition places sand with oblong lensoid shapes, some possibly amalgamated, but generally with some separation laterally and vertically.

Porosity and NTG of Captain Sandstone in the Flank Area of the Blake Oil Field, derived from log interpretation, and average permeability, from core measurement, is summarised in Table 1 above and detailed in Table A3.3.

Attribution of the 'Basin-scale' Captain Sandstone saline aquifer has relied on the understanding of the Blake hydrocarbon field reservoir geology as described above.

**Sedimentological characteristics of the Captain Sandstone**

The Channel Area comprises a north north-west to south south-east oriented, 2 km-wide (possibly an incised valley) fairway filled mainly with deep-water massive sandstones. Within this fairway, good vertical and lateral continuity can be generally expected, whereas outside of the channel, rapid sand bed pinch-outs and increasing reservoir heterogeneity towards the east is possible. The deposition potentially resulted from long run-out high density turbidites, sandy debris flows and mud slumps. Hilton, 1999, identified nine lithofacies, namely structureless sandstone, parallel-stratified sandstone, cross-stratified sandstone, parallel-laminated sandstone, dewatered sandstone, slumped sandstone, mud clast-rich sandstone, argillaceous sandstone and silty mudstone.

The Flank Area consists of non-channelized sandstone lobes, which on lap the Halibut Horst (e.g. interpretation by Rose, 1999). These deposits probably represent slope apron-related deposition (Richards *et al*., 1998).

Overall, the Captain Sandstone comprises dominantly deep-water massive sandstones, bearing similarities with near base-of-slope deposition in sand-rich turbidite systems. The sedimentological characteristics and origin of such deposits are recently summarized by Stow and Johansson, 2000. These authors also list 70 case studies that consist of such strata. This list might be useful when looking for strata analogous to the Captain Sandstone.

The distribution of upper part (Rose *et al*., 2000) of the Captain Sandstone in particular is structurally confined (over part of Halibut Horst), which partially limits the usefulness of depositional analogies where this confined condition might not be represented. Apparently the half-graben topography, which was created by Jurassic tectonism (Rose *et al*., 2000) plays an important role in the distribution of Lower Cretaceous Sandstones in these basins.

The closest depositional analogies will be found from other deep-marine massive sandstone units (See Stow and Johansson, 2000 for examples). Intuitively, the best depositional analogies may be the similar Lower Cretaceous massive deep water sandstone from the Outer Moray Firth area, e.g. the Punt Sandstone; (Argent *et al*., 2000), Britannia Sandstone (Lowe and Guy, 2000). Other examples include outcrops of the Eocene Annot Sandstone in the French Alps, (Sinclair and Tomasso, 2002; Posamentier and Walker, 2006 for references) and Pennsylvanian Jackfork Sandstone in Arkansas (Olariu *et al.*, 2011). Figure 11 illustrates typical dimensions of massive sandstone units.

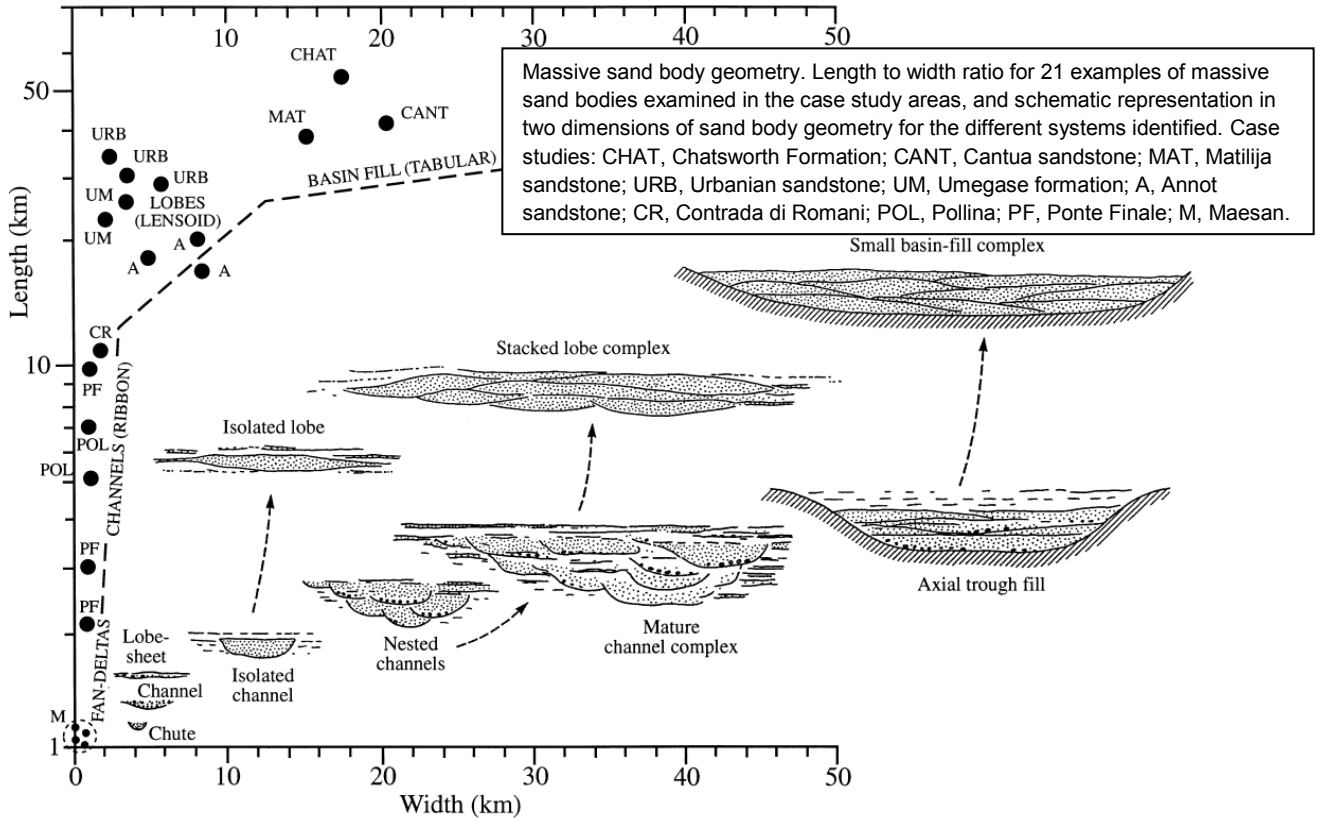


**Figure 11. Examples of dimensions of deep sea massive sandstone units, similar to Captain Sandstone system (from Stow and Johansson, 2000).**

## Formation pressures

A recent study (Munro, 2010) has shown that, regionally, the formation pressure in the Captain Sandstone aquifer is hydrostatic and that there is no observable pressure difference seen in different parts of the 'Basin-scale' 3D model. This suggests that over geological time-scales pressure has equalised over the area and that the Captain Sandstone aquifer may be described as an 'open system'. However, both the Captain and Blake Oil fields use water injection to ensure efficient production of hydrocarbons thus maintaining the pressure in these fields. This suggests that at short timescales the system may not be completely 'open'. In addition, within the Blake Oil Field it is anticipated that the variability in reservoir quality between 'Channel' and 'Flank' areas will mean that some parts of the reservoir are not in pressure communication over shorter timescales.

A geological well report from a well in the Cromarty Field, within the 'Basin-scale' 3D model area, notes pressure increases of over 100 pounds per square inch (psi) (approximately equivalent to 690 Pa), attributing the increase to water injection activities approximately 20 km distant. This corroborates hydraulic connectivity over at least this distance. It is expected therefore that pressure increases in one part of the Captain Sandstone aquifer could be felt in other areas. The spatial and temporal distribution of pressure as a result of $CO_2$ injection

will be assessed through dynamic modelling. In particular, effects on nearby resources (hydrocarbon production) will be studied. Pressure thresholds and an assessment of geomechanical stability will be investigated through geomechanical modelling.

**Lower Cretaceous succession- *the Storage Site seal***

The seal rocks to the storage site are the low permeability sedimentary rocks of the Rodby, Carrack and Valhall formations. The Valhall and Carrack formations are lateral equivalents to the Wick Sandstone Formation and form low permeability barriers between the different Wick Formation sandstone members as well as contributing to the top seal (Figure 3). The Carrack Formation, comprises non-calcareous, carbonaceous, pyritic, micaceous mudstone and siltstone. The Valhall Formation consists of interbedded calcareous and chalky mudstone and thin limestone (Johnson and Lott, 1993). The Rodby Formation, overlies the Carrack, Valhall and Wick formations, and comprises calcareous and chalky mudstone with occasional thin beds of argillaceous limestone (Figures 3 and 12).

For the Captain Sandstone seal, Min Jin *et al*. (2012), used permeabilites of between approximately $1x10^{-4}$ and $1x10^{-6}$ mD, with an average of $1.0x10^{-5}$ mD. For the Upper Jurassic Draupne Fm. (a deep marine shale, sampled at depth of 1057 m), Skurtveit *et al.* (2012), calculated effective $CO_2$ permeabilities at various pressure conditions producing a maximum value of $1.58x10^{-5}$, with average of $5.0x10^{-6}$ mD. For the Lower Cretaceous mudstone seal as a whole (top, lateral and base) the following values are recommended for the Storage Site seal rocks: minimum 0.00001 mD; maximum 0.001mD; mean 0.0001mD.

By comparison, a core from the Sleipner reservoir top seal of a silty mudstone, uncemented and plastic and generally homogenous provided the following information (Chadwick *et al*., 2008):

- Vertical intrinsic liquid permeability between 0.75 to $1.5x10^{-18}$ $m^2$ (~0.75 to $1.5x10^{-3}$ mD); these values sit between the recommended minimum and maximum values;
- Capillary entry pressure 1.7 MPa for super critical $CO_2$.

### 1.3.2 Upper Cretaceous and Palaeogene successions

If the injected $CO_2$ migrates out of the *Storage Site* and through its Primary seal, it will enter the Upper Cretaceous and Palaeogene sedimentary successions of the *Storage Complex*. The $CO_2$ will occupy voids, inter-granular or fracture porosity (secondary containment), and be restricted in further *migration* and ultimate *leakage* by a variety of storage mechanisms (Section 4) including *residual saturation* and *dissolution* and by secondary sealing. Dynamic modelling to be carried out in Task 3.2, led by IFPEN, will define the limits of the *Storage Complex.*

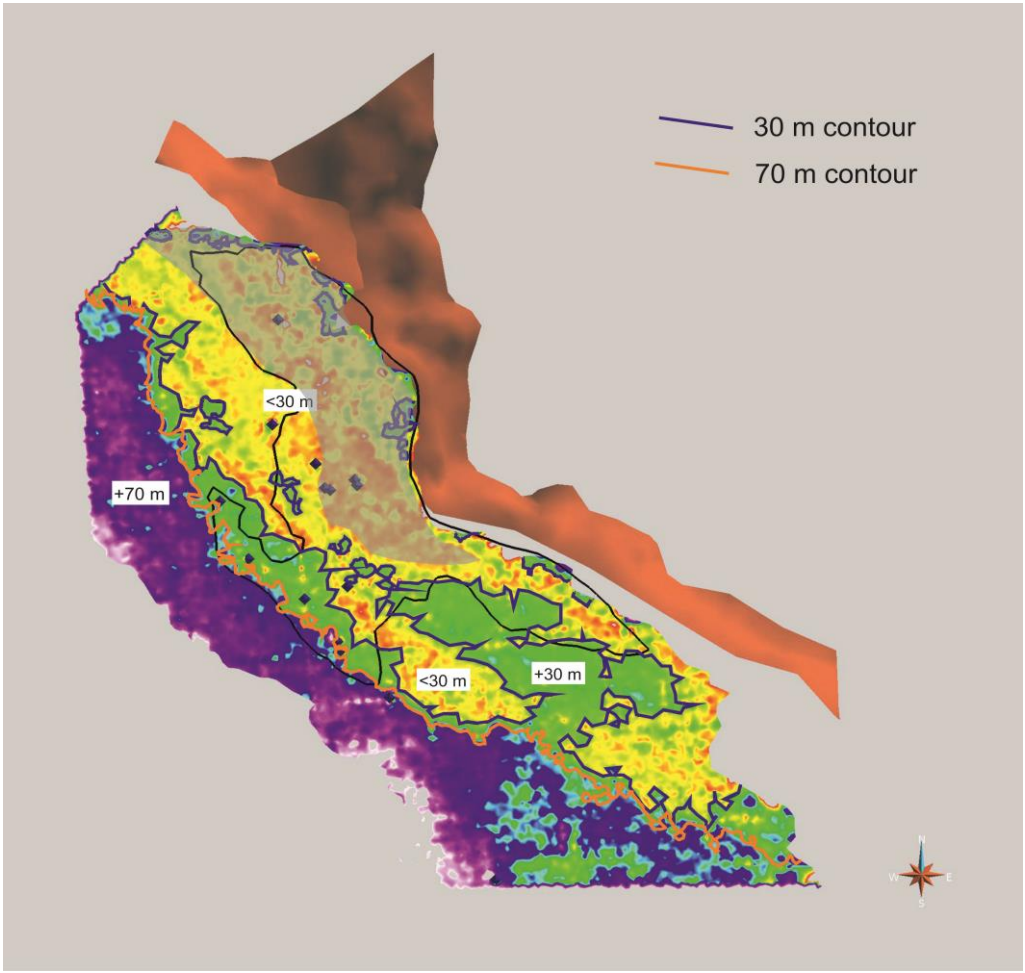


**Figure 12. Thickness map of the primary seal rocks (above and lateral to the Captain. Sandstone) in Detailed model area. Grey shading in north indicates area where seal is potentially less than 10 m thick.**

### Upper Cretaceous succession – *secondary containment or seal*

Upper Cretaceous lithologies within the 'Detailed' 3D model area have generally low porosity and permeability values. However, they could contribute to the secondary containment for any supercritical $CO_2$ migrating out of the *Storage Site* by exploitation of fracture porosity and permeability.

In the Outer Moray Firth area the Late Cretaceous comprises a thick succession of Chalk and Chalk-marl and the deposits represent the longest period of relatively homogenous sedimentation in the area. The Late Cretaceous and Palaeogene were times of little fault activity within an area undergoing post-rift subsidence. Neither sub-aerial dissolution of the chalk nor karst development is expected. In addition, a large number of fractures caused by structural deformation are not anticipated with matrix permeability expected to be dominant.

Horizontal permeability is likely to be greater than vertical permeability, perhaps by a factor of 10. Permeability values for the Chalk Group are quite variable, for example, as high as 7

mD in parts of South Arne Field in Danish sector of the North Sea but the field has an average matrix permeability of 1-2 mD (Mackertich and Goulding 1999). However, Megson and Hardman (2001) quote 0.01 to 0.5 mD as common values in the North Sea, these authors also highlight two efficient intra-Chalk seals, a tight zone at base of Ekofisk and the Plenus Marl shale.

For the Chalk as a whole, horizontal permeability values are recommended as follows: minimum 0.001mD; maximum; 1.0 mD; mean 0.01mD. A ratio of 5:1 horizontal to vertical permeability is suggested.

**Palaeogene succession – *secondary containment and seal***

Examination of the Palaeogene succession in wells within the *Storage Complex*, show that where data is available, substantial thicknesses (36 to 111 m) of potentially sealing rocks are present (Table 2).

| Well | Potential sealing formations (Fm.) and thickness | Potential sealing lithology |
|---|---|---|
| 13/23a- 4 | No available information above the Chalk Group | |
| 13/23b- 5 | No available information above the Chalk Group | |
| 13/24b- 3 | 71 m, Dornoch Fm., 111 m Mousa Fm. | Claystone and siltstone |
| 13/24a- 4, 5, 6 | No available information above the Chalk Group | |
| 13/24a- 7 | 36 m Dornoch Fm., 85 m Mousa Fm. | Siltstone and claystone |
| 13/24b- 9 | No available information above the Chalk Group | |
| 13/29b- 5 | >400 m undifferentiated strata above the Andrew Fm. | Claystone and siltstone (interpreted from Gamma Ray log through well casing) |
| 13/29b- 6 | 51m of undifferentiated strata above the Maureen Fm. sandstone | Siltstone and limestone |
| 13/29b- 7 | No available information above the Rodby Fm. | |
| 13/29b- 8 | No available information above the Chalk Group | |
| 13/29b- 9 | Palaeogene succession thickness is 975 m. The Maureen Fm. comprises 70.7 m interbedded claystone and limestone. The undifferentiated succession above contains thick claystone units. | Claystone |

**Table 2. Potential seal rocks in the Palaeogene succession from wells within the extent of the 'Detailed' geological 3D model.**

However, the lack of well information from the Palaeogene section means the character and thickness of seal rocks is difficult to quantify and where they are known to be present their age is not well known. Mapping the lateral extents of these potential seal rocks is

problematical as it is difficult to match seismo-stratigraphical sequences and seismic reflectors to the potentially sealing horizons due to lack of well time/depth data and lithological description. Seismic survey profiles of the Palaeogene succession show evidence of differential compaction over features interpreted as sand-prone channel deposits. These channels could form high-permeability pathways and so an increased risk *leakage* out of the $CO_2$ store. These risks will be investigated further in Task 3.4 of Work package 3 SiteChar.

## 2. BLAKE OIL FIELD DEVELOPMENT HISTORY

The Blake Oil Field is located 74 km north-east of the St Fergus gas terminal (Figure 1) in approximately 104 m water depth. The Blake Oil Field is located south of and immediately adjacent to the Halibut Horst (Figure 4). Its outline shape reflects in part the reservoir architecture of the field which comprises a North-west-trending amalgamated channel complex ('Channel Area') and associated 'Flank Area' (Figure 13). The Blake Oil Field covers an area of approximately 37.6 km$^2$ and mapped depth to top reservoir varies from approximately 1350 m TVDSS (True-Vertical Depth Sub Sea) in the north-east to a maximum of 1650 m TVDSS in the south-western part of the field (Figure A3.8). A detailed account of the Blake Oil Field production can be found in Appendix 2 of this report.

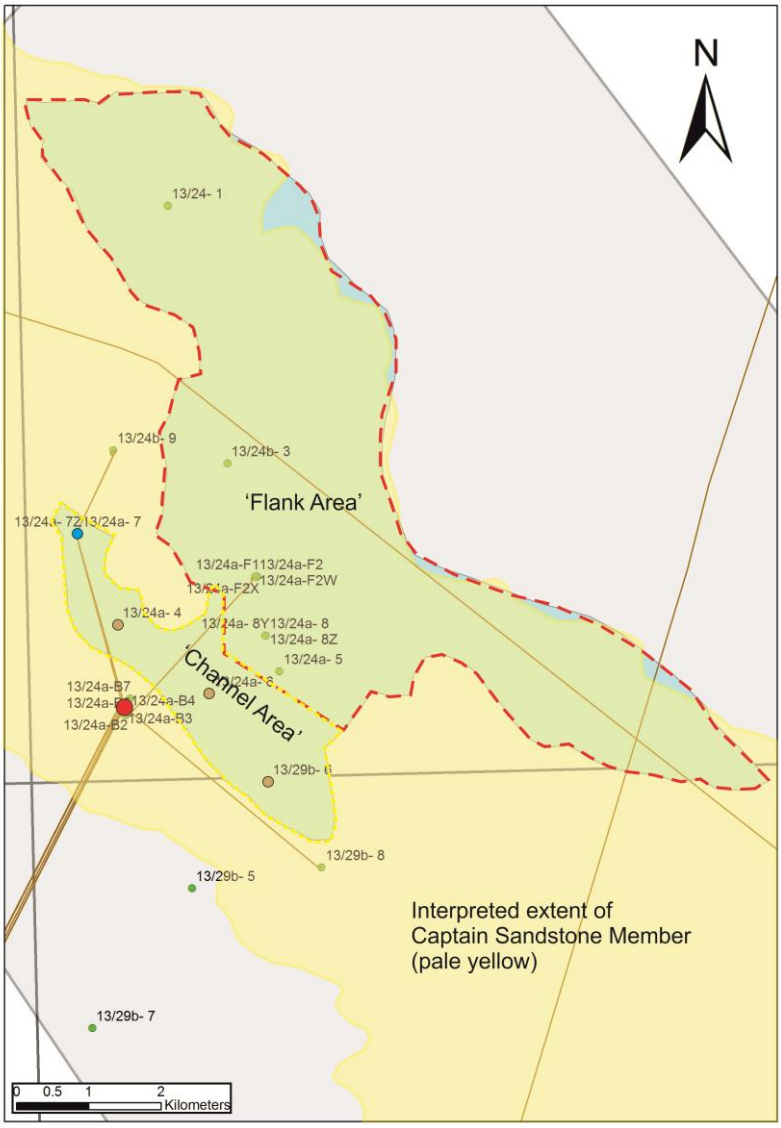


**Figure 13. The Blake Oil Field, showing outline shape (in green), well locations and pipeline configuration. Flank Area (dashed red line); Channel Area (dashed yellow line).**

## 2.1 Blake Oil Field discovery and appraisal

The Blake Oil Field was discovered in March 1997 by well 13/24b- 3 (Figure 15a) that proved the presence of hydrocarbons over an interval of 98.5 m that included a 68.3 m succession of the Captain Sandstone Member and 22.1 m succession of Coracle Sandstone Member separated by a 12.3 m claystone. A single Drill Stem Test (DST) perforated over the Captain and Coracle sandstones flowed more than 2600 barrels of oil per day (BOPD) of saturated oil through a 40/64" choke. Significant sand production was noted which limited the flow rate; a deeper sandstone, the Punt Sandstone Member, was water wet. The discovery was appraised by Well 13/24a- 4 (December 1997), that penetrated 84.4 m of Captain Sandstone and produced 3594 BOPD and 4.97 million standard cubic feet per day (MMscfd) of associated gas from a 44/64" choke. The Coracle Sandstone was present, but separated by a 95 m claystone succession and although moderate gas shows were recorded, no oil shows were present at this down-dip location. The Blake Oil Field was subsequently appraised by 3 further wells, 13/24a- 5, 6 and 8 (Figure 15a, b).

## 2.2 Blake Oil Field development and production

The Blake Oil Field has 36 well penetrations related to exploration, appraisal and development of the field. There are nine plugged and abandoned exploration and appraisal wells and the remaining 27 are development wells sidetracked from a series of 10 pilot holes and deviated to horizontal through the Blake reservoir (Figures 13 and 15a,b).

The Blake Oil Field produced around 14.7 million barrels (2.3 million cubic metres) of oil in its first full year of production (2002). Since then production has steadily declined to 4.7

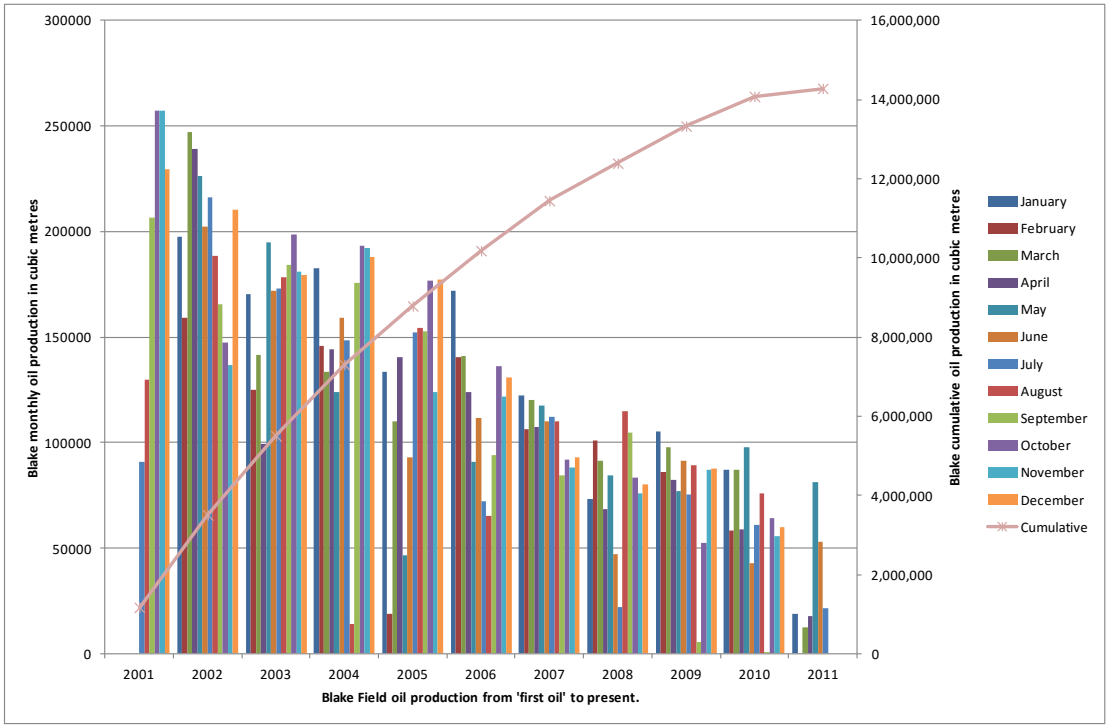


**Figure 14. Blake Field monthly and cumulative oil production in cubic metres to present day.**

million barrels (748,673 cubic metres) of oil in 2010; by contrast, the Captain Field (Figure 4) produced 13.5 MMBBLS of oil in the same year (Figure 14; Table A2.2). In 2010, the field also produced 93.9 million standard cubic metres of associated gas and 1.2 million cubic metres of water (Tables A2.2, A2.3, A2.4). The oil field has been developed utilising a total of 7 horizontal oil producers located at crestal locations supported by 3 water injectors located at the northern and southern ends of the field (Figures 15a and 15b). Producers were completed with sand screens to prevent ingress of sand to pipelines.

The Blake Channel and Blank Flank areas have been developed separately with 7 development wells (5 oil producers and two water injectors – wells 13/24a-7,7z and 13/29b-8) in the Channel area and 3 development wells (2 oil producers and one water injector – well 13/24b-9) in the Flank area.

***Blake Channel Area***

The Channel area of the Blake Oil Field is produced from five horizontal wells (13/24a- B1Z, B2Z, B3Z, B4 and B5, placed to sweep different parts of the amalgamated channel sandstone. The producers are supported by two water injectors, 13/24a 7 and 13/29b- 8 located at the northern and southern ends of the Channel area, respectively (Figures15a and 15b).

Well 13/24a- 7, was first of eight planned development wells. The pilot hole appraised the north-west corner of the field to confirm depth to top and base Captain and indicate reservoir quality, continuity and thickness; its sidetrack well13/24a- 7Z, was completed as a water injector.

Well 13/24a-B1Z was the first horizontal producer to be drilled in the Blake Oil Field and was spudded in June 2000. Well 13/24a- B2Z was placed to sweep the northern part of the field. The well penetrated top of the Captain Sandstone at 1570 m TVDSS. The well has a horizontal section of 1191.2 m. The well was drilled at an average distance of 10.4 m below an assumed Gas-Oil Contact (GOC) of 1576.4 m.

Well 13/24a- B3Z penetrated top of the Captain Sandstone at 1575.2 m TVDSS. The well has a horizontal section of 812.3 m and a net pay of 755 m. The well was drilled at an average distance of 11.6 m below an assumed GOC of 1573.7 m in a vertical corridor between 1584.8 m and 1585.6 m.

Well 13/24a-B4 was placed to sweep the central area of the Field. The well has a horizontal section of 1005.8 m and a net pay of 945.5 m. The well was drilled at an average distance of 13.4 m below an assumed GOC of 1572.0 m in a vertical corridor between 1587.0 m and 1584.6 m.

Well 13/24a-B5 (July 2000) pilot hole was drilled in a general north-west direction, placed to drain oil from the north-west end of the channelized reservoir in a region of greater geological uncertainty than in the Central Area. B5Z producer was drilled at an average distance of 14.6 m below an assumed GOC at 1571.1 m in a vertical corridor between 1585

m and 1586.2 m TVDSS. The horizontal section was 1006.4 m with net pay over oil leg of 940.9 m.

Well 13/24a-B6 (March 2001) was placed to drain oil from the south-east end of the Blake Channel area. The well has a horizontal section of 1155.2 m and a net pay of 1119.8 m. The well was drilled at an average distance of 12.0 m below an assumed GOC of 1571.8 m in a vertical corridor between 1583.0 m and 1585.5 m. B6 proved water saturations of 3.2% (gas zone) and 4.1 % oil zone. However, this well began to produce water. Well 13/24a- B7 was spudded in June 2007 as a sidetrack to 13/24a- B6 to try and remediate this. However, both B7 and subsequent B7z proved much thinner oil columns than expected (8.2 m and 5.5 m respectively. B7 proved water saturations of 3.7% (gas zone), 3.9 % oil zone and 70.8% (flushed zone). B7z proved water saturations of 4.6% (gas zone), 3.0 % oil zone and 71.3% (flushed zone).

***Blake Flank Area***

The Blake Flank is produced from two oil wells (13/24a-F1, F2) supported by a single injector well (13/24b- 9). Initially the development programme for the Flank area of the Blake Oil Field planned production of hydrocarbons from 2 wells, one targeting the Coracle sands (13/24a- F1) and the other targeting the Captain sandstone (13/24a–F2) (Figures 15a and 15b). A single injector well (13/24b- 9) would provide pressure support for both producer wells. The producer wells were drilled at a high angle to best sample the interbedded sand bodies in the Flank area of the field. Well 13/24a-F1T runs horizontally through the Coracle Sandstone between measured depths of 2292.5 m and 2529.5 m with a net pay of 159.5 m (porosity 23.7%, with a water saturation of 15%).

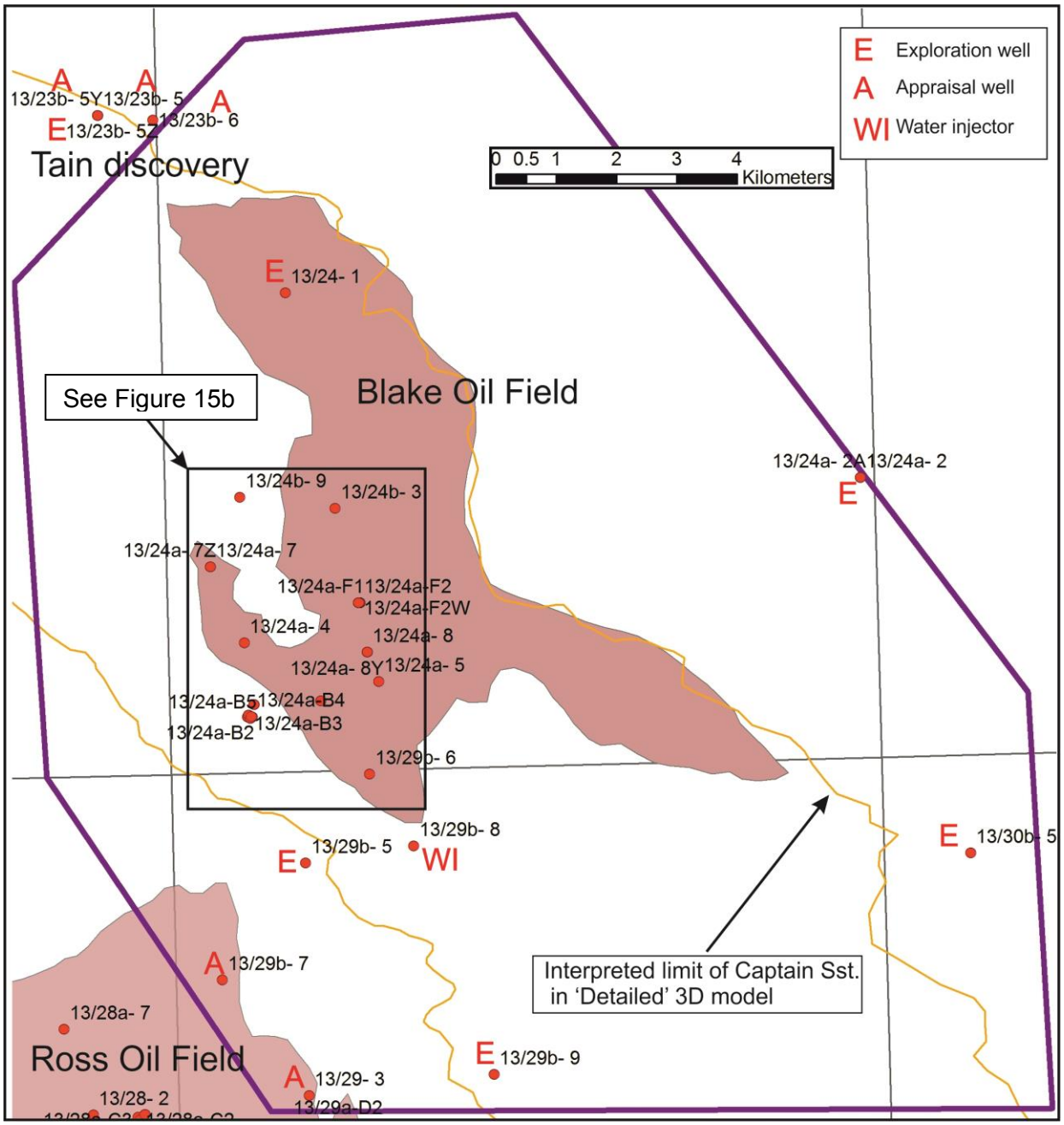


**Figure 15a. Original intent of all wells within 'Detailed' geological 3D model.**

However, the F2 well, although primarily targeting the Captain Sandstone also penetrated the underlying Coracle Sandstone and the F2 producer, Well 13/24a- F2W, also produces from the Coracle Sandstone. It is interesting to note that the F2 well proved an anomalously thicker section of Captain Sandstone that was interpreted as a channel that cut down into the underlying Coracle Sandstone. This observation emphasises the complex nature of the Blake reservoir and the potential tortuous connectivity of the sand bodies within it.

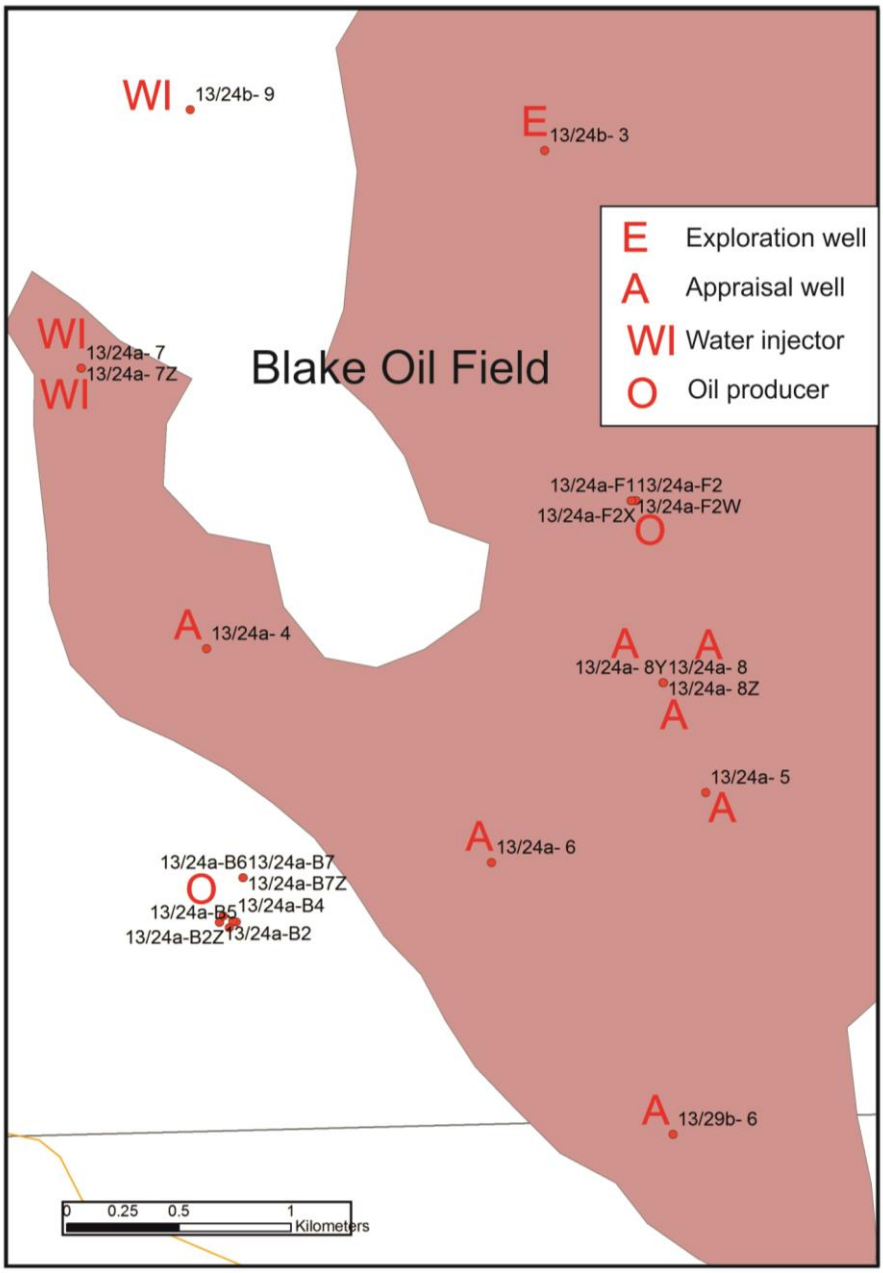


**Figure 15b. Inset from Figure 15a showing original intent of wells within part of Blake Oil Field.**

### Close of production

For this project, estimates of the year of close of production (COP) have been made independently of the current operator. Extrapolation of the yearly decreasing production values from the Blake Oil Field, plotted from data available on the UK Department of Energy and Climate Change website (https://www.og.decc.gov.uk/pprs/full_production.htm) show them to converge on a closure date of 2016. Estimates of Close of production (COP) for producing hydrocarbon fields depend upon a variety of factors, though oil price is a key parameter; the

higher the price the longer the potential field life (Figure 14). In a real licence application it is most likely that the operator of the field would be closely involved in the proposed change of use and COP would be precisely known. By the end of 2010, the Blake Oil Field had produced approximately 88 million barrels of oil (~14 Million $m^3$). Assuming the field produces 4 million barrels of oil annually, from 2010, for the next 5 years the final amount of oil produced would be around 108 million barrels of oil.

### 2.3 Summary of other producing hydrocarbon fields nearby

There are five producing hydrocarbon fields located in the 'Basin-scale' geological 3D model area (Figures 1 and 4; Table 3). The Blake Oil Field has been selected as part of the *multi-store* $CO_2$ storage site and forms part of the 'Detailed' geological 3D model. The Ross Oil Field produces from a deeper Jurassic reservoir and will not be in pressure communication with the Lower Cretaceous sandstones, specifically the Captain Sandstone, which will form the *Storage Site* for injected $CO_2$. Of the remaining three hydrocarbon fields, two, the Atlantic Condensate and the Cromarty Gas fields are located down-dip of the 'Detailed' geological 3D model (Figure 1). The Captain Oil Field lies in an up-dip position in the foot-wall of the West Halibut Fault (Figure 4).

| Hydrocarbon Field | Hydrocarbon reservoir | Ultimate recoverable reserves | Annual production (2010) | Start of production | Estimated close of production |
|---|---|---|---|---|---|
| Captain Oil Field | Lower Cretaceous, Captain Sandstone | 347 MMBBLS | 14.7 MMBBLS | 1997 | 2025 |
| Blake Oil Field | Lower Cretaceous, Captain Sandstone | 108 MMBBLS | 4.6 MMBBLS | 2001 | 2015 |
| Atlantic Condensate Field | Lower Cretaceous, Captain Sandstone | Not available | Not available | 2006 | Production ceased |
| Cromarty Gas Field | Lower Cretaceous, Captain Sandstone | Not available | Not available | 2006 | Production ceased |
| Ross Oil Field | Jurassic sandstone | Not available | 510 733 BBLS | 1999 | Not available |

**Table 3. Summary of hydrocarbon fields located in the 'Basin-scale' geological 3D model. (MMBBLS = million barrels).**

## 3. SUMMARY OF 'DETAILED' GEOLOGICAL 3D MODEL CONSTRUCTION

A range of technical issues need to be addressed to identify and define a *Storage Complex* and *Storage Site* to inform an application to regulators for a *Storage Site*. These activities are to be undertaken in a series of 5 tasks within SiteChar:

- Task 3.1 Construction of a static model of the storage complex;
  - building a structural model with geocellular grids;
  - population of model with petrophysical properties necessary for flow simulation of $CO_2$ in the rock succession;
- Task 3.2 Flow simulation of $CO_2$ injection into both hydrocarbon field and saline aquifer components of the *multi-store site*;
- Task 3.3 Geomechanical and geochemical stability assessments;
- Task 3.4 Assessment of containment risks;
- Task 3.5 Design of monitoring plan and development of a Framework for Risk Assessment and Management.

This section summarises the construction of the static geological 3D models in Task 3.1; a detailed account with additional figures is given in Appendix 3 of this report.

1. A regional 'Basin-scale' static geological 3D model of the Captain Sandstone aquifer was built in an earlier study and made available for this project (Scottish Carbon Capture & Storage, 2011);
2. The 'Detailed' geological 3D model includes the Blake Oil Field and sits within the extents of the 'Basin-scale' 3D model (Figures 1 and 4).

The Storage Site and Complex will be defined through subsequent modelling work in Task 3.2. At this stage, any deductions have come from geological knowledge using the following evidence base and available data. This is referred to throughout the text. In general, values for rock thickness, static capacities etc in the region of the Storage Site have come from data within the detailed model, unless otherwise indicated. The static geological 3D models have been attributed with data acquired for hydrocarbon exploration and production and an account of this is given below.

### 3.1 Seismic interpretation

Construction of the 'Detailed' geological 3D model utilised a 3D seismic survey, a small number of 2D seismic profiles and a comprehensive set of information from oil and gas exploration and production wells (Figure 2). The 'Detailed' geological 3D model comprises six stratigraphical surfaces: Sea bed; Top Chalk; Base Chalk; Top Captain Sandstone; Base Captain Sandstone; and Base Cretaceous (Figure 7).

The seismic reflectors marking the surfaces were identified and then interpreted in two-way travel time (TWTT) from the seismic data constrained by the well information (Figure 16). Faults were also interpreted from the seismic data and correlated between successive seismic sections in order to identify trends and quantify the magnitude of displacements between the different surfaces. The TWTT information was converted to depth using a

velocity model constructed from well information from within the 'Detailed' geological 3D model area. The methodology and data sources used to achieve this are detailed in Appendix 3. Appendix A3.2 describes the specific seismic picks of each stratigraphical surface.

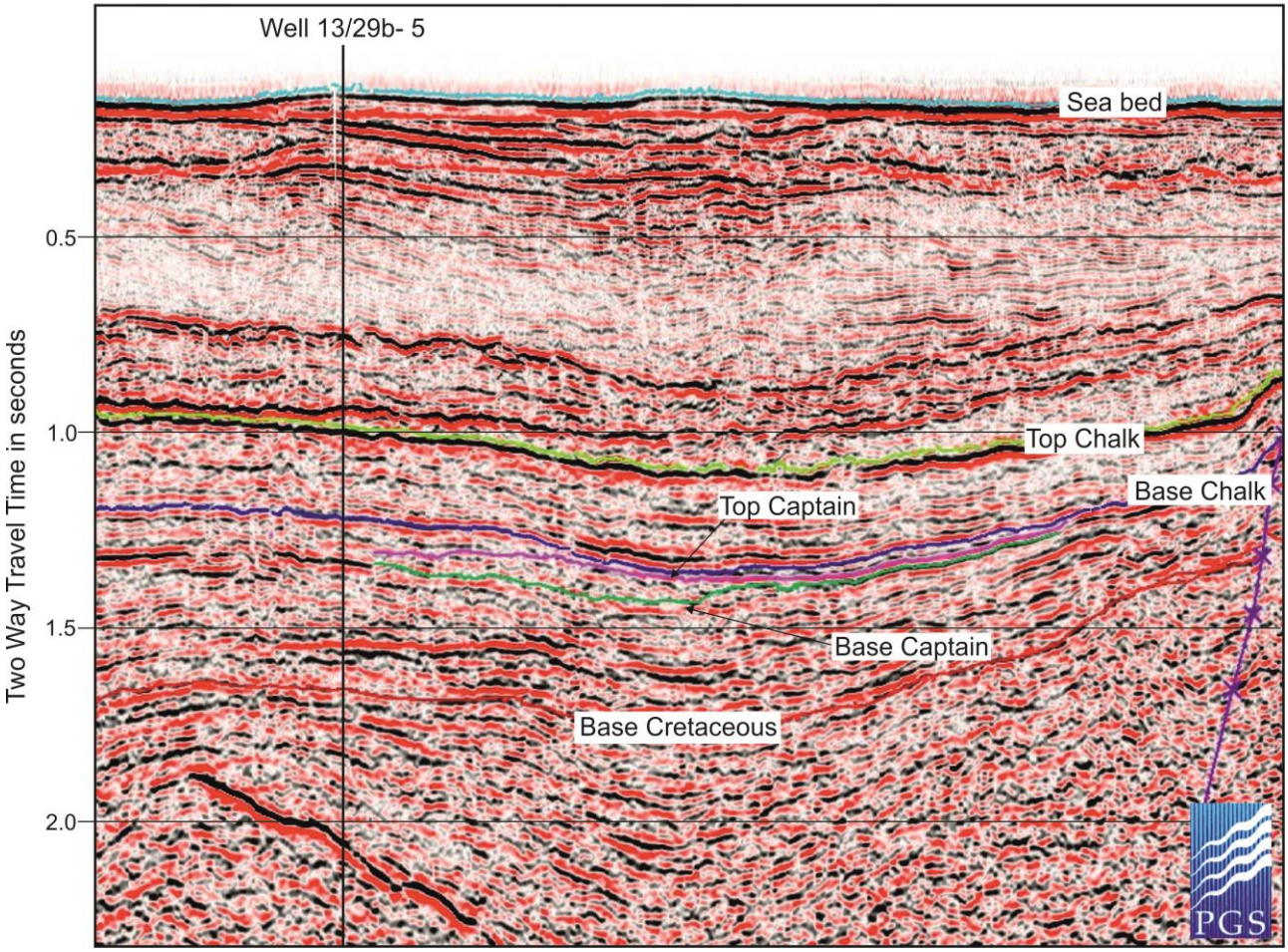


**Figure 16. Seismic profile showing example of seismic reflectors interpreted to construct surfaces for model.**

### 3.2 Construction of the gridded model surfaces

The 'Detailed' model includes an area of approximately 18 by 16.5 km encompassing the Blake Oil Field, the adjacent south-central part of the Halibut Horst and the block-bounding West Halibut Fault System. The regional stratigraphical surfaces were modelled to a 100 m average density triangular mesh and the Captain Sandstone to a 50 m mesh (the greater the density of the mesh, the finer level of detail that the surface can reproduce). The 4 stratigraphical horizons interpreted from the seismic data and Top Captain and Base Captain surfaces were modelled in the GoCad™ workflow. No post-processing smoothing operations

were run. Two planar surfaces were created to emulate the Oil-Water and Gas–Oil contacts published for the Blake Oil Field at 1607 m and 1578 m below sea-level, respectively.

GoCad™ solid (tetrahedron) objects were created from the calculated isopach property mapped for the Captain Sandstone and the primary seal of the Rodby, Carrack and Valhall formations, to determine gross volumes. A third object was created for the Captain Sandstone above the Blake Oil Field oil-water contact to allow calculation of the modelled closure volume of the oil field.

Standard GoCad™ workflow methodology was employed.

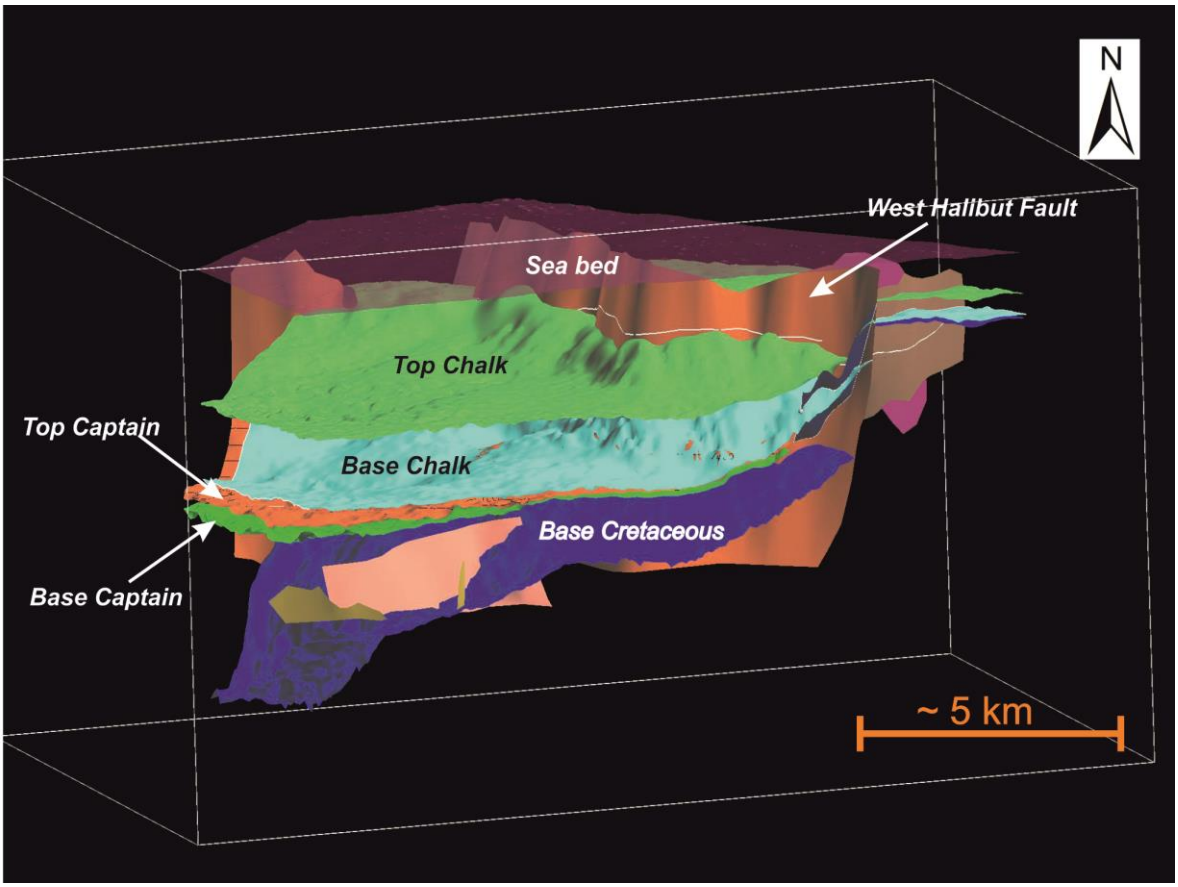


**Figure 17. GoCad™ image of the 'Detailed' geological 3D model.**

### 3.2.1 Faults

Fault polygons were created by interactively editing the curves outlining the extent of individual fault data sets.

The main segment of the West Halibut Basin Fault Zone, which largely defines the boundary between the Halibut Horst and West Halibut Basin, was modelled in two parts. The two faults merge in a conspicuous ramp or transfer zone across the northern part of the model. Fitting of the fault surfaces to the stratigraphical surfaces was achieved within the GoCad™ workflow. Manual editing was also required to achieve a well integrated fit. Subsidiary faults

were modelled within, and at the margin, of the basin, as well as a cross-cutting set defining a small graben feature, inset into the Halibut Horst (Figures 17, A3.7).

No faults were modelled as cutting or bounding the Captain Sandstone.

### 3.2.2 Merging the 'Basin-scale' and 'Detailed' geological 3D models

Slight modifications to the westerly subcrop boundary of the Captain Sandstone and re-fitting of major faults of the regional 'Basin-scale' model, provided from the earlier Scottish Carbon Capture & Storage study, were carried out. The 'Detailed' geological 3D model was merged into the Captain Sandstone 'Basin-scale' 3D model using GoCad™ utilities. Simulation of $CO_2$ injection into the merged model will predict how the injection of $CO_2$ into the hydrocarbon field store would affect the wider connected Captain Sandstone saline aquifer in the proposed *multi-store site* and vice versa. Merging methodology and results is described in Appendix A3.5.

Two static geological 3D models were created:

1. A merged regional 'Basin-scale' and local 'Detailed' geological 3D model;
2. A separate 'Detailed' geological 3D model.

## 3.3 Construction of the geocellular model and flow simulation grids

GOCAD-SKUA - Paradigm™, which is software devoted to the integration of surface and sub-surface data was used in order to build complex structural models and 3D geocellular grids for different purposes including fluid flow simulations. See Appendix 3 for a more detailed description of principles and methodology.

### 3.3.1 Structural modelling

The modelling process began with the creation of the fault network (Figure A3.18) that accommodated all fault relationships present in the area. The initial fault modelling has an impact on final grid quality and must be carried out with care. The next step consisted of modelling the six interpreted horizons, Sea bed, Top Chalk, Base Chalk, Top Captain Sandstone, Base Captain Sandstone and Base Cretaceous using GOCAD-SKUA - Paradigm™ software (see Figures A3.19, A3.20, A3.21, A3.22). Note that the Base Captain surface extends across the 'Detailed' 3D model area, mapped from well data, to enable closure of the Captain Sandstone volume within the GoCAD™ model.

From this surface model, the 3D grids are then generated automatically with very little additional input. The same structural model can be used to generate several customised 3D flow simulation grids at local scale (an area that includes the 'Detailed' geological 3D model) or at regional scale (Figure 18) using all the layers or a subset of layers around the targeted reservoir.

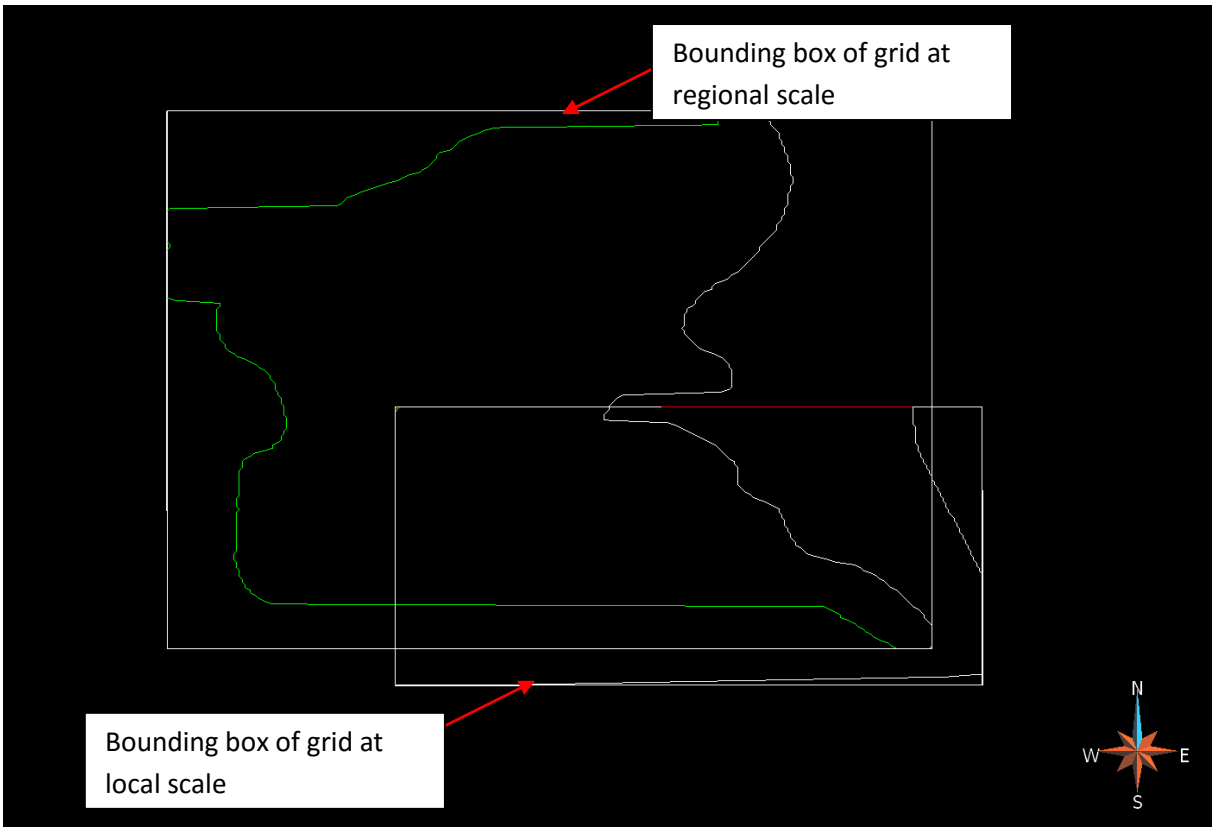


**Figure 18. Bounding boxes of regional and local grids defined on the same structural model.**

### 3.3.2 Flow simulation grids

The flow simulation grid at the 'Basin-scale' regional model is built to study the temporal evolution of the pressure field during $CO_2$ injection. The flow simulation grid at the local scale that includes the 'Detailed' geological 3D model aims to follow all the dynamic parameters during the lifespan of the geological *Storage Complex*.

At this stage all the structural elements are in place to easily generate fluid flow simulation grids. Standard parameters for this are the area of interest, the stratigraphical units, the orientation of the grid and the grid resolution. In this study, in order to speed up fluid flow simulations, the recurring theme was for both local and regional models not to exceed a maximum of 100 000 active cells.

For the 'Basin-scale' model, the grid comprises only the Top Captain Sandstone unit divided into nine layers with grid cells oriented parallel to bounding box (Figure 19). The cell dimensions in the XY plane are 400 by 400 metres. The vertical cell size is variable but the median value is around 40 metres. Since grid orientation is parallel to the bounding box axis, the faults are represented as stair steps in the grid (Figure 20). The regional Top Captain Sandstone grid parameters are given in Table 4 below.

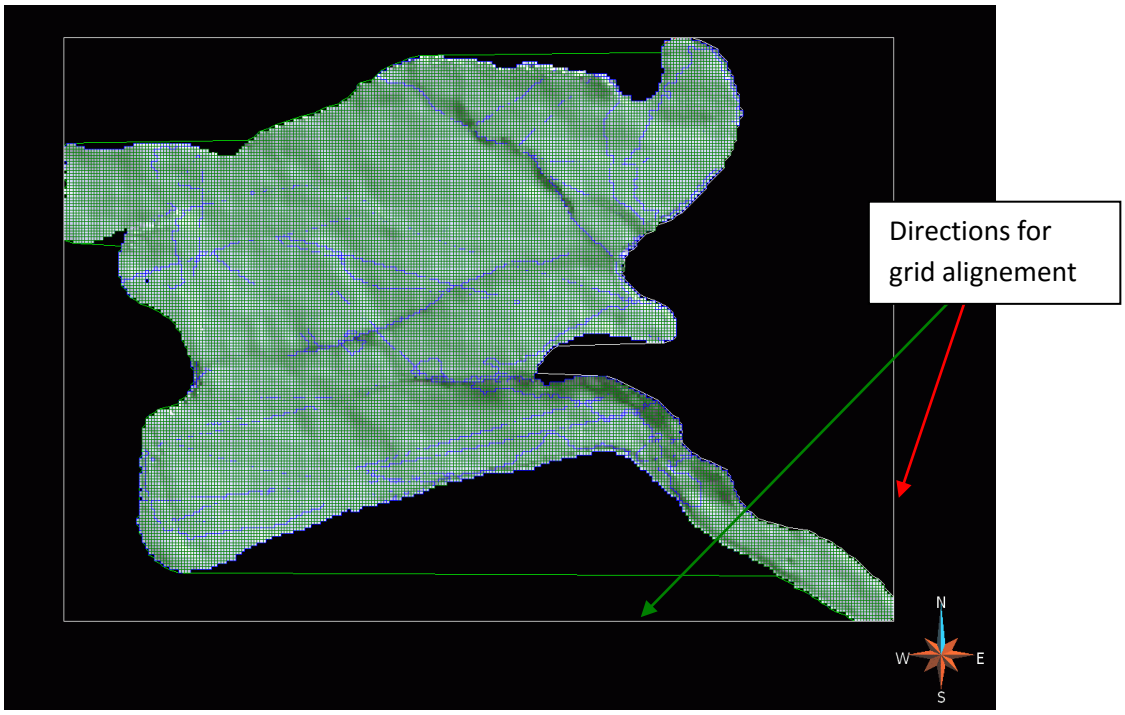


**Figure 19. Grid cells are parallel to red and green axes.**

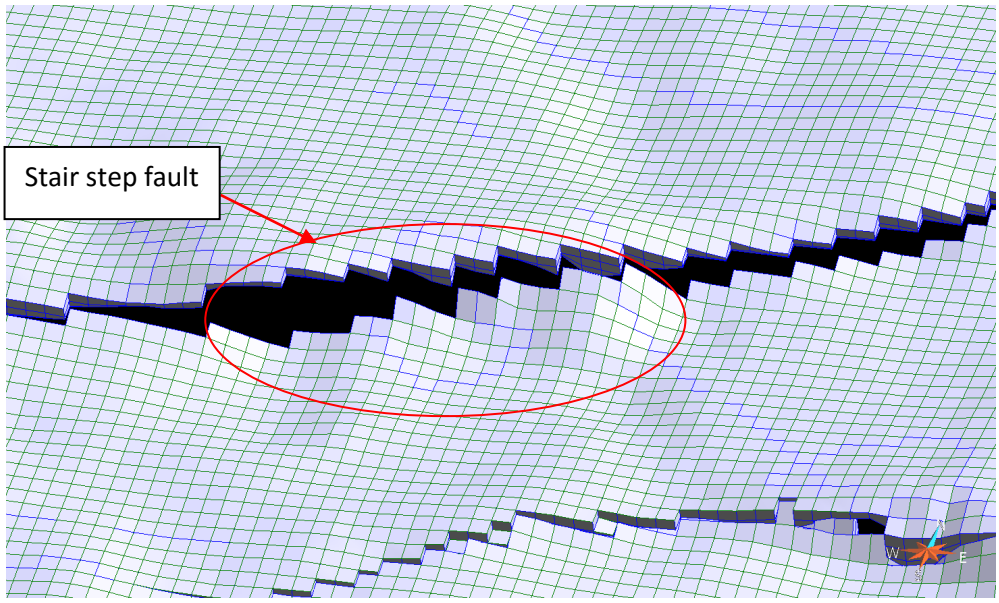


**Figure 20. Illustration of stair-step fault.**

As with the 'Basin-scale' regional grid, the 'Detailed' local grid (geological *Storage Complex* scale) is aligned on the bounding box azimuth and also generates stair-step faults (Figure 21).

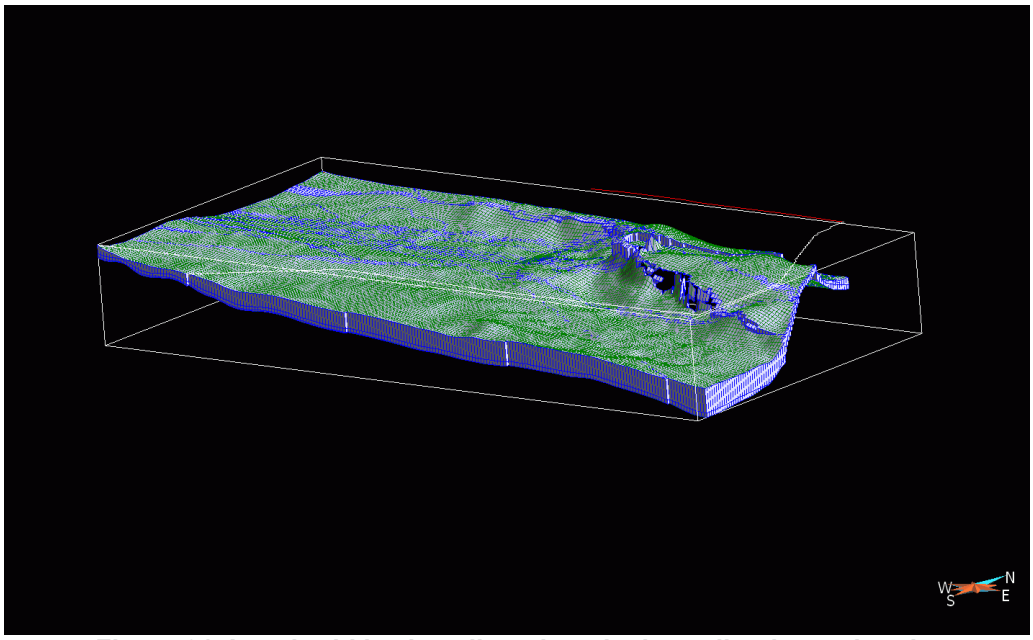


**Figure 21. Local grid is also aligned on the bounding box azimuth.**

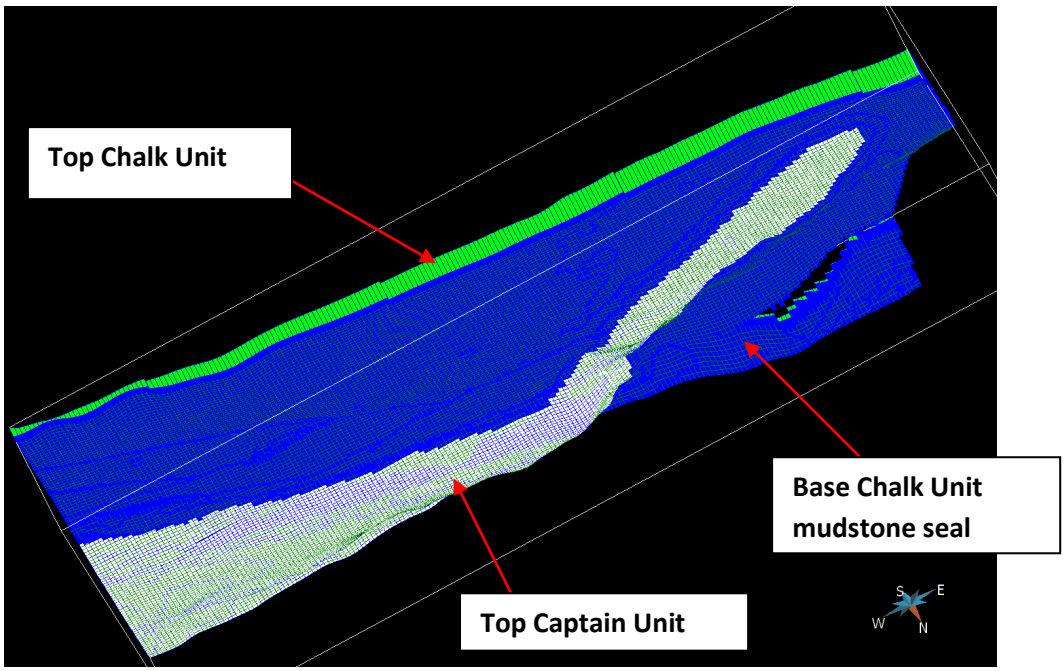


**Figure 22. Bottom view of the local grid in order to visualize the three units.**

The local grid is composed of three stratigraphic units from Top Captain sandstone to Top Chalk (Figure 22):

1. Top Captain Sandstone unit (reservoir): cell thickness median value is around 42 meters with a maximum of 4 layers;

2. Base Chalk unit (mudstone, seal): cell thickness median value is around 62 meters with a maximum of 3 layers.
3. Top Chalk unit: cell thickness median value is around 289 meters with a maximum of 2 layers.

The 'Detailed' model grid parameters are given in Table 4 below.

| GRIDS SPECIFICATION | Regional grid | Field scale grid |
|---|---|---|
| Number of cells along i: | 293 | 211 |
| Number of cells along j: | 230 | 101 |
| Number of cells along k: | 28 | 35 |
| Total number of cells: | 1 886 920 | 745 885 |
| Number of active cells: | 80 610 | 71 784 |
| Property alignment: | Cell centred | Cell centred |

**Table 4. Summary of grid specifications for the 'Detailed' model.**

### 3.4 Wells and logs

A total of 45 wells, both vertical and deviated were loaded into the GoCad™ project including the Blake Oil Field 'B' and 'F' platforms. Stratigraphical marker surface intersections from well data were entered manually. Associated well permeability geophysical log data for the Captain Sandstone Member were imported directly from available digital (LAS format) files.

#### 3.4.1 Well interpretation - Porosity, permeability, NTG – data for attribution of model

Attribution of the 'Detailed' geological 3D model for the dynamic modelling of $CO_2$ injection is by incorporation of measured and interpreted values. The variation in rock porosity, both effective and total porosity, was interpreted from geophysical well logs also from analyses of samples from core. Net sandstone To Gross thickness (NTG), a measure of the proportion of sandstone, was also interpreted from geophysical well logs. Permeability variation was derived from the relationship between measured porosity and permeability values of core

taken from wells within the extent *Storage Complex* and from selected wells in the wider basin-scale model. Detailed methodology for interpretation is described in Appendix A3.6.

### 3.4.2 Well interpretation for porosity and 'facies' attribution

Twenty three wells with suitable geophysical logs were available over the Captain Sandstone Member within the 'Detailed' geological 3D model (Figure 23). In addition, seven wells also within the Captain Sandstone Member, but outside the 'Detailed' 3D model area were also interpreted to enable attribution of the 'Basin-scale 3D model (Figure 23). The logs were analysed in 'Interactive Petrophysics' (IP) software (Version 3.6.2010.399, Senergy Software Limited). Core plug porosity and permeability data was also available for some wells and this was used to compare with log interpretation-derived porosities and also to inform the population of the model with permeability values.

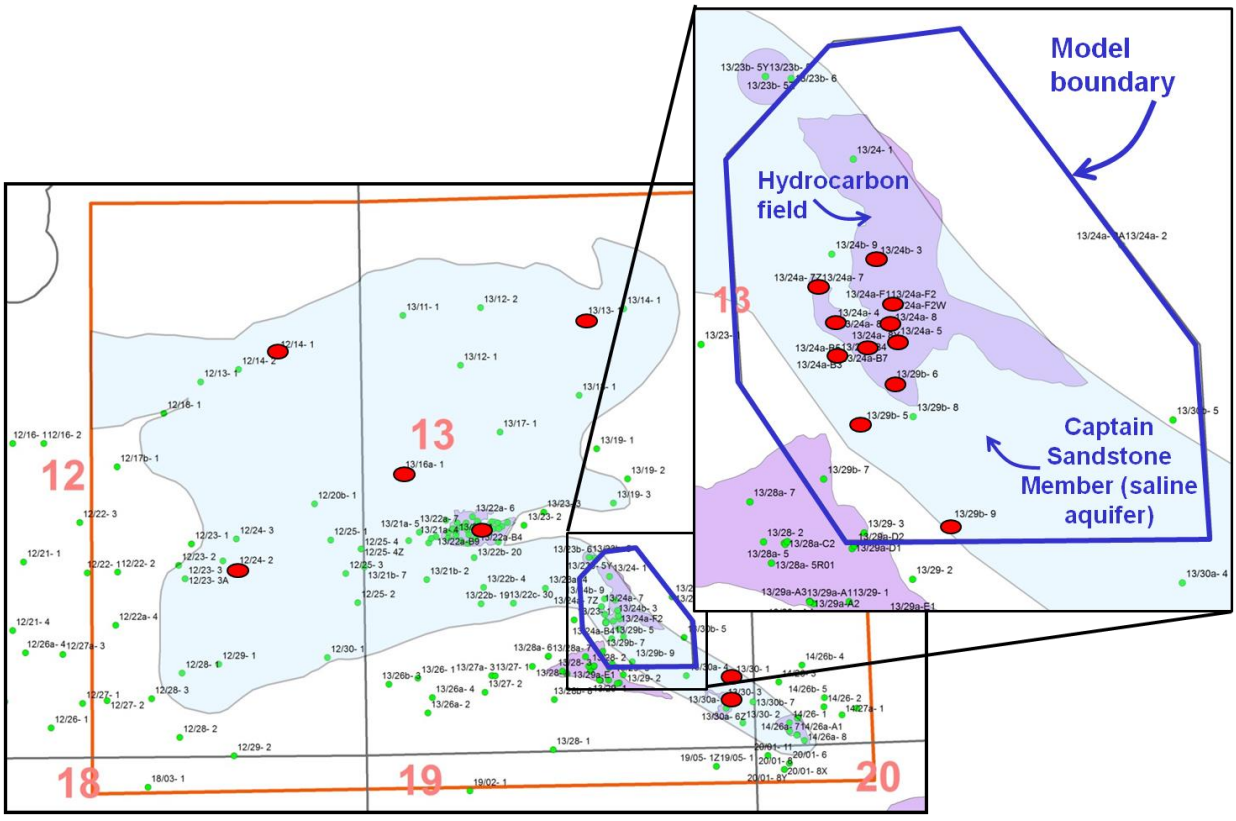


**Figure 23. Map showing locations of wells within the project area. Those interpreted are highlighted in red (and listed in Table A3.3). Note that limit of Captain Sandstone Member within detailed model is from regional model and not the new interpretation.**

### 3.4.3 Log curves, assumptions, quality & corrections

Available well logs include Natural Formation Gamma Ray (GR), sonic transit time, density and neutron logs. Different geophysical log curves were available for different wells and log data was acquired using various tool ages, tool types, conveyance methods and collected at different times. The interpretation methods described here were therefore adapted according

to well logs and data quality available. Areas of poor log quality were identified where possible and discarded.

### 3.4.4 Interpretation to produce a lithological log

A simple, discrete lithological log with a two-fold subdivision was produced for each well to help inform the modelling of 'facies' (Figure A3.24). This was based on an interpreted 'Shale Volume ($V_{sh}$)' log. Input curves were the GR or density-neutron curves (where available).

### 3.4.5 Porosity

Total and effective porosity curves (PHIT and PHIE, respectively) were calculated from the sonic or density-neutron log curves. Areas where density–neutron log quality is poor were identified using the density correction curves and/or calliper curves. Over logs sections where log quality was poor the porosity curve was computed from the sonic log. Some wells had no density-neutron log available and in these instances, the porosity was computed using the sonic log.

The continuous porosity log curves were output from IP software as LAS format files in readiness for import into GoCad™ modelling software.

### 3.4.6 Permeability

No suitable curves were available to calculate log-derived permeability values. Therefore, the relationship between porosity and permeability in core plug samples were used.

Core data was available for seven wells, six within the 'Detailed' geological 3D model area and one adjacent to it.

## 3.5 Population of flow simulation grids with petrophysical properties

The generated grids were populated with petrophysical parameters, mainly porosity ($\Phi$) and permeability (K). Porosity is expressed as a percentage or a fraction and permeability is expressed in milliDarcy (mD).

Without any available stratigraphic correlations in the Captain Sandstone reservoir, the model was populated using a porosity distribution derived from core analyses taken from wells that penetrated the Captain Sandstone reservoir (Figure 24).

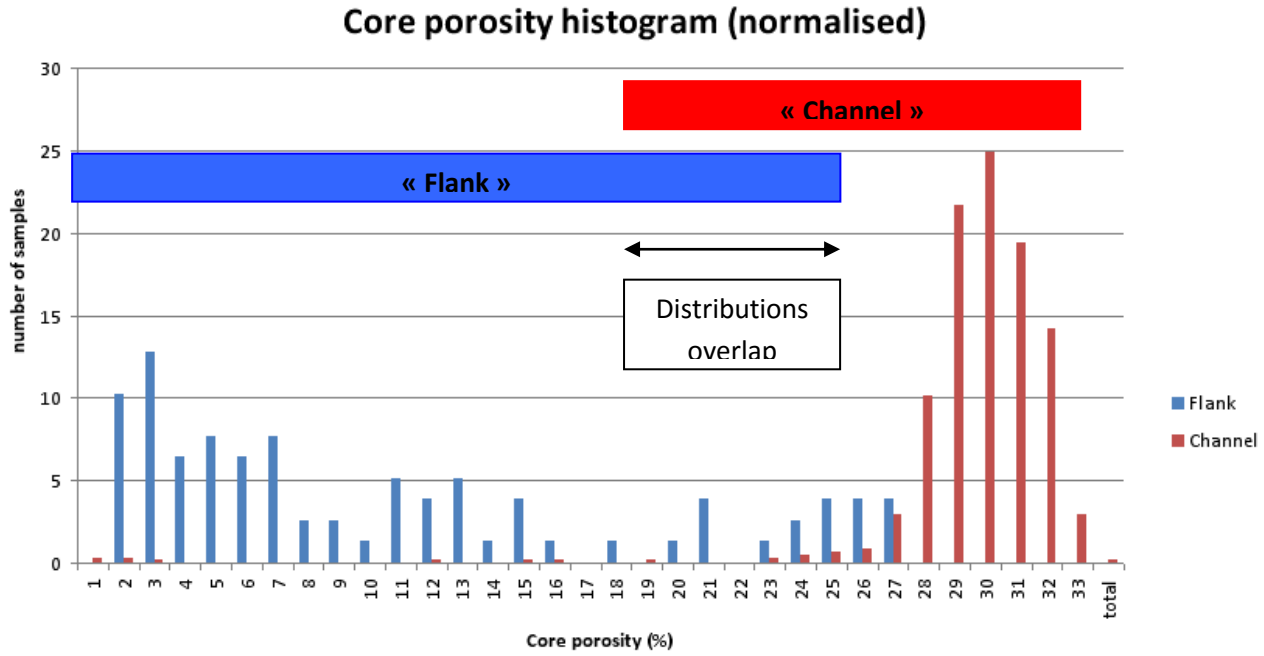


**Figure 24. Porosity distribution from core data and regionalisation (red bars – all data points from Channel facies, blue bars - all data points from Flank facies).**

Understanding of the Blake reservoir geology in terms of the spatial distribution of petrophysical properties, from knowledge of the seismic and well data, enables extrapolation to the wider Captain Sandstone saline aquifer at regional scale. The Blake Oil Field reservoir has been divided into two distinct areas (see Section 1.3.1) whose facies association reflect this range of depositional processes:

- the Channel area in the down-dip, south-western part of the field,
- the Flank area up-dip to north-east.

This geological interpretation informs population of petrophysical attributes over the entire Captain sandstone Regional extent (Figure 25).

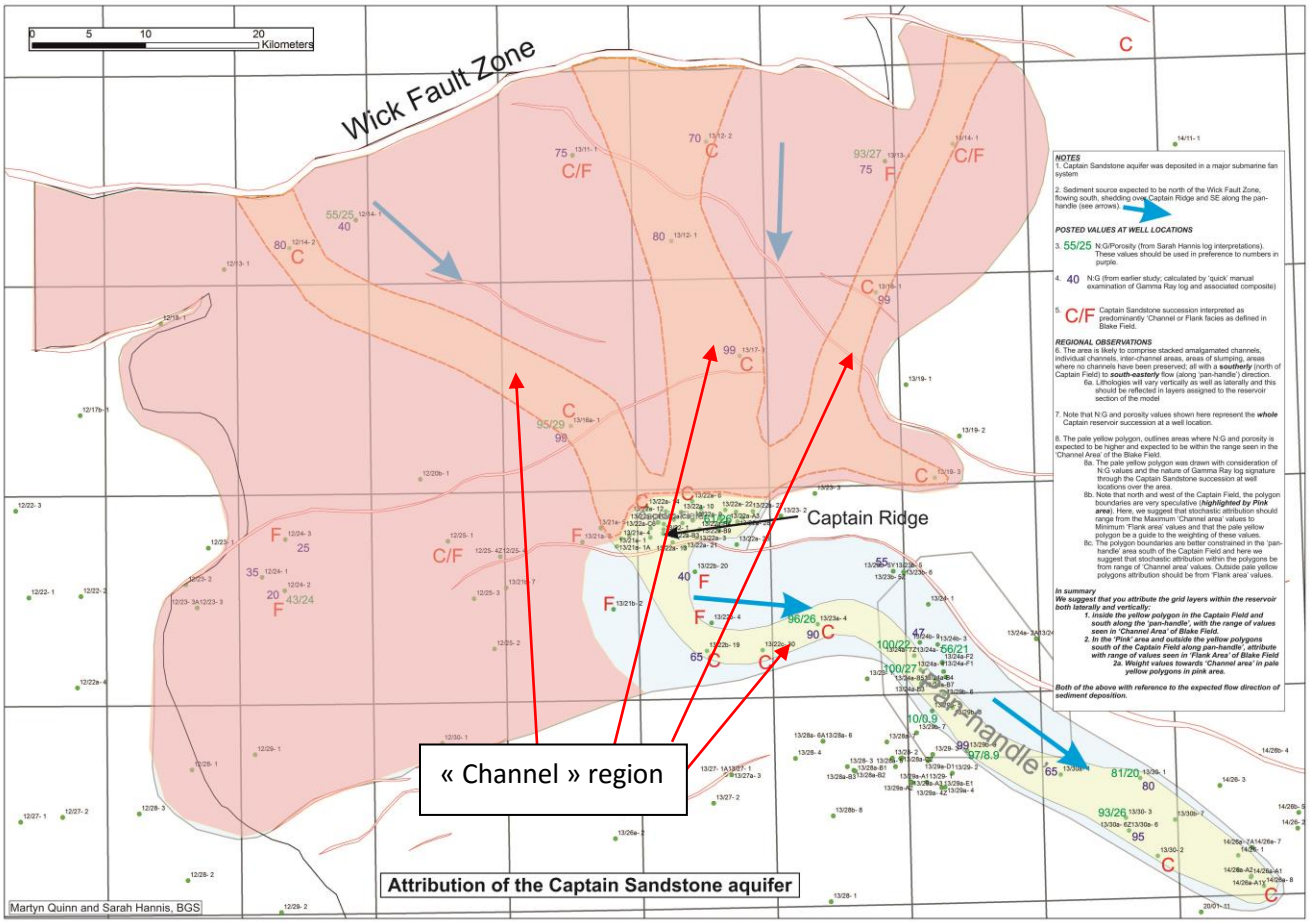


**Figure 25. Regional character of the Captain Sandstone based on geological knowledge.**

Assuming that the porosity distribution derived from core data available for this project is representative of the porosity distribution at basin scale, the method used to populate the reservoir grid aims at respecting this distribution. Most of modelling software offers the possibility to populate the grids using customised scripts. This was applied successfully to Channel and Flank areas as shown in Figures 26 and 27.

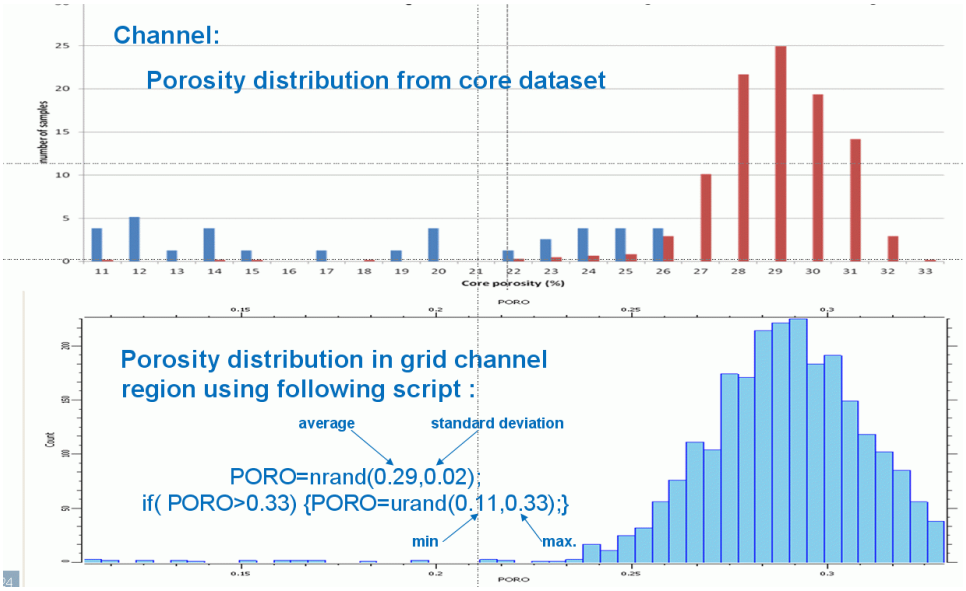


**Figure 26. Porosity distribution comparison between core measurements (top) and grid attributes (bottom) in the Channel area (red bars – all data points from Channel facies, blue bars - selection of data points from Flank facies).**

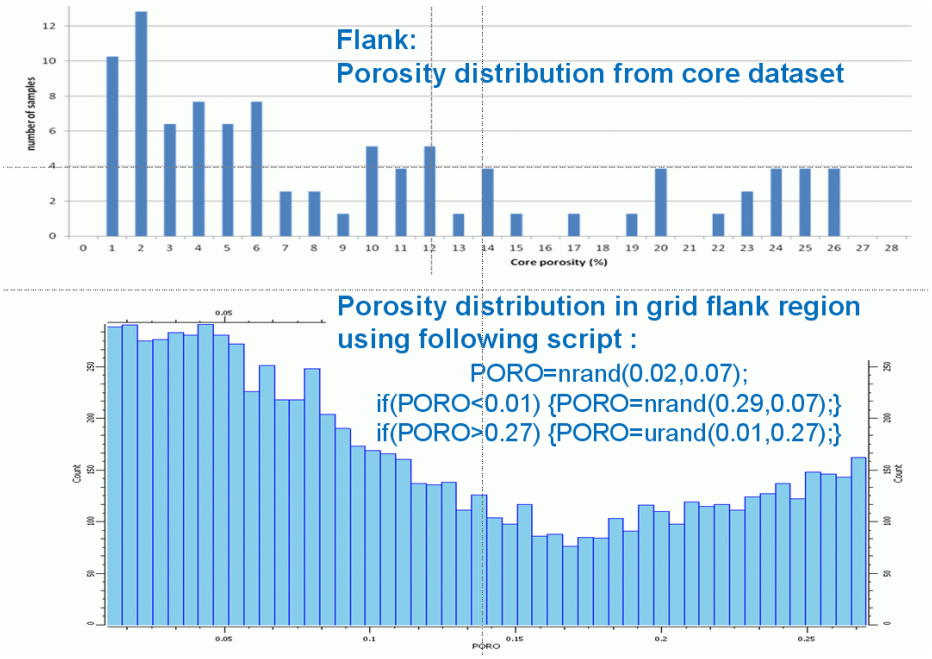


**Figure 27. Porosity distribution comparison between core measurements (top) and grid attributes (bottom) in the Flank area (blue bars – all data points from Flank facies).**

The two scripts used in this study for grid porosity distribution are described in Appendix 3. They allow us to quickly populate the grids in a very simple and efficient way. For more detailed studies, porosity values at the wells could be easily honoured with this method.

### 3.5.1 Porosity distribution

Facies description from well logs in Channel Area is binary. This unit is mainly composed of one reservoir facies (sandstone) associated with one non reservoir (shaly facies). Without any information on stratigraphic correlations in this reservoir (which is a typical issue associated with a turbiditic depositional environment), a purely stochastic process has been used, respecting as a constraint the core porosity distribution.

This way of populating the grid doesn't give the most realistic result in terms of the geology but gives properties distributions which are statistically representative of existing input data. Identification of Channel and Flank regions leads to a spatial regionalisation which is directly related to petrophysical values distribution (Figures 28 and 29; also Figures A3.27, A3.28).

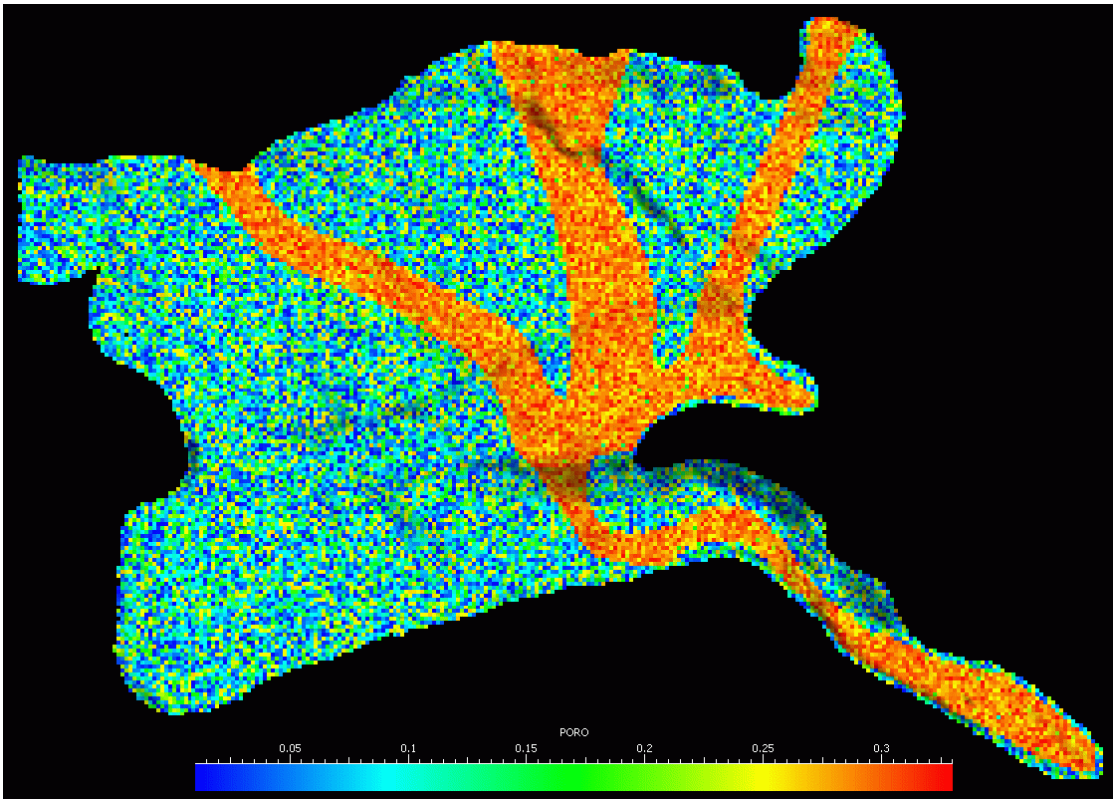


**Figure 28. Modelled porosity distribution over the Captain Sandstone.**

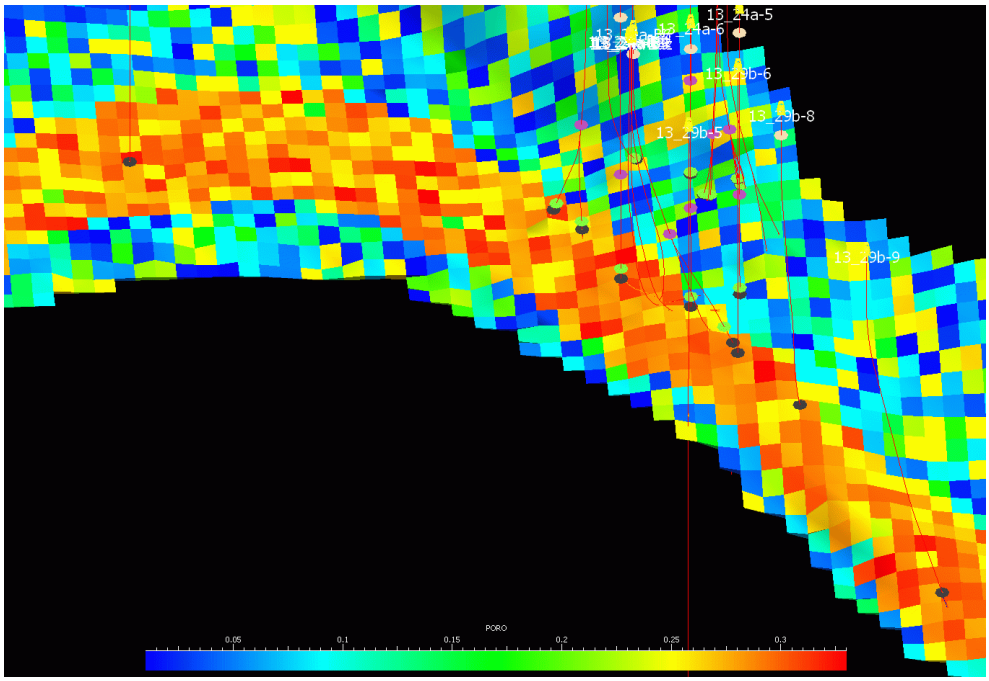


**Figure 29. Point-by-point accurate choice of modelled porosity distribution allows creation of connections between Channel and Flank facies, as shown by Blake Field well trajectory and intersection data in an excerpt of the porosity model.**

### 3.5.2 Permeability distribution

To populate a model with permeability attribution, the standard solution is to establish correlations between porosity and permeability with data values from cores analysis. Figure A3.25 shows the empirical relationship of porosity versus permeability derived from core data.

This approach is often used even if there is no causality between porosity and permeability.

Kozeny-Carman derived equations aimed at introducing a causality relationship between porosity and permeability based on laboratory experiments and quantitative physical parameters for rock reservoir composition are described in detail in Appendix 3. The main steps are listed below:

- A cross-plot of 'Reservoir Quality index' (RQI) against normalised effective Porosity was established based on Kozeny-Carman equations (Figure A3.29). This shows the relationship between porosity and different reservoir properties;
- A number of Flow Units (FUI) present in the core dataset were identified from analysis of relationship between 'Reservoir Quality index' (RQI) against normalised effective Porosity (Figure A3.30);
- Three causal relationships between porosity and permeability were identified from the dataset (Figure A3.31);
    - Flow Unit 1 (FU-1) $K = 133015 \times PHIE^{3.0943}$

- Flow Unit 2 (FU-2) K = 147237 x PHIE $^{3.5726}$
- Flow Unit 3 (FU-3) K = 9292.8 x PHIE $^{3.5982}$

- Figure 30 shows curves generated by above equations superimposed on the dataset; if porosity is known an associated permeability can be assigned;
- The curves were then adjusted to bound the data and so reflect the Channel and Flank facies (Figure 31).

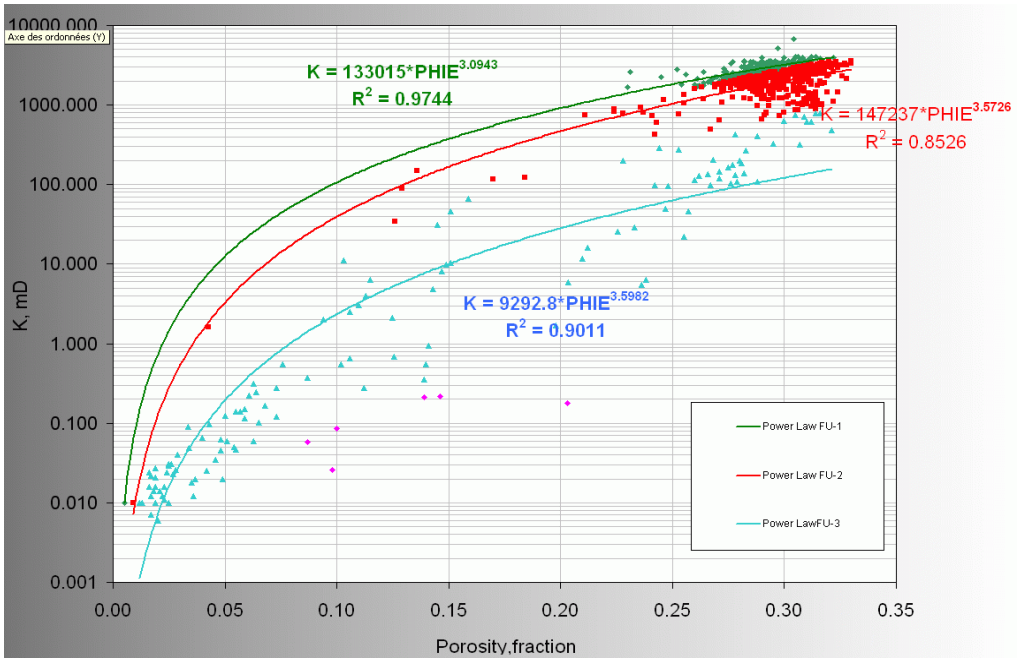


**Figure 30. Illustration of power laws for each significant Flow Unit on a cross-plot of porosity and permeability.**

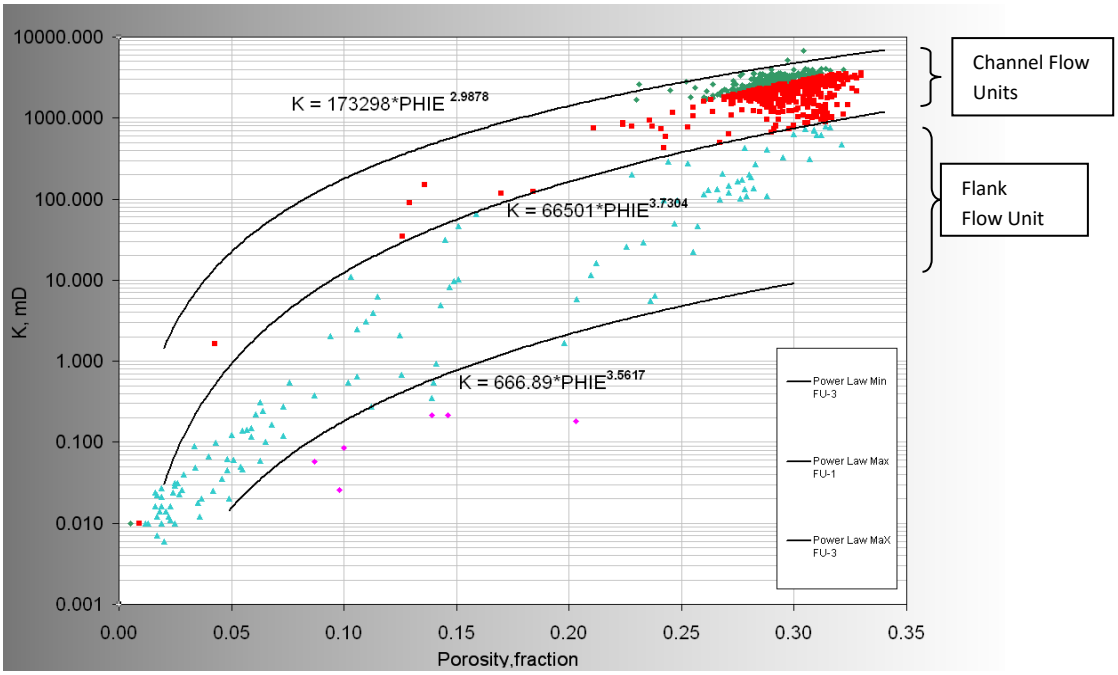


**Figure 31. Additional Power Laws bounding Channel and Flank Flow Units on a cross-plot of porosity and permeability.**

At this stage of the petrophysical interpretation of core data, all the elements based on causal relationship between porosity and permeability are established.

These elements are:

- regional understanding of Channel and Flank areas based on geological knowledge,
- spatial stochastic distribution of porosity values for the Captain Sandstone,
- causal Kozeny-Carman relationships between porosity and permeability.

According to the porosity distribution between Channels and Flank facies, the Channel region appears to be mainly associated with Flow Units 1 and 2, and the Flank region with Flow Unit 3.

Simple scripts have been written to randomly attribute, in a given range, permeability values to already populated porosity values in the grids.

This method is very flexible and powerful: it is possible to take into account geological information, petrophysical information, to establish causal relationships between well logs porosity and permeability, and to determine flow units inside a given stratigraphical unit. Populating grids with this method takes only a few seconds.

An example of script for permeability attribution in channel area knowing porosity distribution is detailed in Appendix 3.

Figures 32 and 33 display the computed permeability distributions in the Channel region and in the Flank. As usually expected, these permeability distributions are log-normal. Figure 34 illustrates the permeability distribution over the whole Captain Sandstone aquifer.

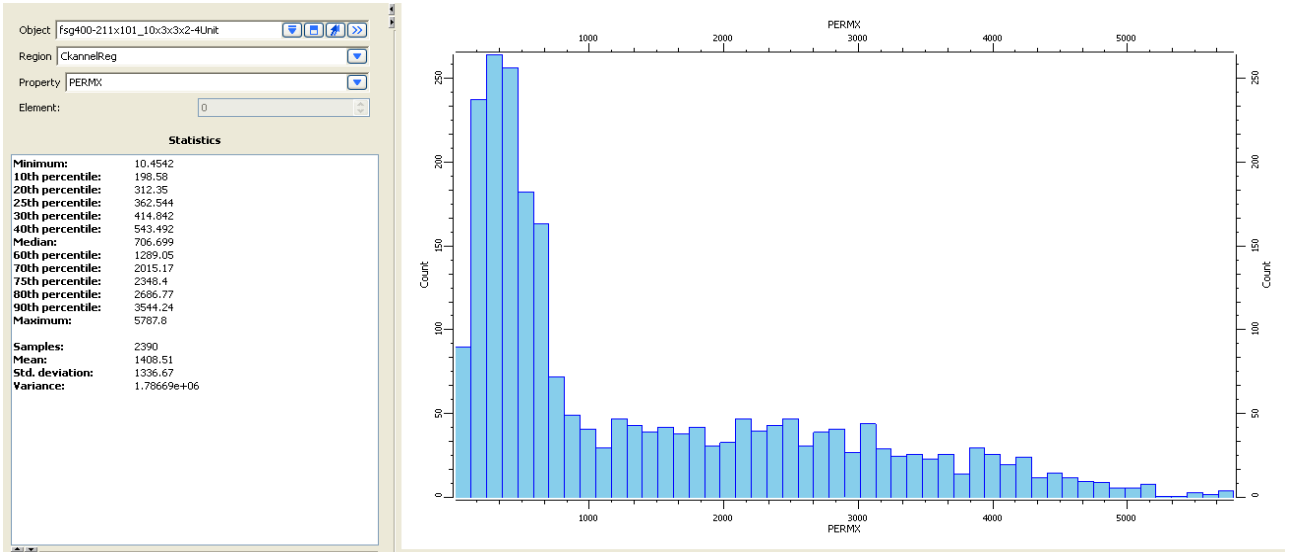


**Figure 32. Permeability distribution in Channel region.**

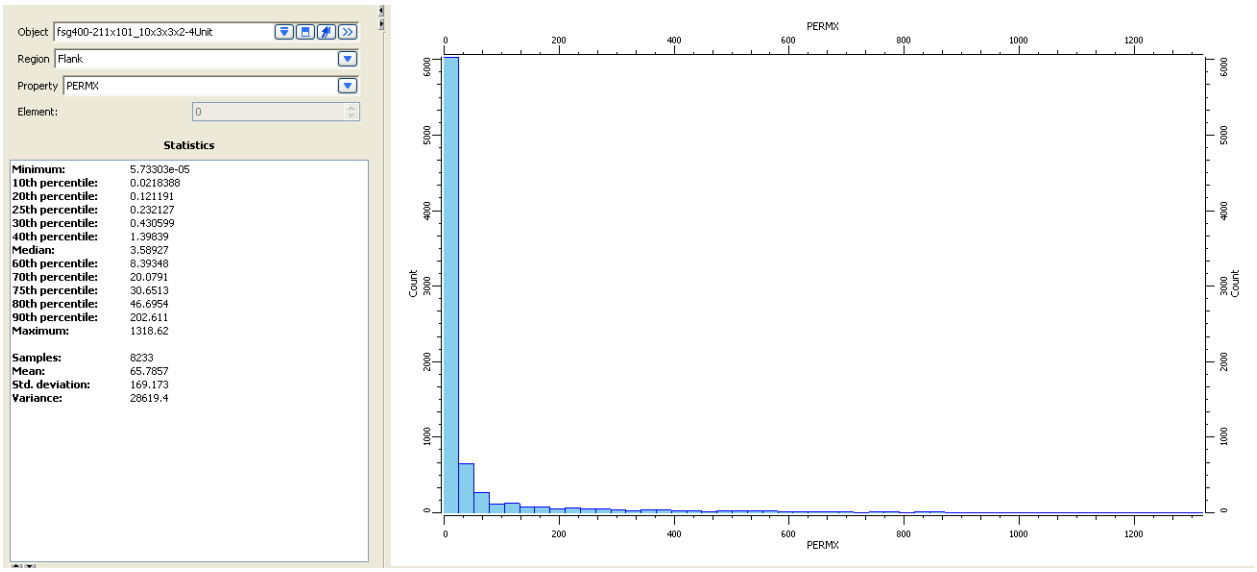


**Figure 33. Permeability distribution in Flank region.**

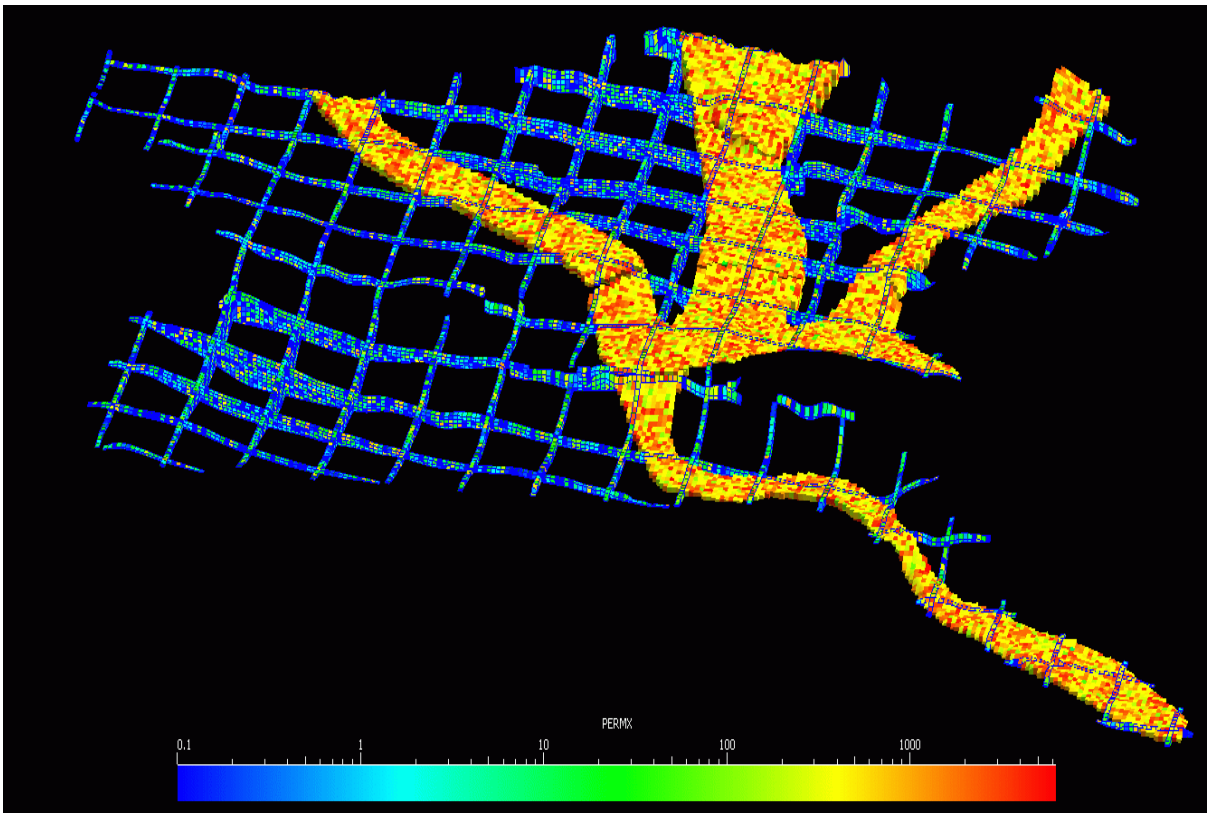


**Figure 34. Fence diagram showing modelled permeability distribution over the entire Top Captain Sandstone.**

## 4. CONTAINMENT

The *Storage Site* is within the Wick Sandstone Formation (Figures 35a & 35b). The primary seal consists of low permeability rocks (the Rodby, Carrack and Valhall formations), that contain the top, base and lateral extents of the Wick Sandstone Formation (Figures 35a and 36). There is an element of structural closure within the *Storage Site* that, combined with the sealing rocks, will contain the injected $CO_2$. The Blake Oil Field will form a significant part of the *Storage Complex*. The Blake Oil Field structural and stratigraphical trap has demonstrated secure containment of hydrocarbons for millions of years.

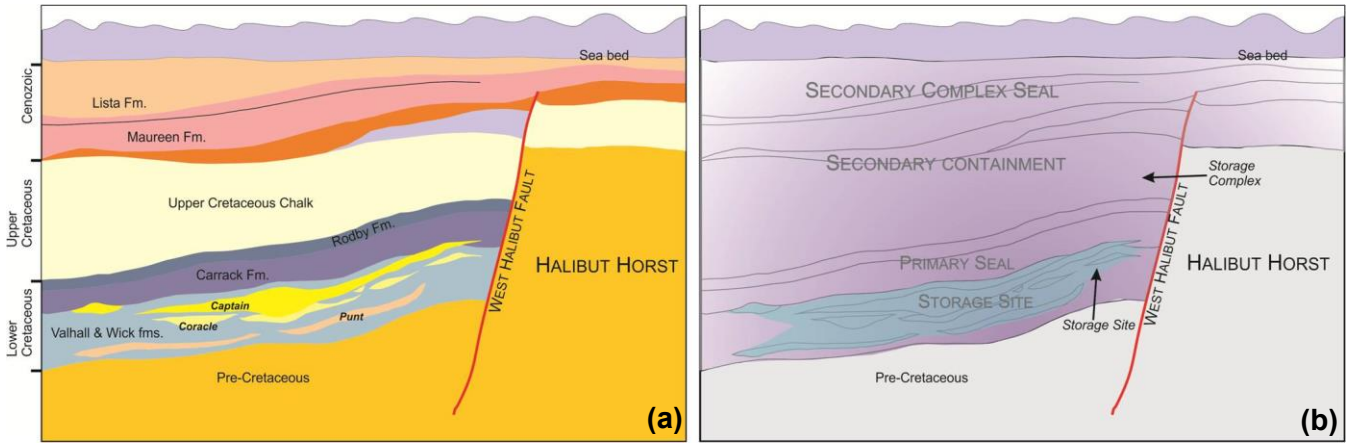


**Figure 35. Diagram showing a) the geological elements of the UK Moray Firth b) the expected *Storage Site* and area in which the *Storage Complex* will be defined.**

The secondary containment reservoirs are located within the *Storage Complex* volume, above the primary seal (Figures 35a & 35b), and comprise Upper Cretaceous Chalk Group strata (average thickness of approximately 460 m) that have relatively low permeability and sandstone and mudstone of the Maureen and Lista formations (average thickness of about 1000 m). The Lista Formation includes the extensive Mey Sandstone Member (Figure 3).

The seal rocks for the volume of secondary containment (the secondary or *Storage Complex* seal), comprise laterally extensive mudstone within the Lista and Dornoch formations (Figure 3; Figure 35a & 35b).

The main components of the *Storage Complex* (Figure 35b) are the:

- *Storage Site*;
- primary seal to the *Storage Site*;
- secondary containment;
- secondary or *Storage Complex* seal.

The main mechanism by which the injected $CO_2$ will be stored is a combination of *structural* and *stratigraphical trapping*. However, other mechanisms such a *residual saturation*, *dissolution* and *geochemical reactions* will also contribute to the total amount held in the *Storage Site* and wider *Storage Complex.*

The attributed 'Basin-scale' and 'Detailed' 3D models of the Captain Sandstone and seal rocks will provide the geological framework from which the *Storage Complex* can be defined and assessed as the project progresses.

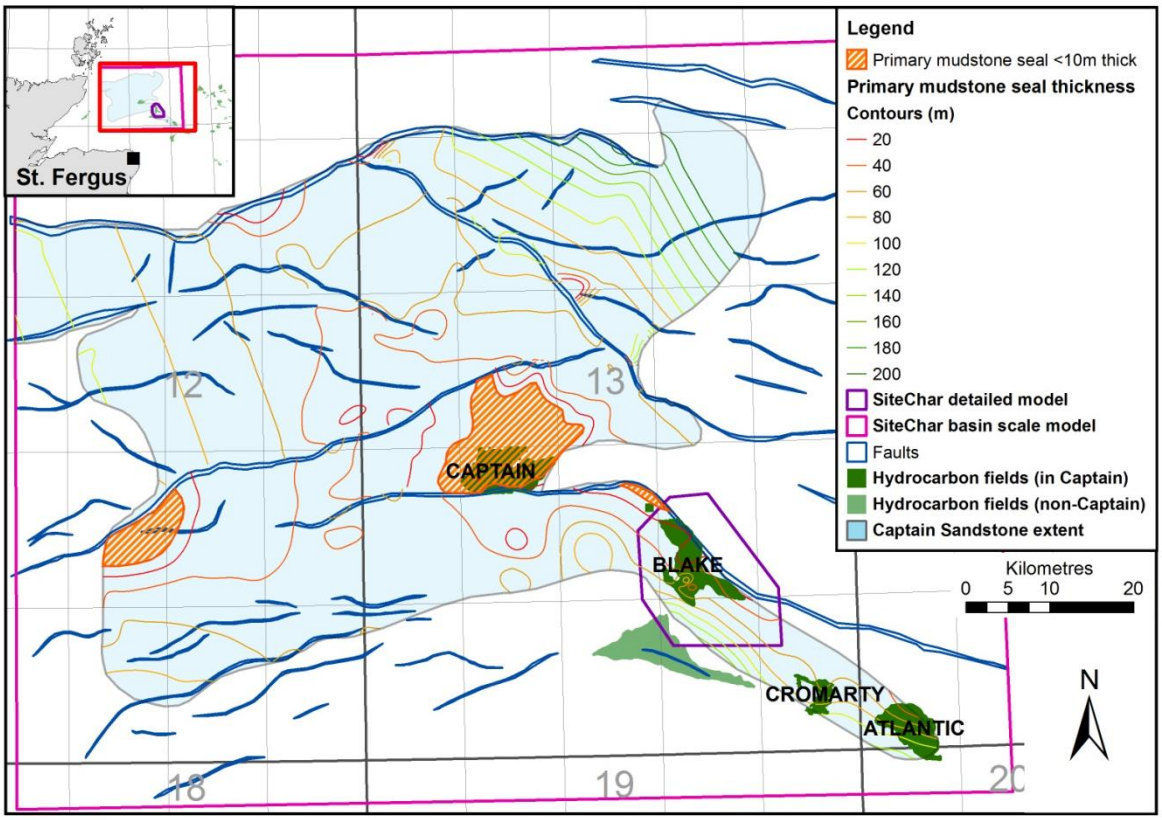


**Figure 36: Thickness map of primary seal (above and lateral to the Captain Sandstone) over whole area contoured in metres from well thickness values.**

### 4.1 The Storage Site – primary reservoir

Immediately north of the Blake Oil Field, the Captain Sandstone has a regional dip to the east, shallowing westwards and cropping out at sea bed at its western boundary. The sandstone reservoir thickens towards and abuts against the Wick Fault Zone to the north, it pinches out and is absent towards the east and south (Figure 4). Within the 'pan-handle' (Figure 4), in the area of the Blake Oil Field, the Captain Sandstone dips towards the south-west and south-east, shallows and pinches out onto the West Halibut Fault.

The 'Detailed' geological 3D model defines the limits of the Captain Sandstone Member in much greater detail than the 'Basin-scale' geological 3D model. The extent of the Captain Sandstone has been re-interpreted from 3D seismic survey data and its boundaries within the 'Detailed' geological 3D model area has been defined (Appendix 3; Figure A3.8). This newly interpreted extent defines the stratigraphical element of the trap within the *Storage Site*. Seismic interpretation shows that the reservoir has a mean thickness of approximately 60 m.

The Blake Oil Field will form a significant part of the total *Storage Site* and is a combined *structural* and *stratigraphical trap*. The field reservoir dips to the west and south providing *structural trapping* to hydrocarbons filling the reservoir. The reservoir sandstone pinches out to the east providing *stratigraphical trapping* of hydrocarbons parallel to the Halibut Horst. However, the nature of the trap to hydrocarbons in the Blake Oil Field along its northern boundary is not clear. There is no structural closure to the field along the field boundaries defined by Department of Energy and Climate Change and no pinch out of the Captain Sandstone can be interpreted that follows this boundary (Figure A3.8). There is a significant discovery, Tain (Figures 15a and A3.8), immediately to the north of the Blake Oil Field that may form the actual northern limit of the Blake accumulation however lack of seismic data precludes confirmation of this. Summarising, the interpretation of data presented here suggests the field boundaries as provided by Department of Energy and Climate Change do not define the full field limits and it is possible that hydrocarbons have migrated beyond the northerly limits of the field, possibly filling a small structure to the north, the Tain discovery (Figures 15a and A3.8).

The Blake Oil Field hydrocarbon reservoir comprises the Lower Cretaceous Captain and Coracle sandstone members of the Wick Sandstone Formation. For this reason the *Storage Site* reservoir is defined as the entire formation within the bounds of the *Storage Complex* as it is uncertain exactly how the Captain, Coracle and deeper Punt Sandstone may be connected (Section 1.3.1). Observations in the Blake Oil Field suggest that it is likely that, in some areas, the Captain Sandstone may directly overlie the Coracle Sandstone and here will be in hydraulic communication. Within the Blake Oil Field there is no evidence of connection with the deeper Punt Sandstone Member; the extents of the Coracle and Punt sandstones are less well known and these may form potential *migration* routes to the fault.

These Lower Cretaceous sandstones comprise a facies association derived from a range of gravity-driven depositional processes and may include high- and low-density turbidites, mud flows, debris flows, slides, slumps and hemi-pelagic deposition (Mayall *et al*. 2006). The environment of deposition of the sandstones has resulted in variable reservoir quality within the *Storage Site* that is well illustrated in the Blake Oil Field (Section 1). The wider Captain Sandstone saline aquifer, beyond the Blake Oil Field where less data is available, is expected to exhibit similar characteristics. Information from exploration, appraisal and development wells has enabled proposed locations for injection wells to be selected. Dynamic modelling of $CO_2$ injection and *migration* within the Blake Oil Field will be fairly well constrained and the model of facies seen here will be applied when simulating $CO_2$ *migration* within the 'Basin-scale' model of the saline aquifer.

The principal sandstone of the *Storage Site*, the Captain Sandstone Member, is interpreted from 3D seismic survey data to pinch out in the hanging wall succession of the West Halibut Fault. The sandstone does not appear to extend to the fault as previously inferred from the interpretation of 2D seismic survey data (Scottish Carbon Capture & Storage, 2011). The *Storage Site* lies within the hanging wall of the West Halibut Fault (Figure 35b). The West

Halibut Fault forms the southern boundary to the Halibut Horst. The *Storage Site* itself contains no mapped faults except for a pair of diverging faults, included in the 'Detailed' 3D model and oriented east to west, that are mapped at the Base Cretaceous surface (Figures 17 and A3.7); these are not interpreted to extend up as far as the Base of the Captain Sandstone Member. The faults mapped within the 'Detailed' geological 3D model are not expected to present a significant risk to the integrity of the *Storage Site* and *Complex*.

### 4.2 The Storage Complex - primary seal to the *Storage Site*

The top of the Captain Sandstone is sealed by overlying low permeability mudstone but in places the mudstone is thin and sometimes directly overlain by the unconformable Base Chalk surface. Seismic mapping does not have the resolution to identify where Chalk rests directly on the Captain Sandstone; Figure 18 illustrates where the mudstone seal is most likely to be thin (less than 10 m) and some wells in these areas (e.g. well 13/22a-28 – Captain Oil Field) show Chalk resting directly on the Captain Sandstone. The Chalk seal may not be as efficient a seal as the mudstone. However, within the potential *Storage Complex* volume, the Captain Sandstone is expected to be overlain by Lower Cretaceous mudstone. The basal seal to the *Storage Site* is mostly low permeability mudstone, but in places the Captain Sandstone may directly overlie the Coracle and Punt members of the same sandstone formation. Any fluid flow into underlying porous sandstone bodies would enable greater dissipation of increased pressure due to $CO_2$ injection (Scottish Carbon Capture & Storage, 2011)

The top seal comprises argillaceous rocks of the Valhall, Carrack and Rodby formations (Figures 3, 35a and 36). The top seal is present over the entire 'Detailed' geological 3D model area, has a mean thickness of 58 m and varies from less than 20 m to a maximum thickness of 227 m. Interpretation of the 3D seismic survey data indicates that the top seal thickens south-westwards from the Halibut Horst reaching the maximum thickness of over 200 m in the south-west of the 'Detailed' 3D model area.

The bottom seal comprises mostly low permeability rocks and any underlying sandstones will add to the storage capacity of the $CO_2$ store and would not be expected to constitute a containment risk (Appendix 4).

All well penetrations in the 'Detailed' 3D model area prove the presence of the top seal which consists of calcareous and non-calcareous mudstone and siltstone of the Rodby, Carrack and Valhall formations.

### 4.3 The Storage Complex - secondary reservoirs and secondary seals

Rock strata that overlie, underlie or are laterally equivalent to the Captain Sandstone present options for both secondary containment and secondary sealing for the storage of injected $CO_2$. *Migration* of injected $CO_2$ beyond the *Storage Site* may be contained within the overlying Upper Cretaceous Chalk Group and Palaeogene succession or the laterally equivalent Coracle and Punt members of the Wick Sandstone Formation.

The Upper Cretaceous Chalk Group succession has an average thickness of approximately 460 m over the 'Detailed' 3D model area. The Chalk Group could provide additional containment for $CO_2$, although the Chalk has low rock porosity and permeability it may have fracture porosity and permeability sufficient to provide storage for $CO_2$. The overlying Palaeogene succession comprises sandstone, mudstone, claystone, siltstone and limestone and has an average thickness of approximately 1000 m over the 'Detailed' 3D model area.

The sandstone could provide very good secondary containment for migrating $CO_2$ while the mudstone and claystone successions present in the Palaeogene Lista and Dornoch formations (Figure 3) could provide a secondary seal to the *Storage Complex*. There is insufficient well information for detailed mapping of the thickness or continuity of the secondary containment and seal lithologies (Section 1.3.2).

### 4.4 Integrity uncertainties - Potential structural leakage pathways

The geological structure within the area of the 'Basin-scale' model of the Captain Sandstone includes a framework of faults defining basins and highs mapped at the Base Cretaceous surface (Figure 4). Not all the faults mapped cut through the Captain Sandstone and shallower modelled surfaces. Those faults that were active after deposition of the seal rocks and extend up to the sea bed are shown as potential *leakage* points (orange in Figure 4). If the injected $CO_2$ migrates and intersects with a fault, there is a risk that the fault plane would provide a conduit to higher levels in the geological succession, bypassing regional seals, and eventually migrating to the sea bed where *leakage* would occur. Alternatively the $CO_2$ could migrate directly up the fault plane and leak at the sea bed. If these structures permit fluid flow the seal may be compromised by *migration* or *leakage* up the faults. Scenarios where fault structures that lie within the calculated *migration* path for injected $CO_2$ are non-sealing will be investigated by flow simulation and geomechanical stability assessments in Tasks 3.2 and 3.3.

The Blake Oil Field has thirty six well penetrations of which eleven are plugged and abandoned exploration and appraisal wells. The remaining twenty five are development wells side-tracked from a series of pilot boreholes and deviated to horizontal through the Blake reservoir. The 'Detailed' geological 3D model area has a total of forty five well penetrations within its boundaries. These wells represent a containment risk and their integrity will be assessed in Task 3.2 of WP3.

The Captain Sandstone is interpreted as an 'open system' and the water held in the saline aquifer is at hydrostatic pressure. The impact of increased pressure will be assessed by dynamic modelling of $CO_2$ injection within the 'Detailed' and 'Basin-scale' 3D models, including an assessment of fault reactivation (Task 3.3) within the 'Detailed' 3D model.

## 5. STATIC ESTIMATES OF STORAGE CAPACITY OF THE POTENTIAL STORES

The proposed injection/storage scenarios will define stores with different boundaries that will be quantified in more detail after the dynamic modelling in SiteChar Task 3.2 is complete. Static storage capacities of the Blake Oil Field and *multi-store site*, comprising the Blake Oil Field and a volume of the saline aquifer down-dip from the Blake Oil Field were calculated. The equation used to calculate the storage capacity is shown (Equation a) and the results are tabulated (Table 5).

Equation (a):

$CO_2$ static storage capacity(Tonnes) = (V($m^3$) x NTG x Porosity x $CO_2$ density($kg/m^3$) x $St^{eff}$ )/1000

where :

$CO_2$ static storage capacity= calculated volume of $CO_2$ that might be stored;

V= store site volume in cubic metres; amounts from static 'Detailed 3D geological model;

NTG= proportion of Net sandstone To Gross thickness within the store site volume (av values taken from Table 1);

Porosity= proportion of the sandstone volume that is pore space (Value taken from av. total porosity, Table A3.3);

$CO_2$density= Density of $CO_2$ in the sandstone at an assumed reservoir pressure of 2342 pounds per square inch (16.15 MPa) and temperature of 54°C (reservoir data from well reports);

$St^{eff}$ = Storage Efficiency factor representing the amount of pore space available to store $CO_2$ (Note this study uses a value of 0.2 (20%) specifically for the Captain Sandstone. The Scottish Study used a maximum $St^{eff}$ of 0.02 (2%) for all saline aquifers in that study).

| STORE | VOLUME in millions of cubic metres ($Mm^3$) | Proportion of sandstone (NTG) | Porosity | $CO_2$density | Storage Efficiency | Static storage capacity (Mt) |
|---|---|---|---|---|---|---|
| Blake Oil Field | 1228 | 0.66 | 0.257 | 691 $kg/m^3$ | 0.2 | 28 Mt |
| Blake Field Channel facies only | 578.8 | 0.985 | 0.257 | | 0.2 | 20 Mt |
| Storage Complex (Total Captain Sandstone in Detailed model) | 7927 | 0.66 | 0.257 | As above | 0.2 | 186 Mt |

**Table 5. Static calculated storage capacity for components of the Moray Firth *multi-store site*.**

## 6. INJECTIVITY

The injectivity of the reservoir into which $CO_2$ is to be injected is an important parameter to quantify and is defined as the product of the permeability of the aquifer and its thicknessin units of Darcy-metre (Dm) (Hosa *et al*., 2010). Injectivity values based on experience from methane gas injection and storage suggest a minimum injectivity of 0.25 Dm for an aquifer to be commercially feasible (Hosa *et al*., 2010). Chadwick *et al*. (2008) highlight cautionary values for key geological indicators of <20 m for net reservoir thickness and <200 mD for reservoir permeability; this equates to an injectivity of 4 Dm. Positive indicators of >50 m for net reservoir thickness and >500 mD for reservoir permeability equates to an injectivity of 25 Dm.

### 6.1 Selection of injection wells for subsequent modelling

Two potential injection sites, at existing well sites, have been identified such that $CO_2$ is injected into high permeability sandstone Channel facies. Calculated injectivity for the two virtual injector wells are shown in Table 6 below. Both injection sites have injectivities suitable for the storage of $CO_2$.

| Injection Well | Reservoir Thickness (m) | Mean effective porosity (%) | Permeability (Darcy) | Injectivity (Darcy-metre) |
|---|---|---|---|---|
| 13/24a- 4 | 84.4 m | 27% | 0.724 D | 61 Dm |
| 13/29b- 9 | 84.1 m | 24.6% (average for all channel reservoirs) | 0.271 D | 23 Dm |

**Table 6. Calculated injectivity for wells 13/24a- 4 and 13/29b- 9 located within the 'Detailed' geological 3D model.**

The geological properties of the Captain Sandstone within and outside the Blake Oil Field reservoir are likely to vary laterally. To ensure SiteChar research is informed by hydrocarbon well data, the location of the $CO_2$ injection well, for the purposes of modelling in WP3 SiteChar and so the dry-run application will be at the location of an existing well site.

These wells have been chosen as the initial points for modelling $CO_2$ injection into the storage formation according to the following criteria:

1. Good data availability
2. Good injectivity
   - high permeability and porosity
   - good thickness of reservoir sandstones
3. Suitable depth and temperature (injection of $CO_2$ in supercritical phase)
4. Accessibility to existing infrastructure (although this may only be important if it is of suitable material tolerances).

These criteria are for the purposes of this SiteChar research desk study only. In a real storage permit application it is anticipated that if necessary, dynamic modelling to determine optimal well locations would be performed.

One proposed injection well will be located within the 'Channel Area' of the Blake Oil Field (Figure 13). The 'Channel area' is penetrated by three appraisal wells (green on Figure 13; Figure 15b) [13/24a- 4, 13/24a- 6 and 13/29b- 6], that are now plugged and abandoned, a water injector well [13/24a- 7, 7z] (blue on Figure 13; Figure 15b) and a series of sidetracked and deviated producer wells (red on Figure 13; Figure 15b) [13/24a-B].

All these wells provide information on the Captain Sandstone and will inform the attribution of the model. However, the three vertical wells (13/24a- 4, 13/24a- 6 and 13/29b- 6) provide the best options in terms of location along the channel and amount of data available and, of these three, the location of the vertical, plugged and abandoned Well 13/24a- 4 is suggested to be optimal for the proposed site for modelled injection. The key reason for choosing this well over the others in the 'Channel Area' is that, at this point the Captain Sandstone is deeper (depth to Top and Base Captain Sandstone are 1574 m TVDSS and 1659 m TVDSS, respectively) than the permeable sands in wells 13/24a-6 and 13/29b- 6. Without trying to pre-empt the dynamic modelling results, the deeper location of the reservoir in this well should allow *migration* of $CO_2$ to access the shallower parts of the reservoir within the Channel Area. Its location should also allow clear access of the injected $CO_2$ to the 'Flank interbedded unit'.

The second virtual injection well site is located south of the Blake Oil Field, within the Captain Sandstone saline aquifer. It is anticipated that dynamic modelling will demonstrate *migration* of the supercritical $CO_2$ up-dip and into the Blake Oil Field. The most southerly well located within the 'Detailed' geological 3D model is exploration well 13/29b- 9 drilled by Talisman Energy UK Ltd in May 2004. The well proved 84 m of relatively clean massive Captain Sandstone with a blocky Gamma Ray log signature. This well will provide the necessary parameters to dynamically model injection at this location.

One of the proposed injection well sites will be used to simulate injection of $CO_2$ into the *multi-store* site. Selection of the simulated injection site will be undertaken at the commencement of Task 3.2 to take account of reservoir properties of the *Storage Site* rocks and the ambition of WP3 SiteChar to investigate a feasible multi-store site with sufficient capacity for commercial-scale storage capacity.

The dynamic simulations will be carried out as part of Task 3.2 and results will inform the final licence application (MS8).

## Appendix 1: DEFINITIONS

- ***Storage Site*** - a defined volume area within a geological formation used for the geological storage of $CO_2$ and associated surface and injection facilities;
- ***Storage Complex*** - the storage site and surrounding geological domain which can have an effect on overall storage integrity and security; that is, secondary containment formations;
- ***Multi-store site*** - a *Storage Site* comprising both a depleted hydrocarbon field and a saline aquifer;
- ***Leakage*** - any release of $CO_2$ from the storage complex;
- ***Migration*** - the movement of $CO_2$ within the *Storage Complex*;
- ***Residual saturation*** occurs during migration of the supercritical $CO_2$. A proportion, between 5-30% of the $CO_2$, is left behind as it migrates upwards, trapped by capillary forces;
- ***Structural trapping*** $CO_2$ become trapped in structural closure at the top of the reservoir;
- ***Stratigraphic trapping*** the $CO_2$ may become trapped as the permeable reservoir becomes impermeable, perhaps by a change in lithology from sandstone to mudstone;
- ***Dissolution*** of $CO_2$ in formation water is potentially a significant contribution to total storage capacity in a reservoir. For instance under typical reservoir conditions and at a salinity of 3%, the solubility of the $CO_2$ in the formation water may be between 47 – 51 kg/m$^3$, this is equivalent to the amount of free $CO_2$ that could be stored in 6.7% - 7.3% of the pore volume in a rock. Thus this mechanism in effect provides the equivalent of 7% extra pore volume in parts of the reservoir filled with formation water. $CO_2$ solubility depends upon the temperature, pressure and salinity of the formation water; the higher the salinity, the lower the solubility of the $CO_2$. The rate at which dissolution takes place is also dependent upon the thickness of the reservoir. If thin, the $CO_2$ will quickly become trapped beneath the cap rock and spread out widely, with the result that a greater surface area of $CO_2$ is exposed to the formation water. As formation water containing dissolved $CO_2$ is about 10% denser than formation water not containing $CO_2$ it will tend to sink causing convection currents to be set up exposing non-carbonated formation water to the $CO_2$ liquid;
- ***Geochemical reaction*** with the surrounding rock formations or formation water is another potential $CO_2$ storage mechanism and is dependent upon pore water chemistry and rock mineralogy and only takes place over long time scales (hundreds to thousands of years);
- ***UKCS –*** United Kingdom Continental Shelf

## Appendix 2 – THE BLAKE OIL FIELD

### Selection of Hydrocarbon Field

All UK hydrocarbon fields have a released 3D seismic dataset and a comprehensive well dataset available. Table A2.1 summarises the 3D seismic data that has been acquired over the hydrocarbon fields considered for this project. The Blake and Cromarty fields had the same surveys available to them, namely the PGS MegaSurvey built from a Amerada Hess survey acquired in 1992 (Section A3.1.1). The Atlantic Condensate Field has a more recent (1997) survey available.

| | Captain | Blake | Cromarty | Atlantic |
|---|---|---|---|---|
| | | | | |
| Fluid | Oil | Oil | Gas | Condensate |
| Operator | Chevron | BG | Hess | BG |
| Field area (approx $km^2$) | 41.918544 | 37.575133 | 8.885847 | 28.846925 |
| ?PRT area (approx $km^2$) | 57.142796 | 67.684088 | 25.963000 | 37.740650 |
| Number of wells within hydrocarbon Field boundaries | 161 | 24 | 3 | 7 |
| MegaSurvey data | Y | Y | Y | N? |
| | | | | |
| Survey | | MF10 | | |
| 2D/3D/4D | | 3D | | |
| Shot by | | TGS Nopec | | |
| When | | 2010 | | |
| Owner | | TGS Nopec | | |
| Released | | No | | |
| | | | | |
| Survey | TX033F0001 | BG07BLAK4D | | JB973D2002 |
| 2D/3D/4D | 3D | 3D/4D | | 3D |
| Shot by | Geco | WesternGeco | | CGG |
| When | 2003 | 2007 | | 1997 |
| Owner | Chevron | BG | | IHS Energy |
| Released | Yes | No | | Yes |
| | | | | |
| | | | | |
| Survey | ET973F0001 | AH923F0002 | | |
| 2D/3D | 3D | 3D | | |
| Shot by | Fugro | SSL | | |
| When | 1997 | 1992 | | |
| Owner | Centrica | Hess | | |
| Released | Yes | Yes | | |
| | | | | |
| Survey | TX903F0001 | | | |
| 2D/3D | 3D | | | |
| Shot by | Geco | | | |
| When | 1990 | | | |
| Owner | Chevron | | | |
| Released | Yes | | | |

**Table A2.1. Summary of data on the four hydrocarbon fields considered for the UK multi-store northern North Sea site, WP3 of the SiteChar project.**

However, the Blake Oil Field has by far the greatest number of well penetrations compared to the Cromarty and Atlantic fields (Table A2.1) and this was seen as advantageous both for constraining the seismic interpretation and for attribution of the reservoir.

The Blake Oil Field lies south of and adjacent to the Halibut Horst (Figure 4) in a water depth of 104 m; the field is 74 km north-east of the St Fergus gas terminal. Its outline shape reflects in part its reservoir architecture that comprises a channel complex, trending north-west, that is 6 km long and about 700 m wide and parallel to the West Halibut Fault (Figure 12). The Blake Oil Field covers an area of approximately 37.6 $km^2$ and mapped depth to top reservoir varies from approximately 1350 m TVDSS in the north-east of the field to a maximum of 1650 m TVDSS in the south-western part of the field. The Blake Oil Field has 36 well penetrations related to exploration, appraisal and development of the field. There are 9 plugged and abandoned exploration and appraisal wells and the remaining 27 are development wells sidetracked from a series of 10 pilot holes and deviated to horizontal through the Blake reservoir (Figures 13 and 15).

**Reservoir spatial facies associations and derivation**

The Blake reservoir was deposited in a deep water submarine environment, derived from a sediment source to the north and west of the area and deposited by a range of gravity flow processes including high and low density turbidites, mud flows, debris flows, slides and slumps and hemi-pelagic rain. The Blake Oil Field reservoir has been divided into two distinct areas whose facies associations reflect this range of depositional processes (Figures 9 & 13):

- The Channel area in the down-dip, south-west part of the field;
- The Flank area up-dip to the north-east.

The areas are defined from log and seismic information. Well log interpretations give point locations of where channel sandstones are present and where the more interbedded sandstone/shale slumped succession of the Flank area occurs. Seismic mapping also gives an indication of the orientation (north-west) of the Channel area and its approximate extents (Figure A2.1).

The nature of the boundary between these two areas, and its precise location, is difficult to define in detail though this is important as it will impact on the dynamic modelling of the $CO_2$ through the reservoir. The isochore map between top and base Captain Sandstone provides a guide to the location of the boundary between the two facies associations (Figure A2.1).

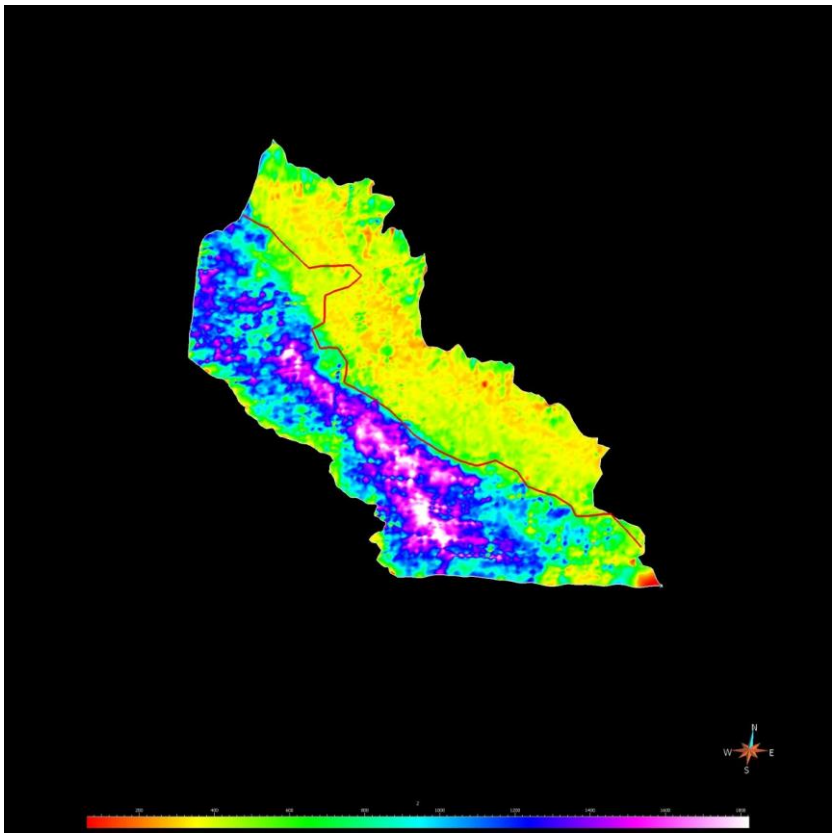

**Figure A2.1. Isochore (metres) of Captain Sandstone Member, blue indicates thicker succession and corresponds to Channel Area in Blake Oil Field.**

In addition, an investigation suggested by Imperial College was carried out to ascertain if changes in the interpreted Base Captain Sandstone surface might reveal a change in character that could be related to the Channel/Flank boundary. Their analysis of the nature of the Base Reservoir surface, that had been interpreted by BGS, in relation to angle and gradient (rate of change) (Figure A2.2) of base reservoir surface enabled a boundary, interpreted to represent the change from Channel to slumped Flank facies to be drawn (Figure A2.3). This is shown as a red line in Figure A2.1 and shows good correlation with the isochore values.

The juxtaposition of the Channel and Flank area facies will result in a wide range of contact relationships. The Channel area is likely to comprise a sandstone with a relatively consistent high NTG character with good permeability and porosity. However the Flank area will be much more variable with juxtaposition of sand on sand, sand on shale and a high number of variations between these two end members. The Channel and Flank areas of the Blake Oil Field have been developed separately with the Flank area exhibiting complex reservoir architecture with possible compartmentalisation of reservoir sands (see below).

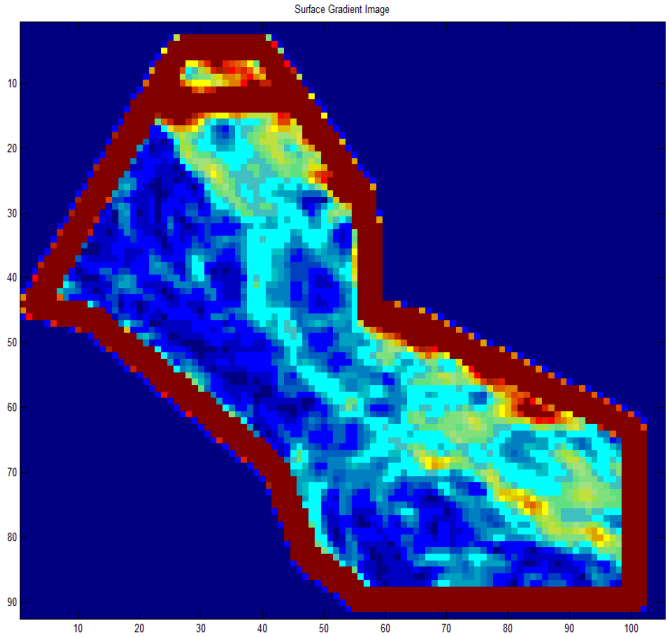


**Figure A2.2. Base Captain Sandstone surface gradient (rate of change). Analysis provided by Imperial College.**

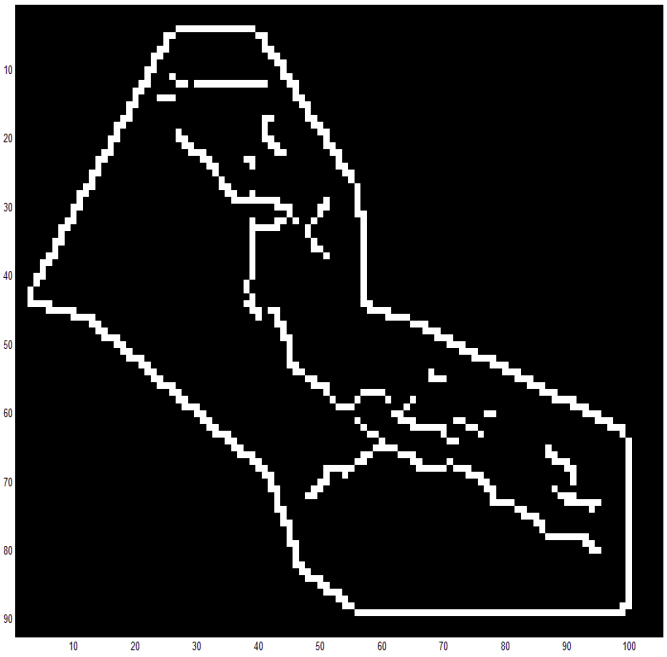


**Figure A2.3. Edge detection result derived from a combination of angle and gradient of interpreted Base Captain Sandstone surface. Analysis provided by Imperial College.**

Interpretation of geophysical logs from 23 wells (including deviated wells) within the Blake Oil Field enabled porosity, permeability and NTG values to be derived for both Channel and

Flank facies areas for attribution of the 'Detailed' geological 3D model (Section 1; Appendix 3). These log interpretations were compared to actual core measurements and are tabulated in Table A3.3. Porosity and permeability values taken from core analyses enable a relationship between porosity and permeability to be established so that the model could be attributed with permeability values (Figure A3.25).

**Blake Oil Field development and production**

The Blake Oil Field produced a little over 14.7 MMBBLS (2.3 Million $m^3$) of oil in its first full year of production (2002) (Table A2.2). Since then production has steadily declined to 4.6 MMBBLS (748,673 $m^3$) of oil in 2010 and to the present day (Section1, Figure 14). The oil field has been developed utilising a total of 10 horizontal oil producers located at crestal locations supported by 3 water injectors located at the northern and southern ends of the field (Section 2, Figure 15). Producers were completed with sand screens to prevent ingress of sand to pipelines. The Channel and Flank facies areas in the Blake Oil Field have been developed separately with 8 development wells (6 oil producers and two water injectors) in the Channel area and 3 development wells (2 oil producers and one water injector) in the Flank area (Section 2, Figure 15).

In 2010 the Blake Oil Field produced 748,673 cubic metres of oil (627,840 tonnes, 4.6 MMBBLS) (Section 2, Figure 14; Table A2.2), 93.9 $MMsm^3$ of associated gas (Figure A2.4; Table A2.3) and 1.2 $MMm^3$ of water (Figure A2.5; Table A2.4).

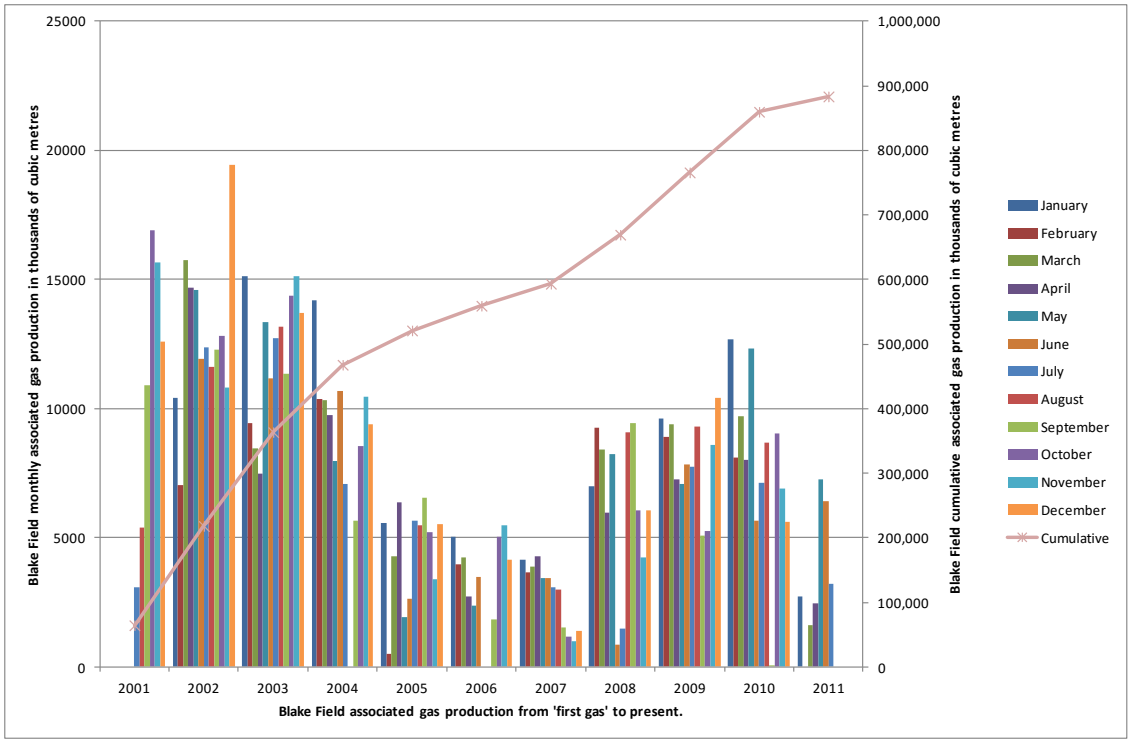


**Figure A2.4. Blake Oil Field monthly and cumulative associated gas production in thousands of cubic metres to present day.**

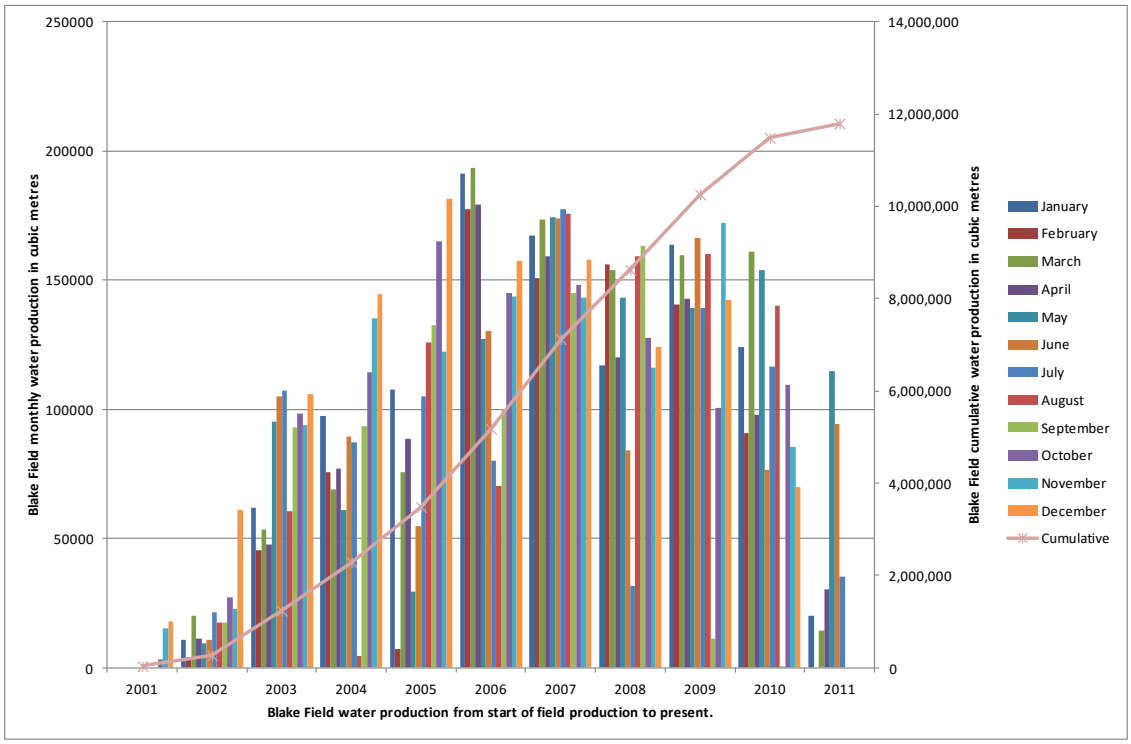


**Figure A2.5. Blake Oil Field monthly and cumulative water production in cubic metres to present day.**

| | Jan | Feb | Mar | Apr | May | Jun | Jul | Aug | Sep | Oct | Nov | Dec | Yearly Total |
|---|---|---|---|---|---|---|---|---|---|---|---|---|---|
| 2001 | | | | | | | 90,658 | 129,693 | 206,726 | 257,148 | 257,412 | 229,304 | 1,170,941 |
| 2002 | 197,350 | 159,136 | 247,284 | 239,010 | 226,063 | 202,213 | 216,432 | 188,228 | 165,300 | 147,487 | 136,540 | 210,333 | 2,335,376 |
| 2003 | 170,467 | 124,841 | 141,447 | 99,532 | 194,625 | 171,950 | 172,966 | 178,258 | 184,144 | 198,713 | 181,051 | 179,237 | 1,997,231 |
| 2004 | 182,782 | 145,870 | 133,759 | 144,346 | 123,655 | 159,362 | 148,691 | 14,274 | 175,560 | 193,026 | 192,286 | 187,743 | 1,801,354 |
| 2005 | 133,371 | 19,058 | 109,847 | 140,699 | 46,668 | 92,961 | 152,035 | 154,221 | 152,774 | 176,560 | 124,165 | 177,281 | 1,479,640 |
| 2006 | 171,936 | 140,355 | 140,798 | 123,792 | 91,065 | 111,683 | 72,023 | 65,094 | 93,888 | 136,000 | 121,729 | 130,697 | 1,399,060 |
| 2007 | 122,565 | 106,107 | 120,247 | 107,578 | 117,761 | 110,043 | 112,331 | 109,879 | 84,181 | 92,084 | 88,201 | 92,939 | 1,263,916 |
| 2008 | 73,292 | 100,851 | 91,153 | 68,507 | 84,223 | 46,890 | 21,999 | 114,601 | 104,457 | 83,509 | 76,098 | 80,076 | 945,656 |
| 2009 | 105,251 | 86,282 | 97,744 | 82,427 | 76,885 | 91,473 | 75,565 | 89,224 | 5,551 | 52,384 | 87,274 | 87,523 | 937,583 |
| 2010 | 87,175 | 58,522 | 87,090 | 58,674 | 97,788 | 42,806 | 60,856 | 76,081 | 216 | 64,190 | 55,439 | 59,836 | 748,673 |
| 2011 | 18,793 | 0 | 12,406 | 17,790 | 81,001 | 52,773 | 21,290 | 0 | | | | | 204,053 |
| | | | | | | | | | | | | | 14,283,483 |

**Table A2.2. Blake Oil Field monthly oil production in cubic metres.**

| | Jan | Feb | Mar | Apr | May | Jun | Jul | Aug | Sep | Oct | Nov | Dec | Yearly Total |
|---|---|---|---|---|---|---|---|---|---|---|---|---|---|
| 2001 | | | | | | | 3,093 | 5,388 | 10,895 | 16,903 | 15,664 | 12,592 | 64,535 |
| 2002 | 10,393 | 7,019 | 15,769 | 14,679 | 14,600 | 11,921 | 12,378 | 11,612 | 12,290 | 12,805 | 10,809 | 19,453 | 153,728 |
| 2003 | 15,126 | 9,426 | 8,472 | 7,473 | 13,331 | 11,175 | 12,709 | 13,165 | 11,341 | 14,375 | 15,104 | 13,693 | 145,390 |
| 2004 | 14,191 | 10,348 | 10,336 | 9,755 | 7,955 | 10,692 | 7,069 | 0 | 5,640 | 8,526 | 10,470 | 9,386 | 104,368 |
| 2005 | 5,591 | 510 | 4,272 | 6,352 | 1,930 | 2,638 | 5,660 | 5,496 | 6,539 | 5,226 | 3,403 | 5,504 | 53,121 |
| 2006 | 5,028 | 3,987 | 4,221 | 2,719 | 2,365 | 3,465 | 0 | 0 | 1,843 | 5,041 | 5,496 | 4,148 | 38,313 |
| 2007 | 4,147 | 3,673 | 3,867 | 4,281 | 3,454 | 3,433 | 3,068 | 3,007 | 1,509 | 1,158 | 1,003 | 1,381 | 33,981 |
| 2008 | 6,975 | 9,269 | 8,403 | 5,990 | 8,232 | 842 | 1,474 | 9,082 | 9,419 | 6,048 | 4,222 | 6,047 | 76,003 |
| 2009 | 9,597 | 8,893 | 9,386 | 7,280 | 7,078 | 7,856 | 7,747 | 9,296 | 5,074 | 5,257 | 8,583 | 10,405 | 96,452 |
| 2010 | 12,680 | 8,116 | 9,700 | 8,020 | 12,335 | 5,673 | 7,133 | 8,673 | 2 | 9,059 | 6,889 | 5,634 | 93,914 |
| 2011 | 2,713 | 0 | 1,630 | 2,480 | 7,279 | 6,436 | 3,195 | 0 | | | | | 23,733 |
| | | | | | | | | | | | | | 883,538 |

**Table A2.3. Blake Oil Field monthly associated gas production in thousands standard cubic metres.**

| | Jan | Feb | Mar | Apr | May | Jun | Jul | Aug | Sep | Oct | Nov | Dec | Yearly Total |
|---|---|---|---|---|---|---|---|---|---|---|---|---|---|
| 2001 | | | | | | | 0 | 0 | 0 | 3,050 | 15,261 | 17,889 | 36,200 |
| 2002 | 10,845 | 4,213 | 20,064 | 11,189 | 9,350 | 10,730 | 21,292 | 17,325 | 17,498 | 27,268 | 22,726 | 60,846 | 233,346 |
| 2003 | 62,059 | 45,559 | 53,322 | 47,851 | 95,340 | 105,056 | 107,417 | 60,470 | 93,043 | 98,452 | 93,943 | 106,021 | 968,533 |
| 2004 | 97,553 | 75,584 | 69,018 | 77,226 | 60,908 | 89,678 | 87,322 | 4,485 | 93,560 | 114,534 | 135,340 | 144,425 | 1,049,633 |
| 2005 | 107,898 | 7,426 | 75,495 | 88,793 | 29,307 | 54,649 | 105,211 | 126,034 | 132,520 | 164,864 | 122,278 | 181,659 | 1,196,134 |
| 2006 | 191,061 | 177,308 | 193,460 | 179,189 | 127,112 | 130,405 | 80,105 | 70,204 | 100,149 | 144,955 | 143,557 | 157,517 | 1,695,022 |
| 2007 | 167,048 | 150,615 | 173,282 | 159,061 | 174,484 | 174,039 | 177,513 | 175,571 | 144,980 | 148,147 | 143,425 | 157,979 | 1,946,144 |
| 2008 | 116,866 | 156,199 | 153,972 | 120,028 | 143,276 | 84,006 | 31,675 | 159,285 | 163,052 | 127,791 | 116,050 | 124,132 | 1,496,332 |
| 2009 | 163,903 | 140,720 | 159,899 | 142,883 | 139,078 | 166,583 | 139,035 | 160,297 | 11,155 | 100,383 | 172,150 | 142,359 | 1,638,445 |
| 2010 | 124,278 | 90,824 | 161,110 | 97,867 | 153,967 | 76,806 | 116,376 | 140,069 | 304 | 109,291 | 85,265 | 70,132 | 1,226,289 |
| 2011 | 20,335 | 0 | 14,589 | 30,244 | 114,917 | 94,160 | 35,323 | 0 | | | | | 309,568 |
| | | | | | | | | | | | | | 11,795,646 |

**Table A2.4. Blake Oil Field monthly water production in cubic metres.**

## Appendix 3 - MODEL CONSTRUCTION: METHODOLOGY AND DATA SOURCES

A 'Detailed' geological 3D model of the Blake Oil Field and adjacent area was generated from 6 mapped depth structure surfaces that were identified and interpreted on a 3D seismic dataset and a small number of 2D seismic profiles and constrained by well information (Figure A3.1). The surfaces mapped, from shallowest to deepest, were Sea bed (top of model), Top Chalk, Base Chalk, Top and Base Captain Sandstone and Base Cretaceous (base of model). Areal extents of the 'Detailed' geological 3D model were constrained by a polygon that included the Blake hydrocarbon field and adjacent area (Figure A3.1).

The methodology carried out to achieve this was as follows:

- Identify the surfaces on the seismic data by transferring the two-way-travel-time (TWTT) recorded against that surface at all available well-seismic profile intersections;
- Interpret each surface away from the well-seismic profile intersection to provide an interpretation of that surface over the extents of the 'Detailed' geological 3D model area;
    - This included interpretation of faults over the area;
    - Interpretation of the limits of the Captain Sandstone reservoir;
- Generate a velocity model, comprising TWTT/depth pairs to enable depth conversion of the geological interpretation;
- Depth convert the surfaces in time structure to surfaces in depth structure below mean sea level;
- Export depth-converted stratigraphical and fault surfaces, and extent polygons to GoCad™ modelling software;
- Generate stratigraphical and fault surfaces in GoCad™;
- Clip faults surfaces to stratigraphical surfaces in GoCad™;
- Merge 'Basin-scale' and 'Detailed' geological 3D models;
- Build a structural model with geocellular grids;
- Populate model with petrophysical properties necessary for flow simulation of $CO_2$ injection into the rock succession;

### A3.1 DATA

The raw data available for the mapping of the area, defined by the 'Detailed' geological 3D model polygon (Figure A3.1) comprised a 3D seismic survey, eleven 2D seismic profiles and a large well dataset comprising more than 60 released wells covering the area of interpretation and also the adjacent area. The seismic datasets were used under license from the seismic company providers. The well data was available for academic use by BGS from the CDA. Well data required by project partners were purchased from IHS under a licensing agreement between BGS and IHS; project partners signed individual indemnifying agreements with BGS.

### A3.1.1 3D Seismic dataset

The 3D seismic data was licensed from the Petroleum Geo-Services (PGS) and provided in SEGY format with an accompanying navigation file. The data forms part of the PGS 3D MegaSurvey which covers large parts of the UK offshore area. The areal extent of the survey licensed to BGS was defined by a polygon outlining the study area, the Blake hydrocarbon field and adjacent area (Figure A3.1). The survey covers an area of 234 $km^2$ and comprises a set of north-north-west-trending inlines and east-north-east-trending crosslines with 12.5 m spacing between each line (Figure A3.1). The seismic data is displayed in TWTT from mean sea level to a maximum of 5.0 seconds TWTT. The 3D seismic data in the licensed part of the PGS MegaSurvey was originally acquired in 1992 for the Amerada Hess Oil Company (Survey name: AHL-92-13).

### A3.1.2 2D Seismic dataset

The 2D seismic profiles form part of two speculative surveys acquired by Fugro Seismic Imaging (IMF97, OMF98re99) and WesternGeco (MG86) that were originally used to map the Captain Sandstone aquifer in the earlier Scottish Development Study and from which the regional 3D model of the Captain Sandstone was built (Scottish Carbon Capture & Storage, 2011). The Fugro surveys were acquired and processed in 1997 and 1998. The WesternGeco seismic profiles were acquired in 1986 but reprocessed in 2004. The majority of the 2D seismic profiles are orientated north-west to south-east, with a smaller number orientated approximately east to west; a total of 10 lines cross the area. Data quality of all three surveys is good although all suffer from the presence of multiples within the first 200 milliseconds (msecs) below sea bed.

### A3.1.3 Well information

Through its membership of CDA, BGS has access to a large database of released commercial wells comprising scanned images of well logs and reports; digital versions of some well logs are also available. The information from these wells constrained the mapping of the surfaces and also contributed to the attribution of the model.

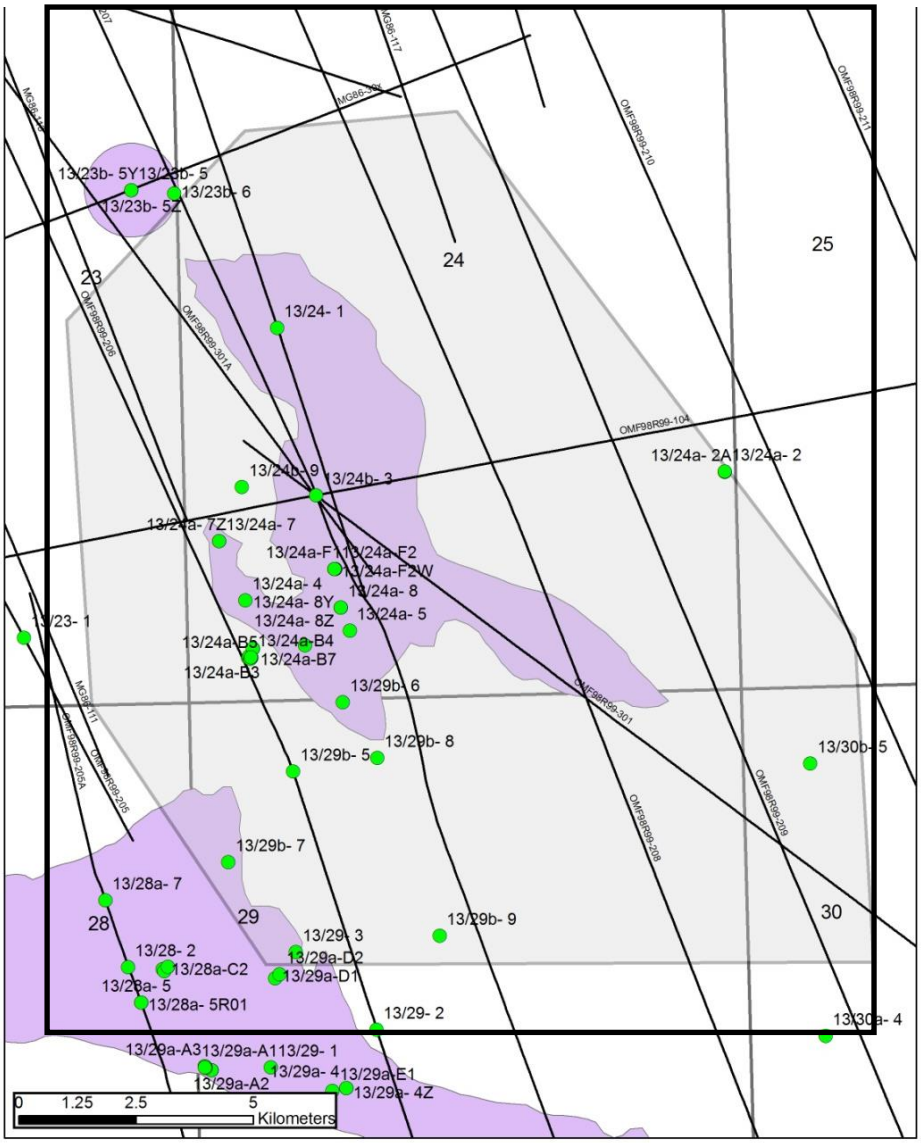


**Figure A3.1. 2D and 3D seismic and well datasets used in this study. 2D seismic profiles licensed shown as black lines, Shaded polygon defines extent of 3D seismic survey and 'Detailed' geological 3D model.**

## A3.2 SEISMIC INTERPRETATION

Seismic interpretation of the 3D MegaSurvey dataset was carried out on a seismic workstation using Kingdom seismic interpretation software. In addition to the seismic 3D dataset, ten 2D seismic lines and 45 released commercial wells (including sidetracks), all part of the dataset used in interpretation of the 'Basin-scale' geological 3D model, are present in the 'Detailed' geological 3D model area. A total of six seismic horizons were picked over the study area these being, Base Cretaceous unconformity, Base and Top Lower Cretaceous Captain Sandstone Member, Base and Top Upper Cretaceous Chalk Group and Sea bed. Six depth structure maps and an isopach map for the Captain

Sandstone reservoir, all at a scale of 1:75,000, are presented in this report and are listed below. These surfaces were exported from the Kingdom software and form the basis of the 'Detailed' geological 3D model discussed in Section A3.4.

The 3D seismic dataset interpreted in this study displays the seismic horizon marking the boundary between a lower velocity succession above (slower sonic travel time) and higher velocity succession below (a positive acoustic impedance contrast) as a red peak. A negative acoustic impedance is displayed as a black peak.

### A3.2.1 Base Cretaceous Unconformity (Figure A3.7)

The quality of the Base Cretaceous seismic horizon varies in character over the study area and in places it is difficult to recognise and, due to the limited number of wells that penetrate Base Cretaceous, difficult to constrain. The seismic horizon was picked on a black peak representing a negative acoustic impedance contrast reflecting the change from higher velocity Lower Cretaceous siltstone to lower velocity Upper Jurassic mudstone. However, due to varying lithologies above and below the unconformity the quality of the seismic response was variable resulting in a discontinuous seismic reflector at this level.

The seismic package that represents the Lower Cretaceous succession, between the Base Cretaceous Unconformity surface and the Base Upper Cretaceous Chalk surface, displays strong and relatively continuous seismic reflectors in some parts and less continuous lower amplitude reflectors elsewhere, possibly reflecting changes in lithology and/or changes in fluid composition within the pore spaces (Figure A3.2). The Lower Cretaceous seismic package includes the Captain Sandstone (Section A3.2.2) and the variability in seismic response is discussed further in that section.

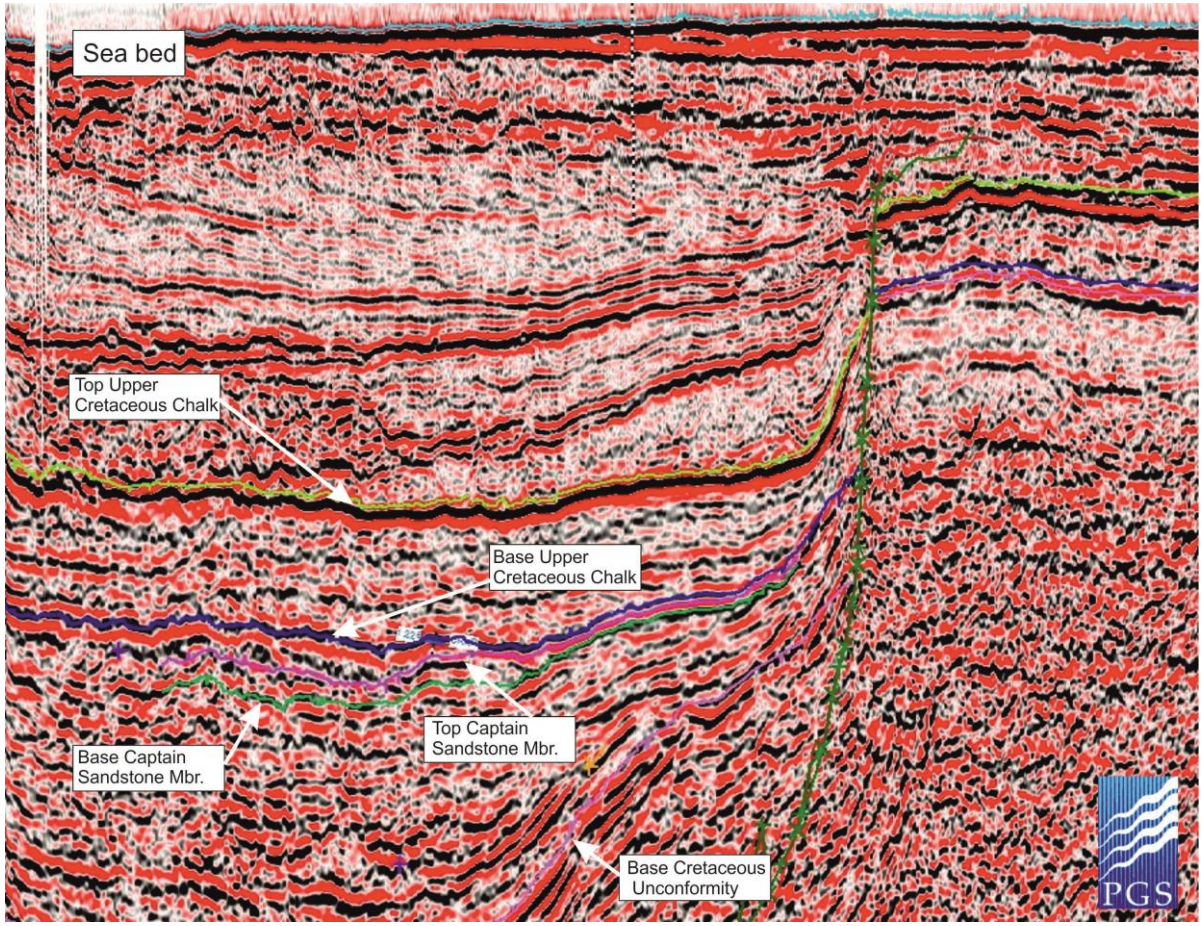


**Figure A3.2. Seismic profile illustrating the character of seismic reflectors and the interpreted surfaces.**

### A3.2.2 The Captain Sandstone

The Captain Sandstone is difficult to define on conventional 2D seismic reflection data due to the small and variable acoustic impedance between the reservoir sandstone and surrounding shale (Law *et al*. 2000). Law *et al*. (2000) examined the change of acoustic slowness and density measurements with depth for water-wet, oil filled and gas-filled sandstone. Combining acoustic slowness and density gives a range of acoustic impedance values, the higher the contrast, the better the strength of the seismic reflection. These authors showed that at depths greater than about 3000 m TVDSS water-wet sandstone may show a small positive reflection, the presence of hydrocarbons reduces the impedance contrast even further (Figure A3.3; Law *et al*. 2000). However, the impedance contrast between gas-charged and water-wet sandstones is greater suggesting that differences in fluid fill within the reservoir may be more visible. Interpretation of the seismic data has tended to confirm this.

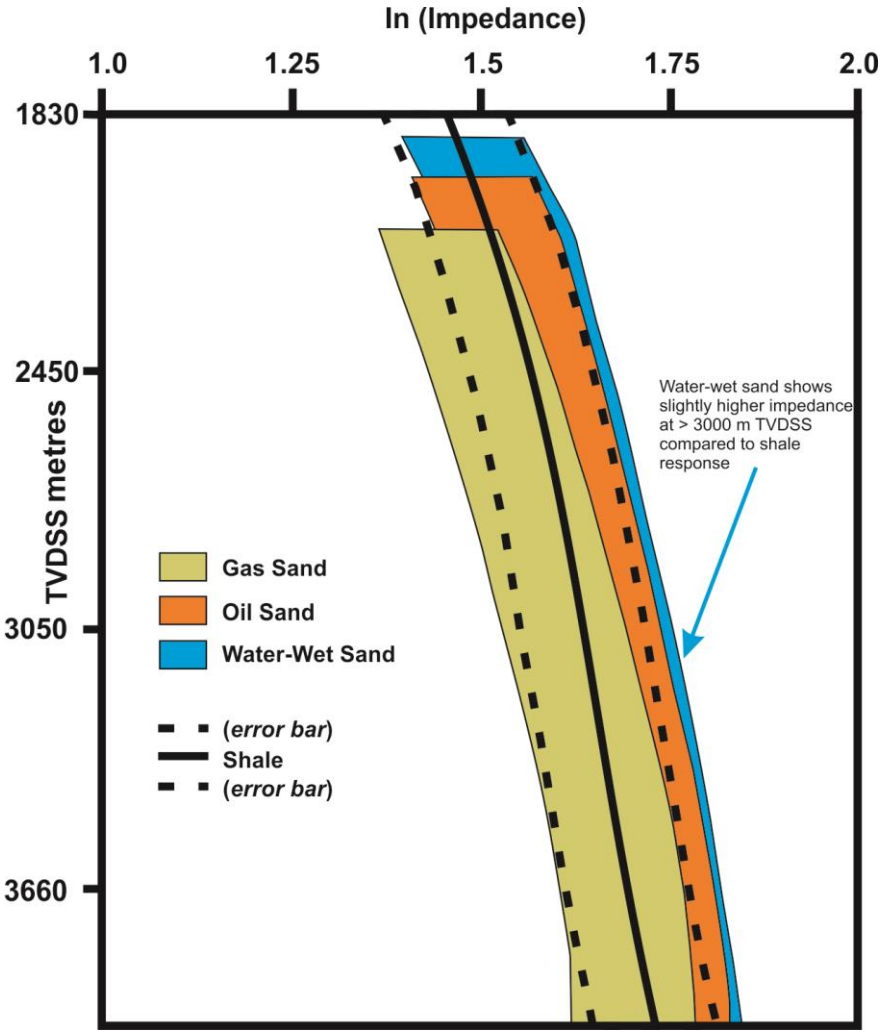


**Figure A3.3. Illustration of variation in acoustic impedance in different fluid filled sands at different depths (modified after Law *et al*., 2000).**

Commercial well penetrations within the study area, that prove Captain Sandstone and have associated TWT information, provided a sparse network of fixed depth points for top and base reservoir and enabled the seismic reflectors to be tied to the seismic database at these specific locations. Top and base reservoir were interpreted away from these data points following seismic reflectors thought to be close to reservoir boundaries and encompassing a seismic package that sometimes included high amplitude reflectors caused by contained hydrocarbon fluids.

#### *A3.2.2.1 Base Captain Sandstone reservoir*

The Base Captain Sandstone seismic reflector was picked on a black peak representing a negative impedance contrast reflecting the change from generally higher velocity Captain Sandstone Member interval and underlying Lower Cretaceous mudstone.

#### *A3.2.2.2 Top Captain Sandstone reservoir (Figure A3.8)*

The Top Captain Sandstone seismic reflector was picked on a red peak representing a positive impedance contrast that reflects the change from lower velocity mudstone and claystone to Captain Sandstone.

#### *A3.2.2.3 Identification of Captain Sandstone reservoir limits*

The Captain Sandstone is known to be limited in its depositional extent and several published outlines exist defined by well penetrations and understanding of regional structure and depositional setting. Detailed seismic interpretation in this study has enabled the limit of sandstone here to be refined (Figure A3.8) by mapping of seismic reflectors associated with the reservoir seismic package (Figures A3.4a, A3.4b & A3.5a, A3.5b). These seismic reflectors sometimes show evidence of termination in the form of decreasing amplitude strength or converging and pinching out of seismic reflectors, all taken to represent the edge of sandstone and thus enabling refinement of the Captain Sandstone limit in this area (Figures A3.4a, A3.4b & A3.5a, A3.5b).

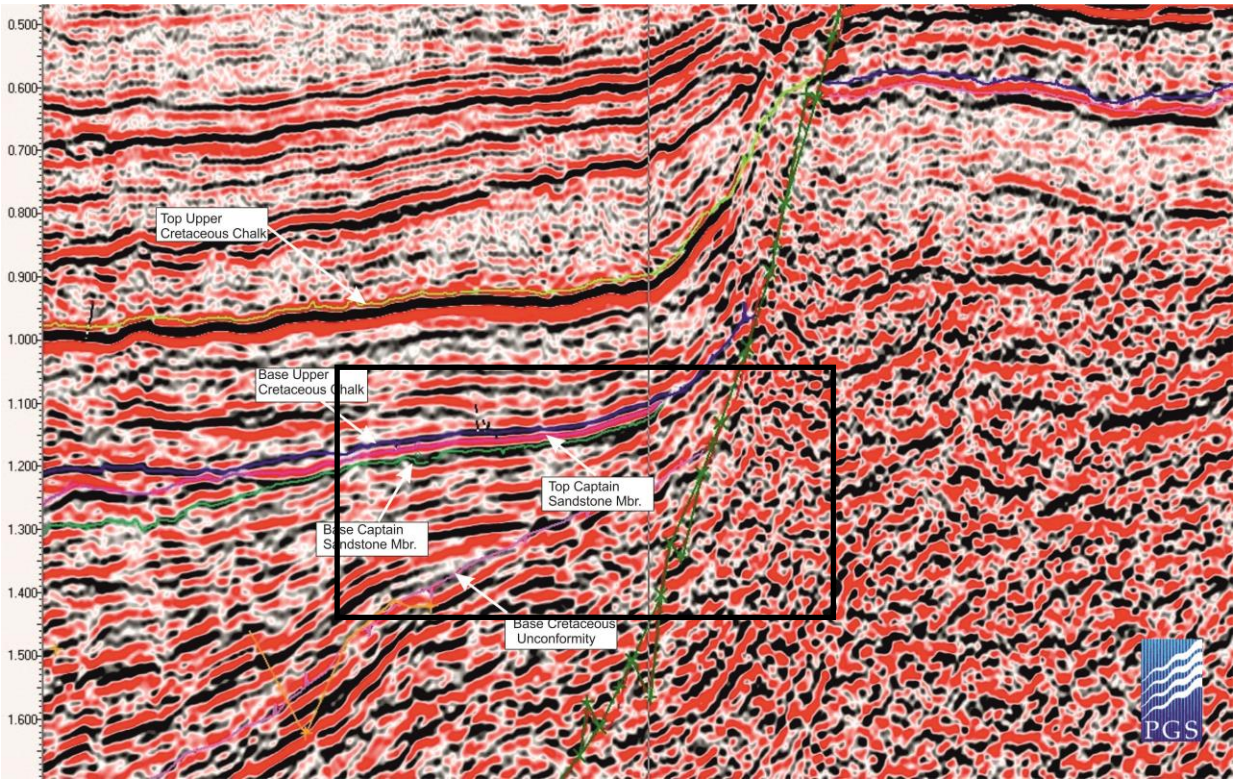


**Figure A3.4a. Interpretation of limit of the Captain Sandstone Member up-dip towards West Halibut Fault (For location see Figure A3.8). Vertical scale in seconds Two-Way Travel Time.**

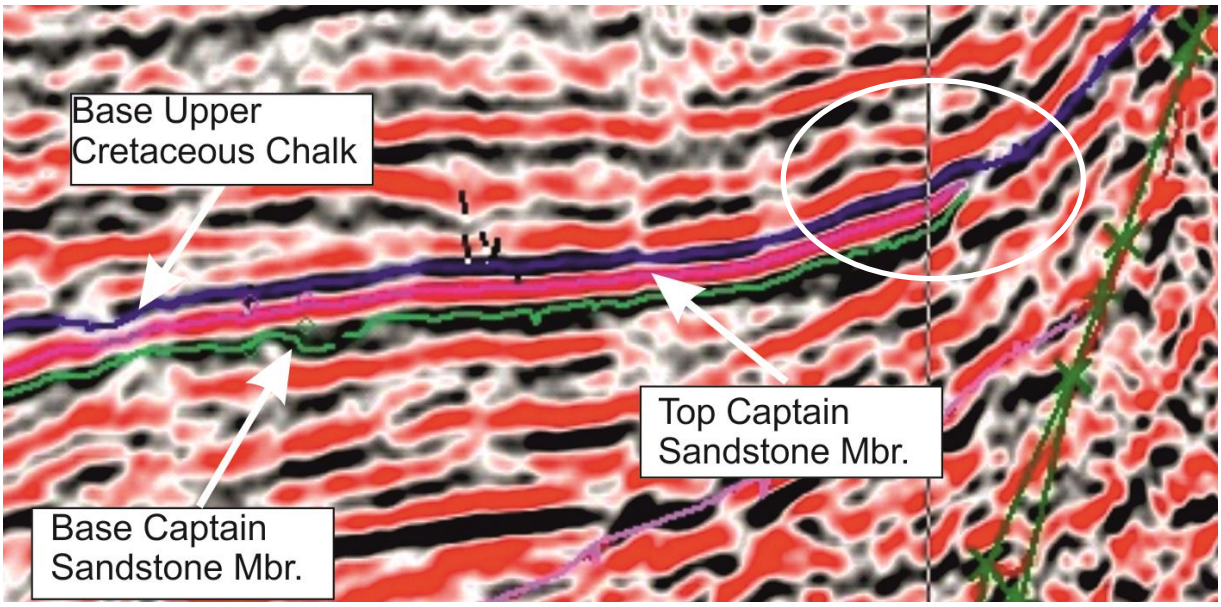


**Figure A3.4b. Detail (inset on Figure A3.4a) of the interpretation (within white oval) of limit of the Captain Sandstone Member up-dip towards West Halibut Fault.**

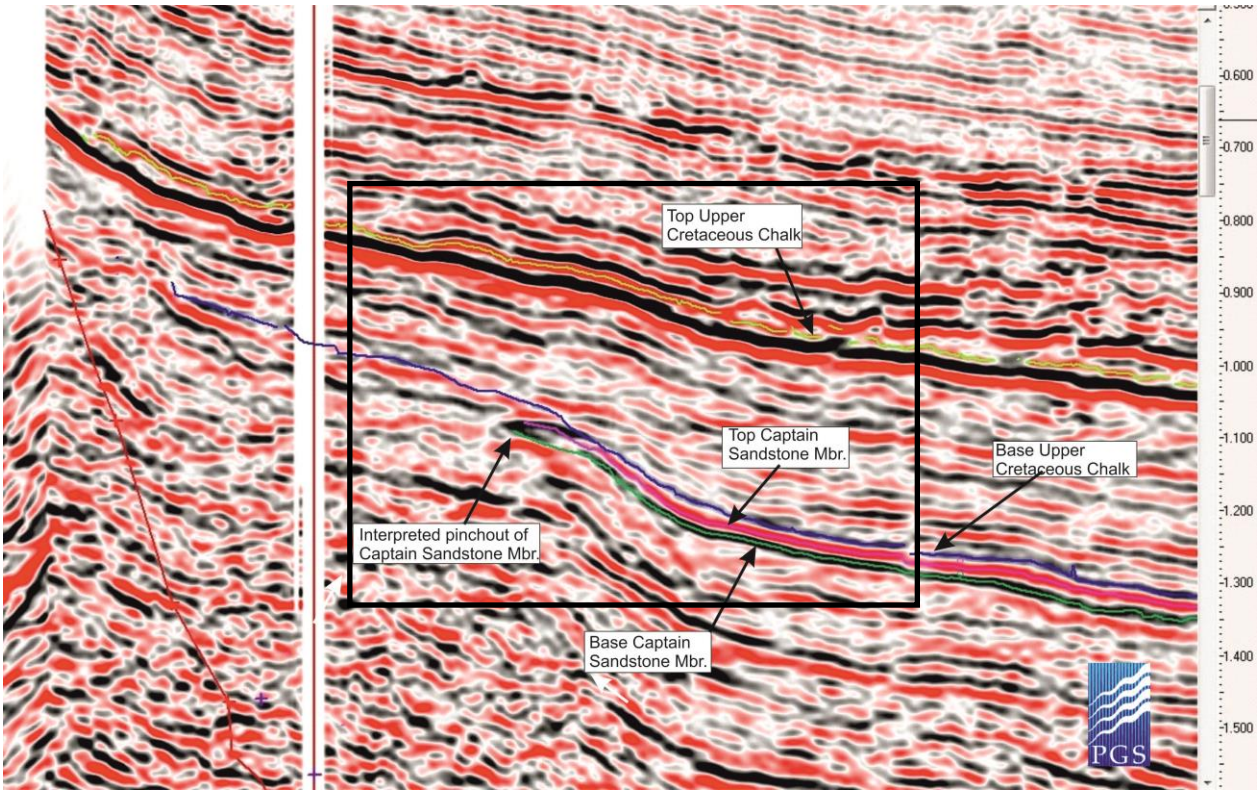


**Figure A3.5a. Interpretation of pinch out of the Captain Sandstone Member up-dip in the north of the Blake Oil Field (For location see Figure A3.8). Vertical scale in seconds Two-Way Travel Time.**

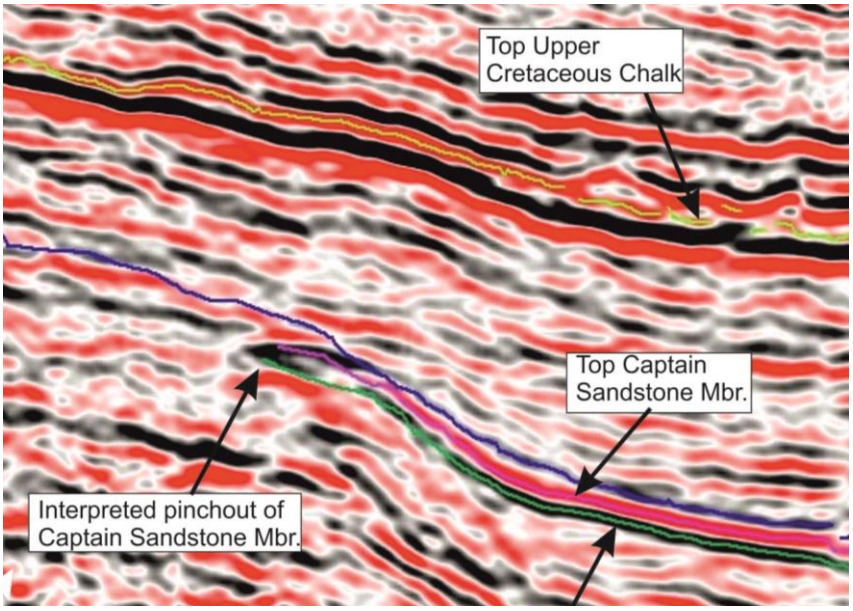


**Figure A3.5b. Detail (inset on Figure A3.5a) of the interpretation of pinch out of the Captain Sandstone Member in the north of the Blake Oil Field.**

### A3.2.3 Base Upper Cretaceous Chalk (Figure A3.9)

This geological boundary is represented by a marked seismic reflector (black) generated by a strong negative acoustic impedance contrast between the high velocity Upper Cretaceous Chalk and lower velocity Rodby Formation mudstone (Figure A3.2). Depending on the thickness of the Rodby and Sola formations mudstone the Base Chalk seismic horizon may be quite close to Top Captain Sandstone surface (Figures A3.2, A3.4, A3.5).

The Base Upper Cretaceous Chalk generates a strong multiple that tends to obscure weaker seismic reflectors such as that generated by the Captain Sandstone.

### A3.2.4 Top Upper Cretaceous Chalk (Figure A3.10)

This geological boundary is represented by a set of high amplitude seismic reflectors generated by a strong positive acoustic impedance between the relatively low velocity Palaeogene sandstone and mudstone succession and relatively higher velocity Upper Cretaceous Chalk (Figure A3.2). Top Upper Cretaceous Chalk was interpreted on a strong and relatively continuous red peak directly above a strong and continuous black peak.

The Upper Cretaceous seismic package displays both strong relatively continuous reflectors and areas where amplitudes are dimmed and internal seismic reflection is weak. Where seen, the seismic reflectors tend to parallel Top and Base Chalk surfaces. The high velocity Upper Cretaceous Chalk succession tends to mask underlying events by absorbing seismic energy so less of the higher frequency energy penetrates to deeper levels.

### A3.2.5 Sea bed (Figure A3.11)

The boundary between sea water and sea bed is represented by a marked seismic reflector generated by a strong positive acoustic impedance between the relatively low velocity water column and the sandstone and mudstone succession beneath. The Sea bed is interpreted on a relatively weak and discontinuous red peak guided by a strong and continuous black peak directly beneath. On the 2D seismic profiles, a strong sea bed multiple is seen in the shallow section at around 300 mS. This is also present on the 3D seismic profiles but is more diffuse and in places cannot be seen.

The seismic package between Sea bed and Top Upper Cretaceous Chalk is composed of a variety of strong continuous reflectors and more chaotic reflections reflecting the diverse Palaeogene lithology comprising thick sandstone some interpreted as channel sandstone interbedded with mudstone. Seismic reflectors are seen to diverge and converge adjacent to the West Halibut Fault indicating its influence on Palaeogene sedimentation. Lack of TWTT information from wells that have penetrated the Palaeogene succession has made it difficult to constrain events with these seismic packages.

### A3.2.6 Mapping of faults

In the ‘Basin-scale’ geological 3D model, the West Halibut Fault was simplified into one continuous fault strand stretching for more than 95 km. The fault trends east to west from Block 12/25 eastwards passing south of the Captain Field before veering north-west to south-east through block 13/24 north-east of the Blake Oil Field and then east-south-east

into Block 13/30 and beyond (Figure 4; Scottish Carbon Capture & Storage, 2011). However, in the 'Detailed' geological 3D model area, a series of faults were interpreted that define the southern boundary of the Halibut Horst (e.g. Figure A3.9). The disposition of the faults is complex and to aid description have been named South, Central and Northern segments (Figure A3.9). In the south of the area the north-west-trending South segment, approximately 4 km long, exhibits a steeply dipping fault plane and throws ranging from 300 m to 600 m at Base Chalk level. The northern extent of this segment is cut by an east-north-east-trending graben (Figure A3.9). Beyond this graben the Central segment continues the north-west trend for approximately 3.2 km, before veering to a nearly northward trend which it continues for at least 8 km to the northern edge of the 'Detailed' 3D model area. The dip of the fault plane in the Central segment is relatively shallow in the north-west-trending part of the fault but steepens after it veers to the more northerly direction. However, the north-west trend that defines the edge of the Halibut Horst is taken up by another well-defined fault, the Northern segment that intersects with the Central segment forming a relay ramp.

### A3.3 DEPTH CONVERSION

Depth conversion was carried out within the Kingdom Suite software. A velocity model was created by plotting Two-Way-Travel-Time (TWTT) values downhole against their TVDSS (m) depth equivalents from 13 wells located within the study area. The time-depth pairs showed good cohesion and an exponential line could be plotted through the data (Figure A3.6). The equation for this line (Equation b) was applied to the gridded TWTT surfaces to convert them to depth.

Equation (b), $y=1149.7x^{1.4706}$

A slight bulge in the plotted TWT/Depth pairs at between 1000 and 1700 m TVDSS reflects the higher velocity Upper Cretaceous Chalk succession. Between these depths, the TWTT is less than if the bulge was absent i.e. the sound waves travel more quickly within this section (Figure A3.6). This effect will be expected to produce slight error in the depth conversion.

Depth converted values at well locations were compared to actual depths at the wells to validate the depth conversion process. Mean error was greatest at Top Chalk level (6.9%), 2.8% at Base Chalk, 2.3% at Top Captain Sandstone, 2.6% at Base Captain Sandstone and 3.36% at Base Cretaceous.

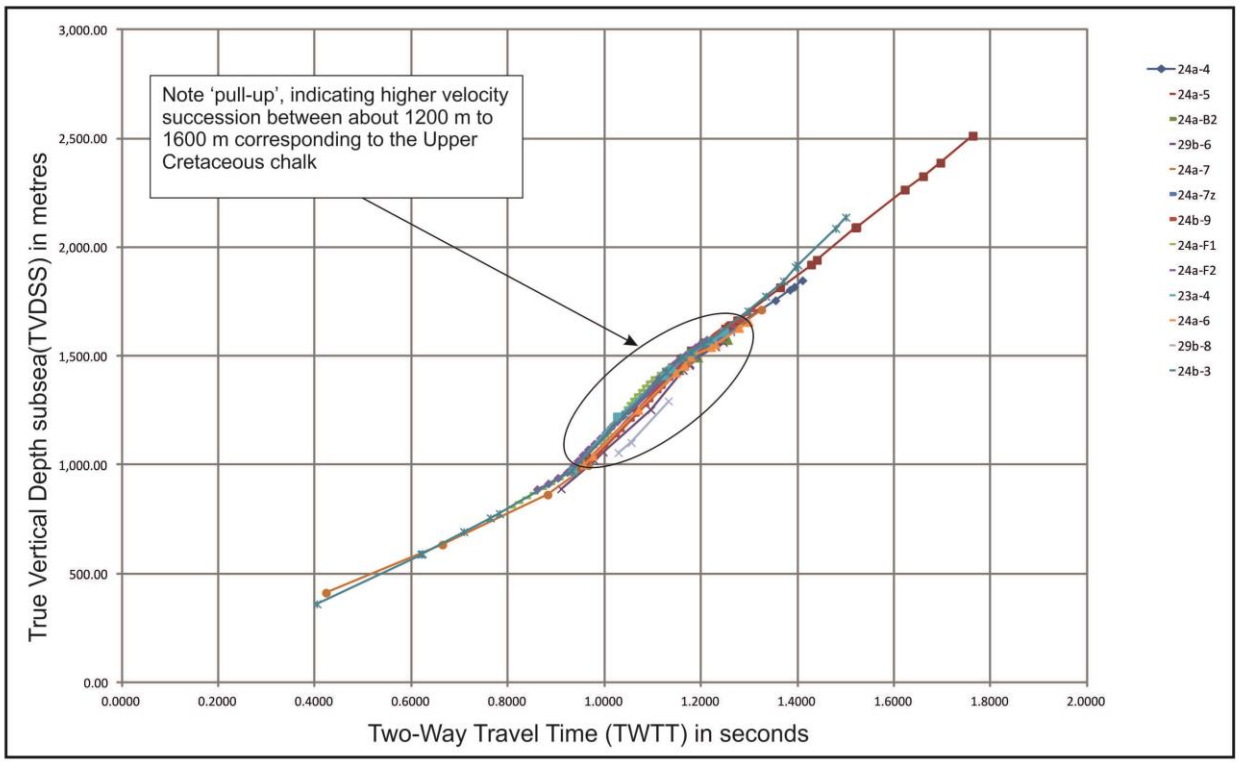


**Figure A3.6. Velocity model used in depth conversion of interpreted TWTT surfaces.**

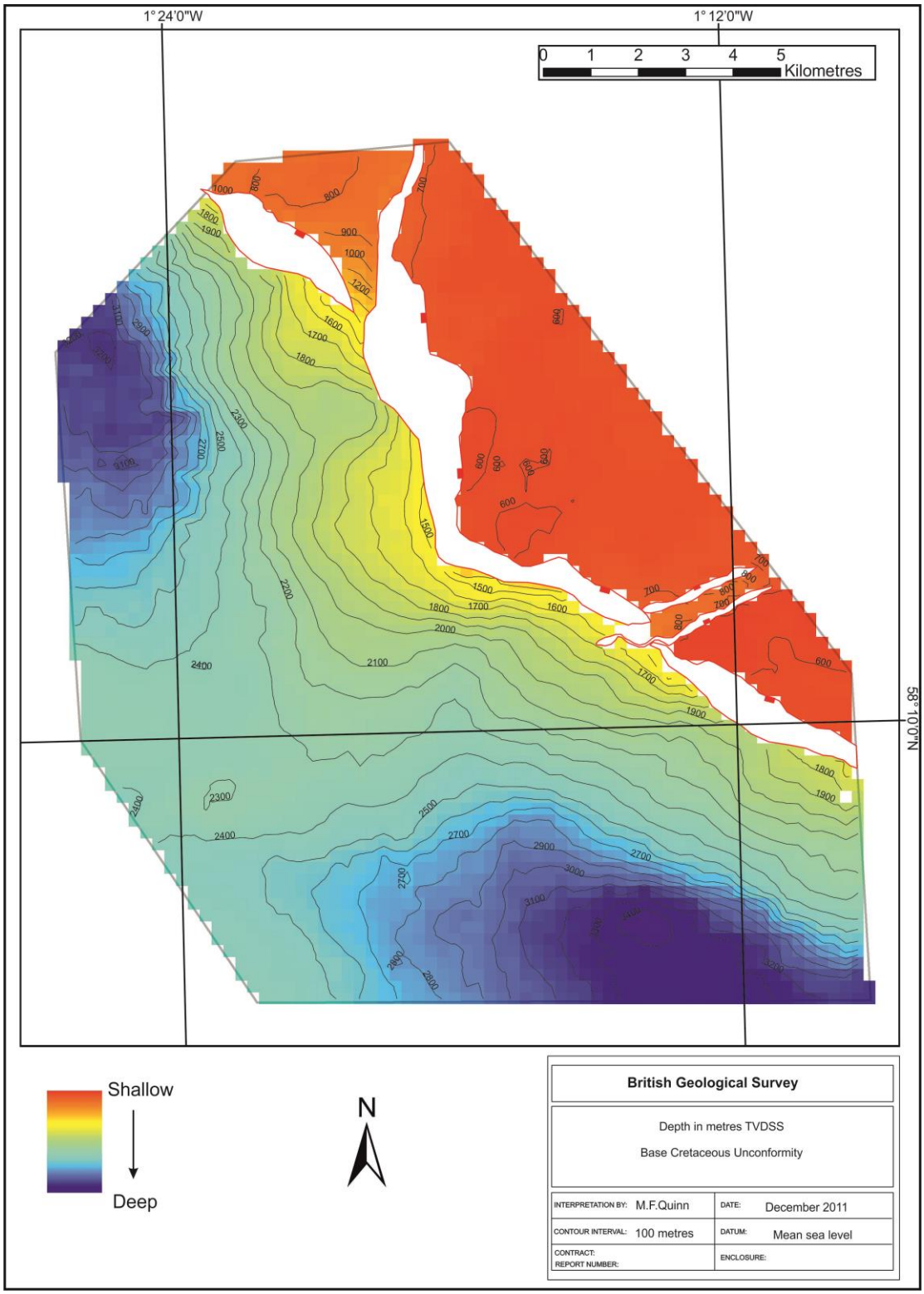


**Figure A3.7. Depth structure map of Base Cretaceous Unconformity, contours in metres below sea level, 'Detailed' geological 3D model.**

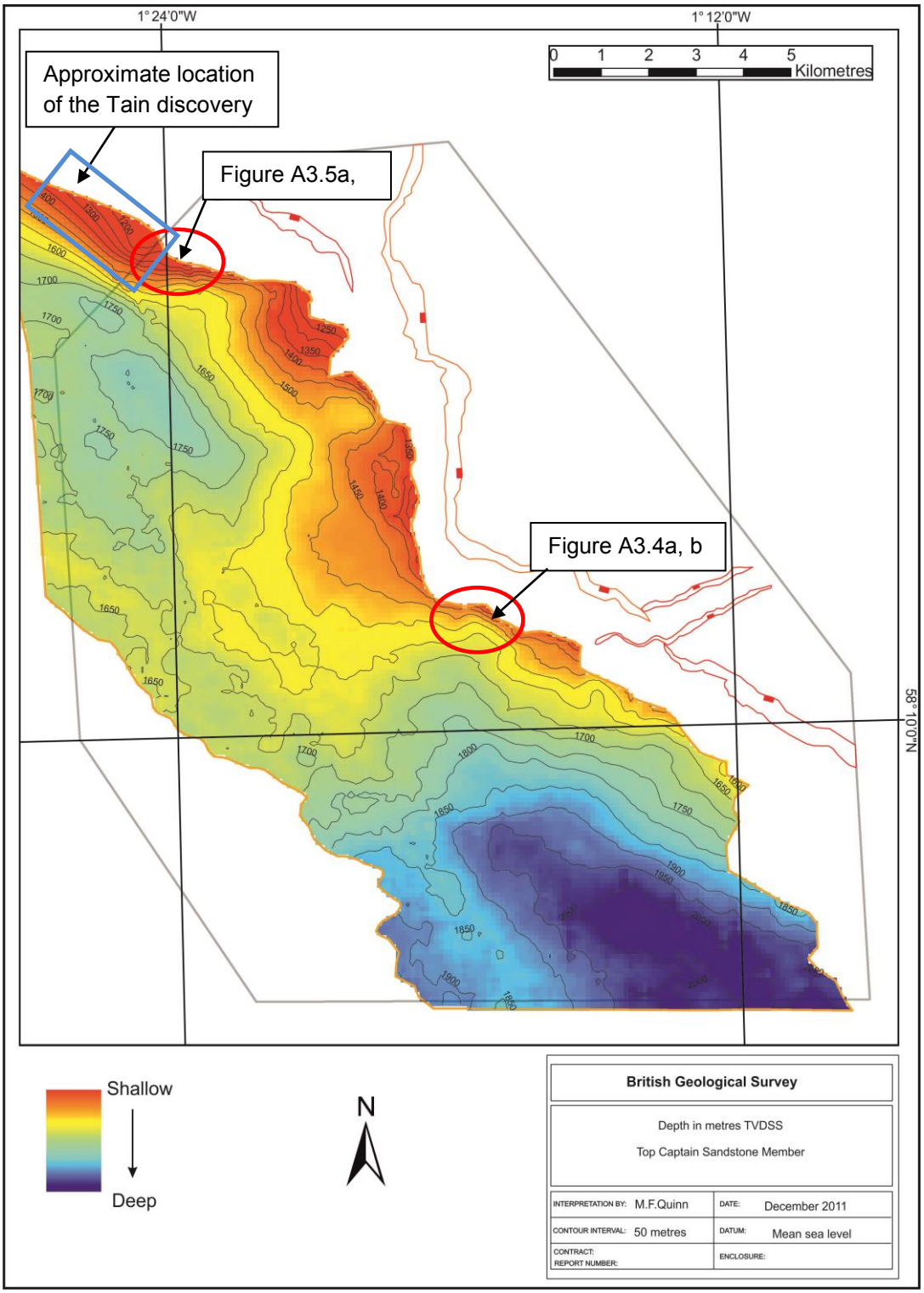


**Figure A3.8. Depth structure map of Top Captain Sandstone Member, contours in metres below sea level. Red ovals highlight locations of seismic profiles illustrating pinch out of the Captain Sandstone Member. Polygon marks extent of 'Detailed' geological 3D model.**

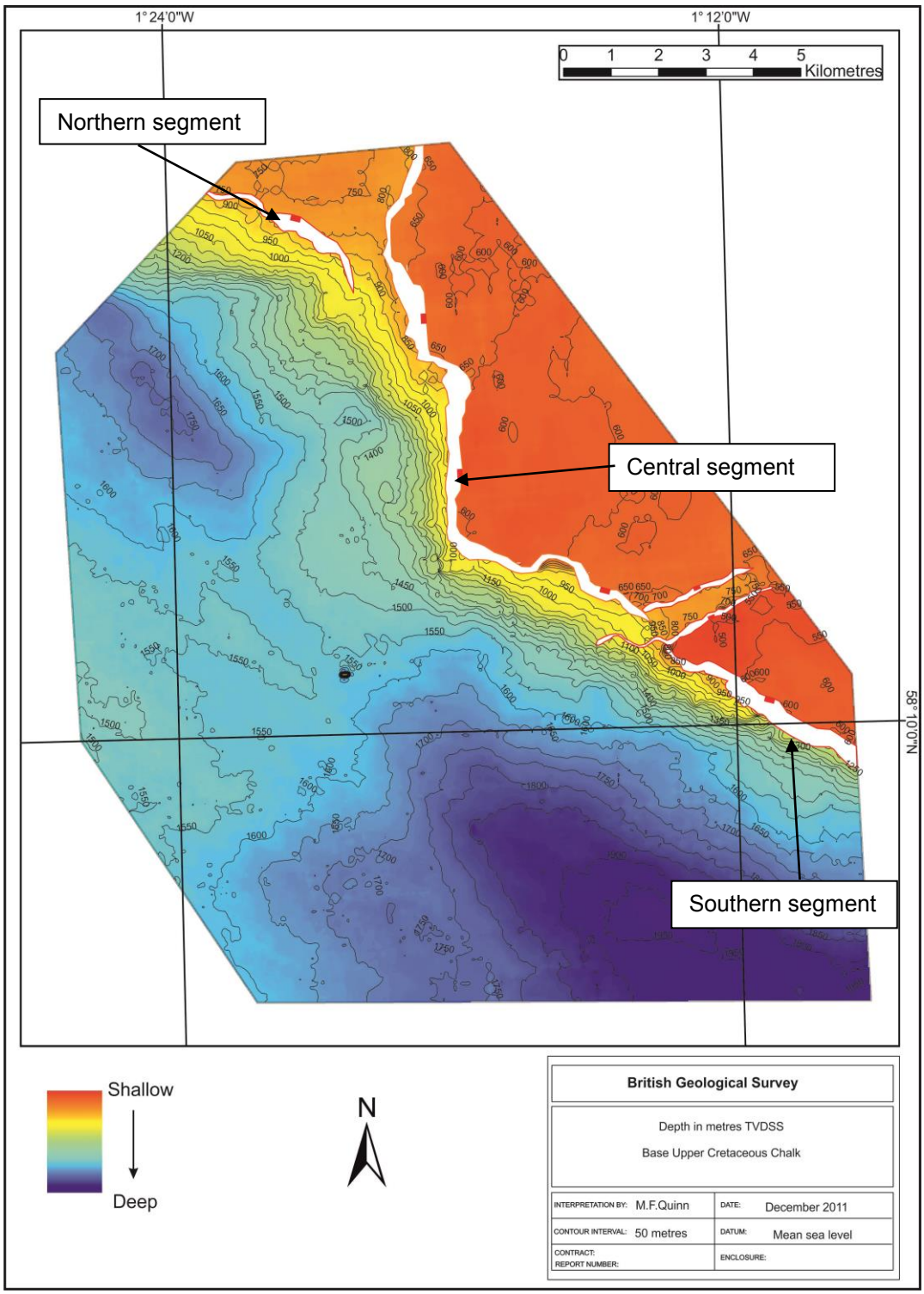


**Figure A3.9. Depth structure map of Base Upper Cretaceous Chalk, contours in metres below sea level, 'Detailed' geological 3D model.**

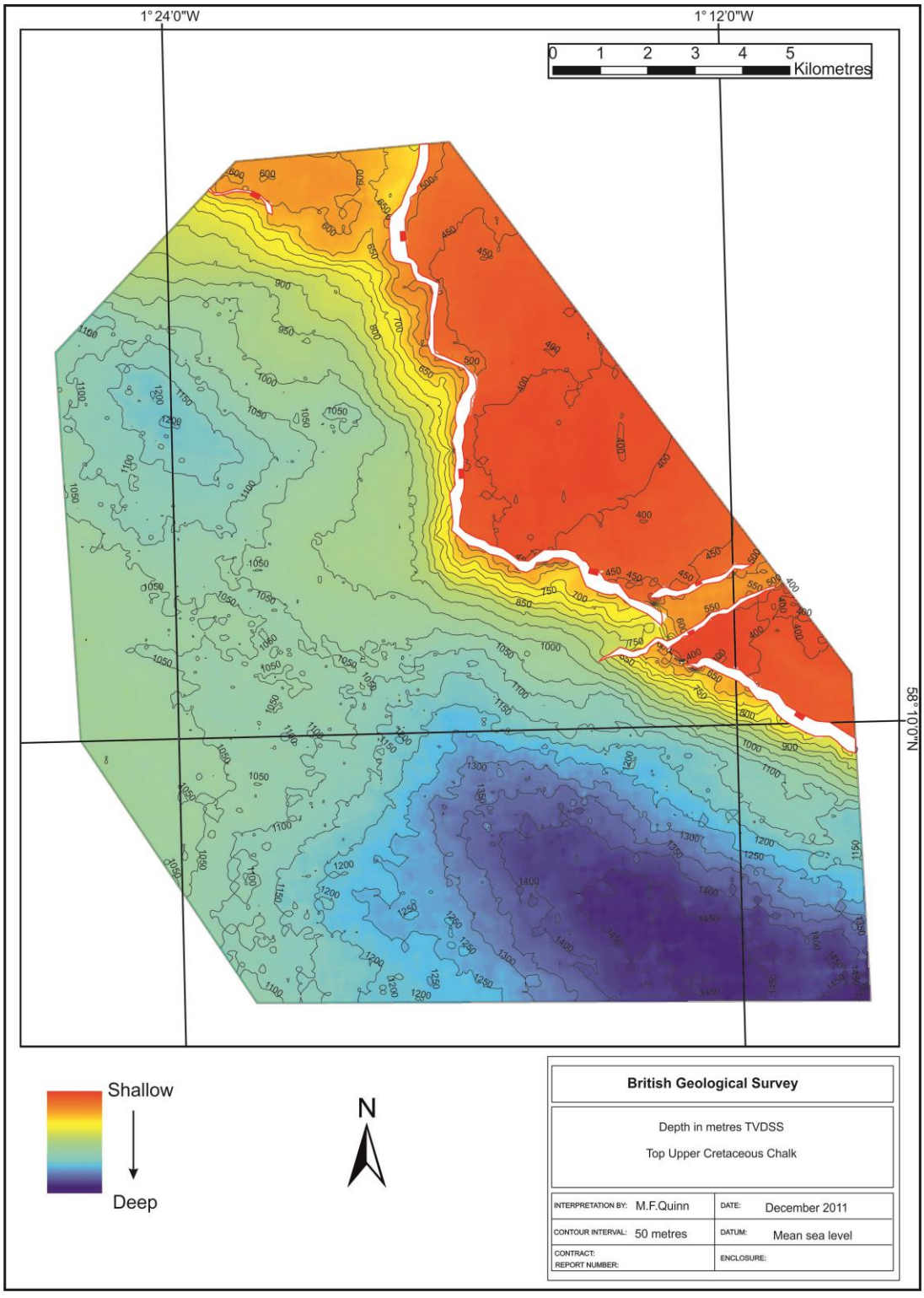


**Figure A3.10. Depth structure map of Top Upper Cretaceous Chalk, contours in metres below sea level,'Detailed' geological 3D model.**

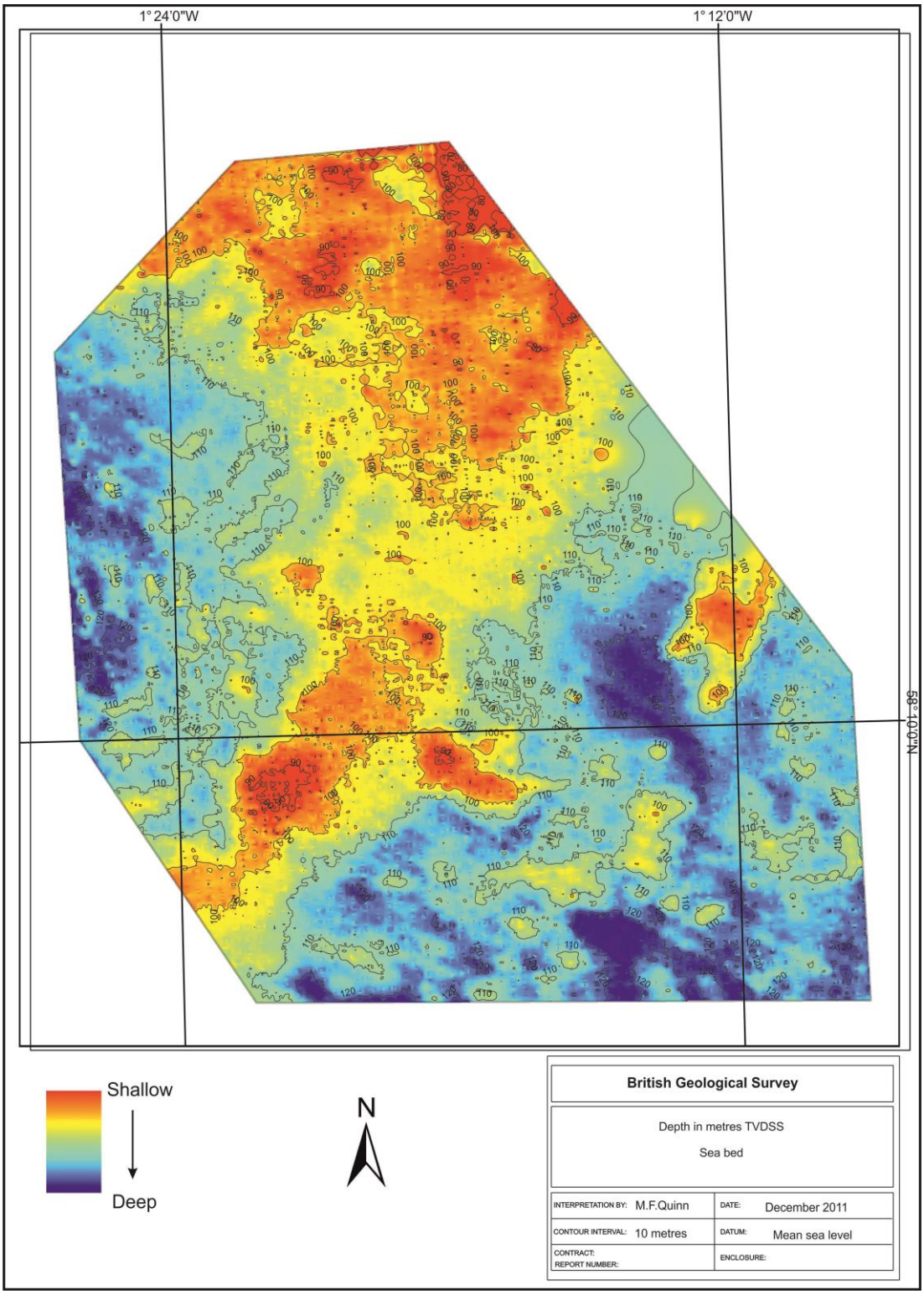


**Figure A3.11. Depth structure map of the Sea bed, contours in metres below sea level, 'Detailed' geological 3D model.**

## A3.4 CONSTRUCTION OF 3D GOCAD™ GRIDDED SURFACES MODEL

The Storage Site and Complex will be defined through subsequent modelling work in Task 3.2. At this stage, any deductions have come from geological knowledge using the following evidence base and available data. This is referred to throughout the text. In general, values for rock thickness, static capacities etc in the region of the Storage Site have come from data within the 'Detailed' model, unless otherwise indicated.

The model includes an area of approximately 18 km by 16.5 km encompassing the Blake Oil Field, the adjacent south-central part of the Halibut Horst and the block-bounding West halibut fault system.

### A3.4.1 Model Data

The GoCad™ model was based on an interpreted and depth converted 3D seismic dataset (refer to seismic survey identifier) for six stratigraphic horizons (Sea bed, Top Chalk Group, Base Chalk Group, Top and Base Captain sandstone and Base Cretaceous Unconformity) and eight single or intersecting fault planes.

Initial attempts to import proprietary data grids, generated by the seismic interpretation software, produced undesirable patterning of the derived model surfaces. Modelling was hence based on the interpreted seismic point data for the horizons and fault surfaces, imported to GoCad™ as XYZ point sets.

### A3.4.2 Horizon modelling

Standard GoCad™ workflow methodology was employed. A rectilinear model boundary line was constructed to fit the seismic data areal extents. This model boundary was used as the outline polygon in the stratigraphic horizon surface creation. The outline polygon for the Captain Sandstone was derived from the interpreted stratigraphical pinch-out of the aquifer when within the licensed 3D seismic data and elsewhere from the areal extent of that data set.

The regional stratigraphical surfaces were modelled to a 100 m average density triangular mesh and the Captain Sandstone to a 50 m mesh. The stratigraphical surfaces mapped from seismic data and the Captain Sandstone top and base surfaces were modelled in the workflow without notable problems. No post-processing smoothing operations were run. However, the 'fit to well markers' utility was run on all surfaces to honour the well intercepts. This process gave satisfactory results for most surfaces but caused a laterally extensive pull up of the Top Captain Sandstone surface, beyond the controlling well locations. This forced, in turn, local intersections of the Top Captain Sandstone surface with the overlying Base Chalk surface, especially along the northern, eastern and southern borders as mapped.

The result was unrealistic modelling of the seal rocks (Rodby Formation mudstone), which is believed to be continuous in the 'Detailed' 3D model area. To compensate, a minimum vertical separation was enforced between the two surfaces (GoCad™ 'remove crossovers'). This 'quick fix' utility was not wholly successful and construction of a laterally competent seal may need to be addressed within subsequent modelling work.

Two planar surfaces were created to emulate the Oil-Water and Gas–Oil contacts published for the Blake Oil Field at 1607 m and 1578 m below sea-level respectively.

GoCad™ solid (tetrahedron) objects were created from the calculated isopach property for the Captain Sandstone layer and the seal rock, to determine gross volumes. A third solid was created for the Captain Sandstone above the Oil-water contact to allow calculation of the modelled closure volume of the Blake Oil Field.

### A3.4.3. Faults

Modelling of the fault system proved somewhat problematic due to the irregular surface geometries forced by the seismically interpreted point data. Fault polygons were created by interactively editing the curves outlining the extent of individual fault data sets.

After some 'trial and error' modelling, the main segment of the West Halibut Basin Fault System, which largely defines the block/basin margin, was modelled in two parts (faults numbered 4 and 19 in the model files). The two faults merge in a conspicuous ramp or transfer zone across the northern part of the model. The fault to horizon fitting process was achieved in the workflow but considerable manual editing of both point control data and surface geometry was required to achieve a well integrated fit along the fault/horizon contact lines. Subsidiary faults were modelled within, and at the margin, of the basin, as well as a cross-cutting set defining a small graben feature, inset into the Halibut Horst.

No faults were modelled as cutting or bounding the Captain Sandstone.

### A3.4.4 Wells and Logs

A total of 45 wells were loaded to the GoCad™ project including the Blake Oil Field 'B' and 'F' platforms. The majority of wells were deviated and the well paths were imported from column-based text files containing measured depth, azimuth and inclination values. Vertical well data (Wellhead location in UTM coordinates, KB height and depth to TD) were manually entered from the composite log or other log headers.

Stratigraphical markers were entered manually, either from a spreadsheet previously prepared for the seismic interpretation, or from a composite log. Associated well permeability logs for the Captain Sandstone interval were imported directly from available digital LAS format files.

## A3.5 Construction of the gridded model surfaces (GoCad™ project file name *Blake_regional_merged_model*)

The second part of the modelling project was to merge the Blake Oil Field model, described above, with the previously created Outer Moray Firth Captain Sandstone regional model (Scottish Carbon Capture & Storage, 2011). This account will deal solely with the process of merging the local and regional models using GoCad™ utilities.

A comparison of the 'Detailed' and 'Basin-scale' models showed that, despite being derived from quite different data sets, there are no major differences in the overall depth profiles of individual surfaces. Any initial differences in the extent and geometry of the main basin-

bounding fault system are due to the coarser scale and lower resolution of the 'Basin-scale' model. However, marked differences in the extent and geometry of the main basin-bounding fault system are apparent, as is the mapped extent of the Captain aquifer sands. After some experimentation, it was found that, because of these configuration differences, simply 'snapping' the regional surfaces, locally, to the Blake Oil Field model was not a viable option.

It was decided to 'cookie-cut' the regional model along the project boundary outline, drop in the Blake Oil Field surfaces, then weld across the surface joins. Similarly, the relevant segment of the regional West Halibut Fault would be deleted out and the free ends grafted onto the fault system mapped in the 'Detailed' model.

Cutting the space to accommodate the 'Detailed' model surfaces was accomplished simply by projecting the model outline curve vertically down through the regional model surface stack and running the GoCad™ 'surface cut by curve' utility. The now disconnected surface parts were then deleted. New regional surfaces were then created incorporating the relevant Blake Oil Field surface parts. The GoCad™ utility to weld, or sew, together adjoining, but disconnected surfaces was applied, resulting in seamless joins.

The join of the West Halibut Fault System was processed in a similar manner, although the cutting and deletion of the regional fault surface was done manually and trimmed to afford a smooth join. The overall model merging process resulted in a loss, at least in part, of the horizon/fault contacts and further manual editing was required to restore an integrated fit.

The inevitable drawback of this method is that where there is a marked change in elevation across the model joins, a noticeable step feature can result. The join is also highlighted by the change in surface texture, engendered by the contrasting fine to coarse model surface control-data density (A3.12).

With the current merged model, these edge effects appear not to be a major issue, especially if imaged without vertical exaggeration. A visually improved, that is smoothed, model can be obtained in GoCad™ by running a re-interpolation of the regional surfaces onto the relevant merged controlling data-sets (A3.13). However, rather than applying heavy-handed smoothing algorithms, it is recommended that the model be taken forward as it stands, but with a clear declaration of the inherent limitations of the modelling process.

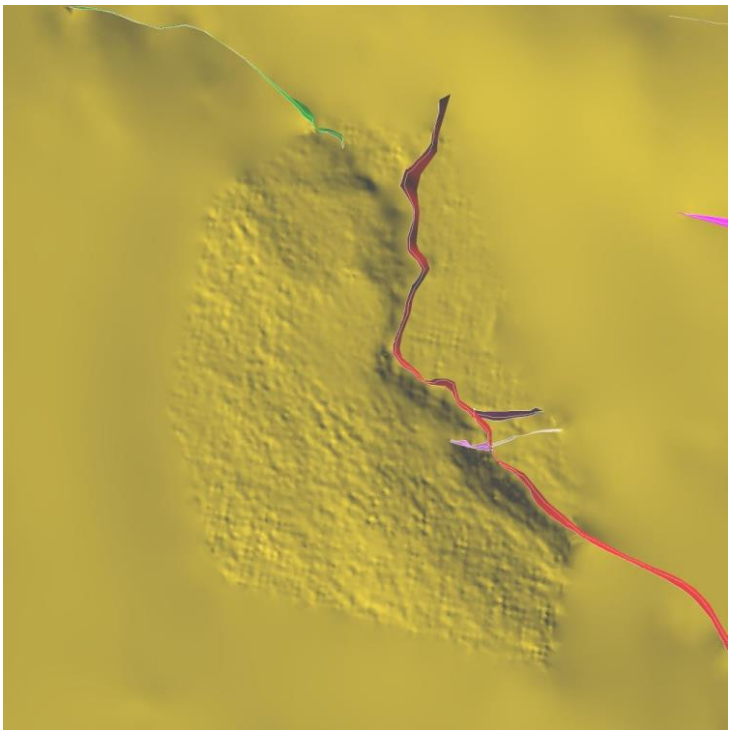

**Figure A3.12. Merged and smoothed model surfaces; Top Chalk.**

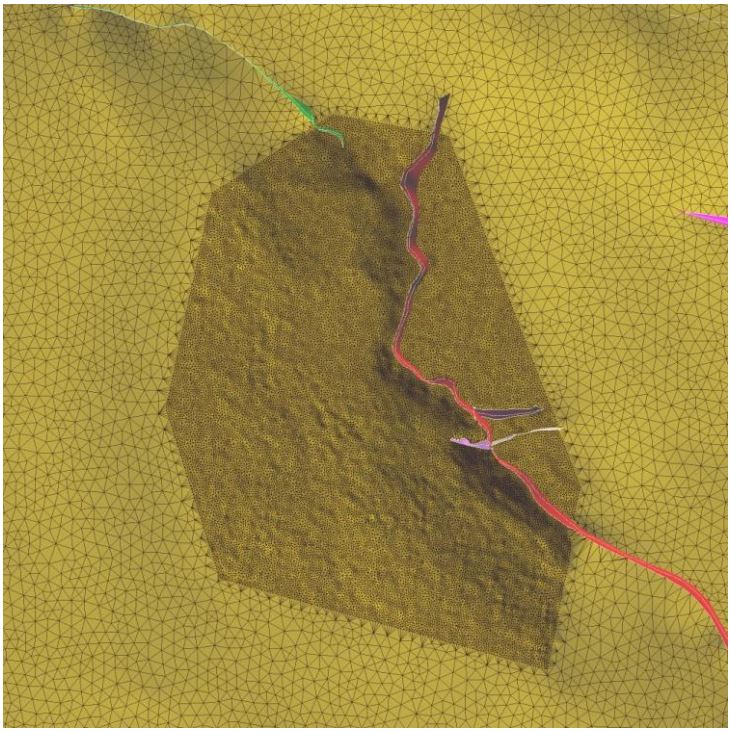

**Figure A3.13. Contrast in surface texture.**

The merged 'Basin-scale' and 'Detailed' geological 3D model and a separate 'Detailed' 3D model were used for the construction of the geocellular model.

**A3.6 Construction of the geocellular model and flow simulation grids**

GOCAD-SKUA - Paradigm™, software devoted to the integration of surface and sub-surface data, was used to build complex structural model and 3D geocellular grids for fluid flow simulations.

Usually this kind of software is used in petroleum industry to create sub-surface models at field scale (few hundred kilometres square) with a rather good resolution both in vertical and horizontal directions. Dealing with regional scale increases the horizontal dimensions (than become greater than 100 by 100 km) and may induce a loss in vertical resolution. This is a challenge for the geomodelling for CCS studies where building reservoir models at both regional and local scales is now becoming the standard.

The number of active cells in the final grid (cells effectively used for fluid flow simulations) was limited to less than 100 000, following discussions with the reservoir engineer leading Task 3.2 fluid flow simulations. This constraint speeds up the fluid flow simulations, and consequently increases the number of possible simulation scenarios to test different hypotheses. These scenarios, related to assumptions on multiple parameters for $CO_2$ injection, faults and model boundary conditions, will be described in details in the fluid flow simulation report for Task 3.2.

The main added-value of SKUA is that surface modelling is constrained by geological rules defined by the users. This means that all surfaces of a model are built in a same run accounting for, of course, the input data but also some given geological rules (stratigraphic scale, relationship between surfaces, defined depositional area, *etc*…). This new approach thus requires all input data to be geologically consistent and stringent quality control to check this consistency and the associated geological rules. This methodology guarantees that the structural model can be used to build geometrically and topologically consistent 3D grids.

A key lesson learned from this CCS study is that the whole team (the work being often split between different institutions) must pay attention at each step of the process to geological consistency. There must be consistency from raw data to surface model production, quality control and geological reality.

**Principles**

Horizons, faults surfaces, and also well markers are the usual basic inputs for structural modelling. Horizons define unit boundaries of each stratigraphical unit and faults are used to define fault blocks, which are key features to correctly create 3D grids.

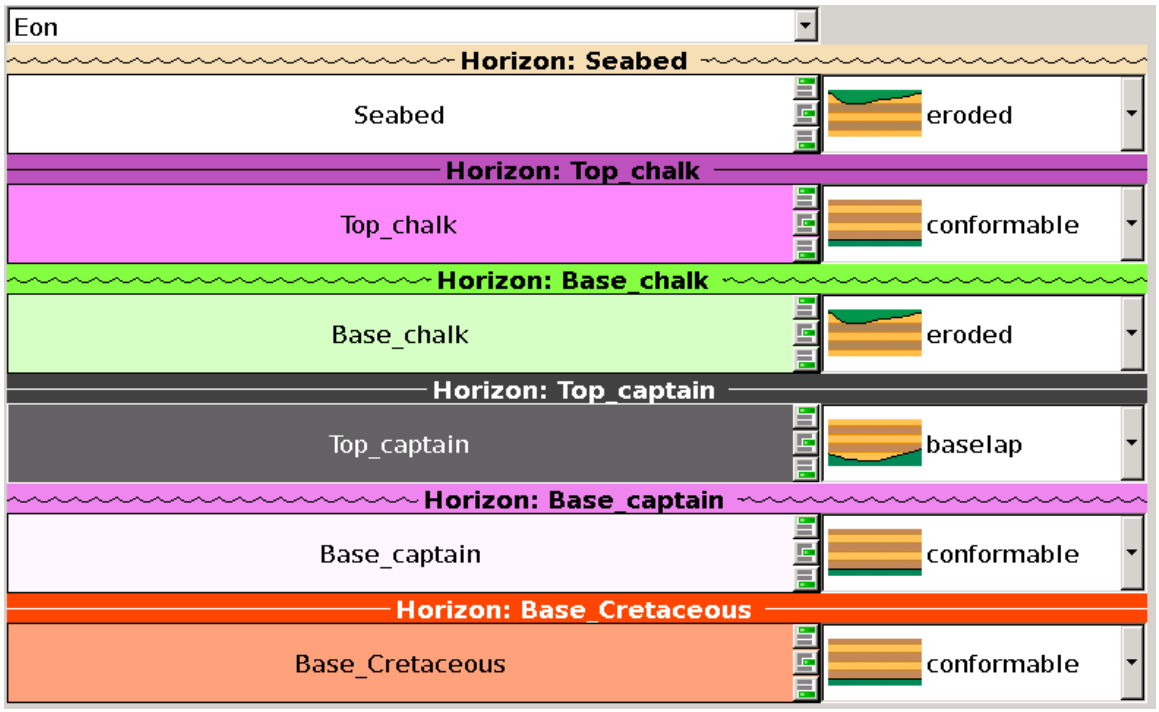


**Figure A3.14. Stratigraphical scale and associated geological features.**

Normal, reverse or unknown is an attribute that could be attached to each fault to add some control on the horizon geometry modelling.

When using SKUA, it is mandatory to define the stratigraphical scale of the model. This scale is used to define the chronological ordering of the horizons (Figure A3.14). It defines the rules, which constrain the geological and therefore the geometrical relationships between horizons that are used for structural modelling. The stratigraphical scale finally controls the depositional mode for each stratigraphic unit that can be defined as conformable, non-conformable, eroded or with baselap. This information serves as a guide for the grid structure.

Optional geological features such as deposition outline, non-deposition outline, erosion outline and non-erosion outline could in addition be attributed to each horizon in order to better constrain surface modelling.

All these data and constraints based on some geological knowledge are introduced in SKUA in order to improve the structural modelling. In counterpart, as already underlined in the introduction, raw input data horizons, faults and well markers must absolutely be consistent with these geological constraints.

**The Captain Model**

From Sea bed to base Cretaceous, the initial surface model (Figures A3.15 and A3.16) is composed of six layers: Sea bed; Top Chalk; Base Chalk; Top Captain Sandstone; Base Captain Sandstone; Base Cretaceous.

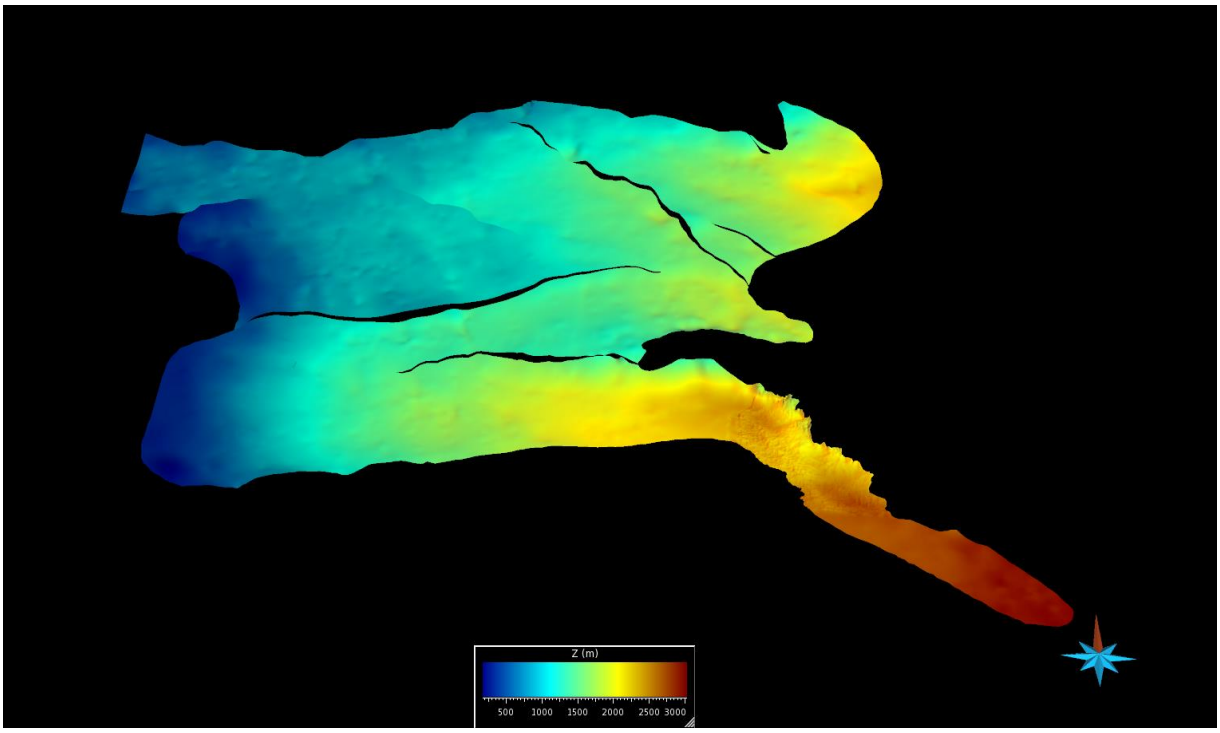


**Figure A3.15. Initial Top Captain Sandstone horizon provided as a surface.**

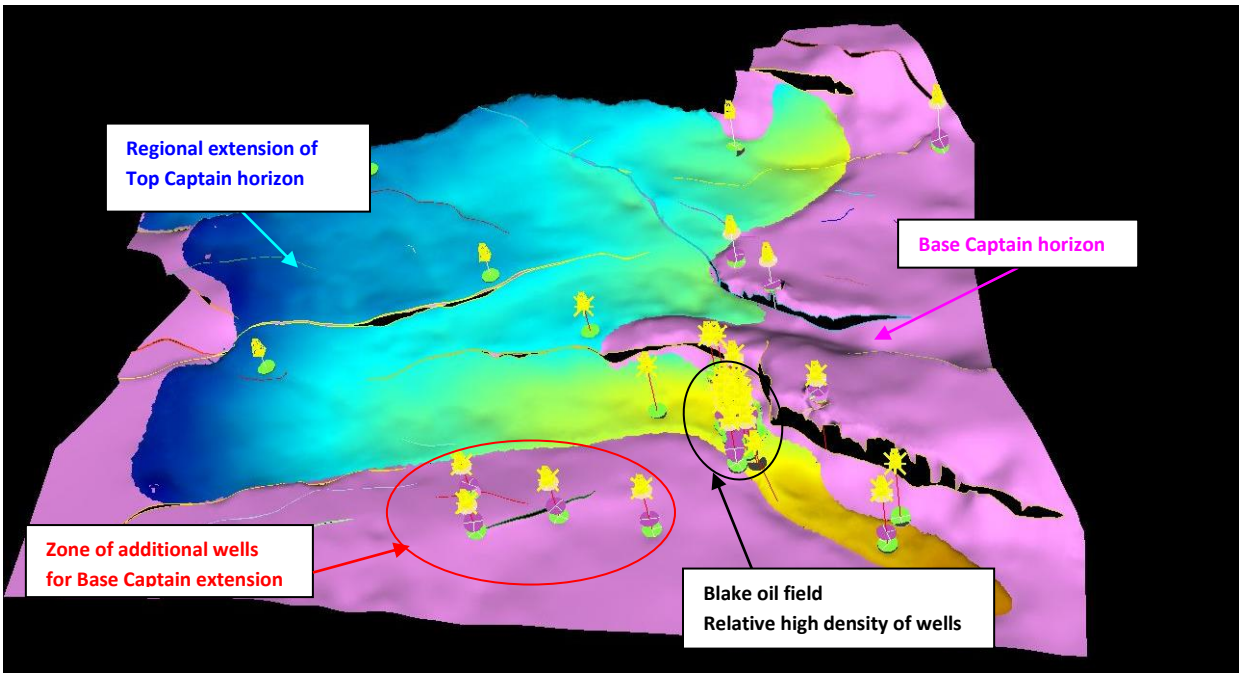


**Figure A3.16. 3D view of Top Captain and Base Captain Sandstone horizons at regional scale showing all wells used in this study. Black oval around area of detail shown in Figure A3.17.**

In addition, some wells (Figure A3.17) have also been provided with horizon markers and well logs interpreted in terms of effective porosity in the Captain Sandstone reservoir. The spatial distribution of these wells is not homogeneous and their density is of course much higher where hydrocarbons fields have been discovered and put in production.

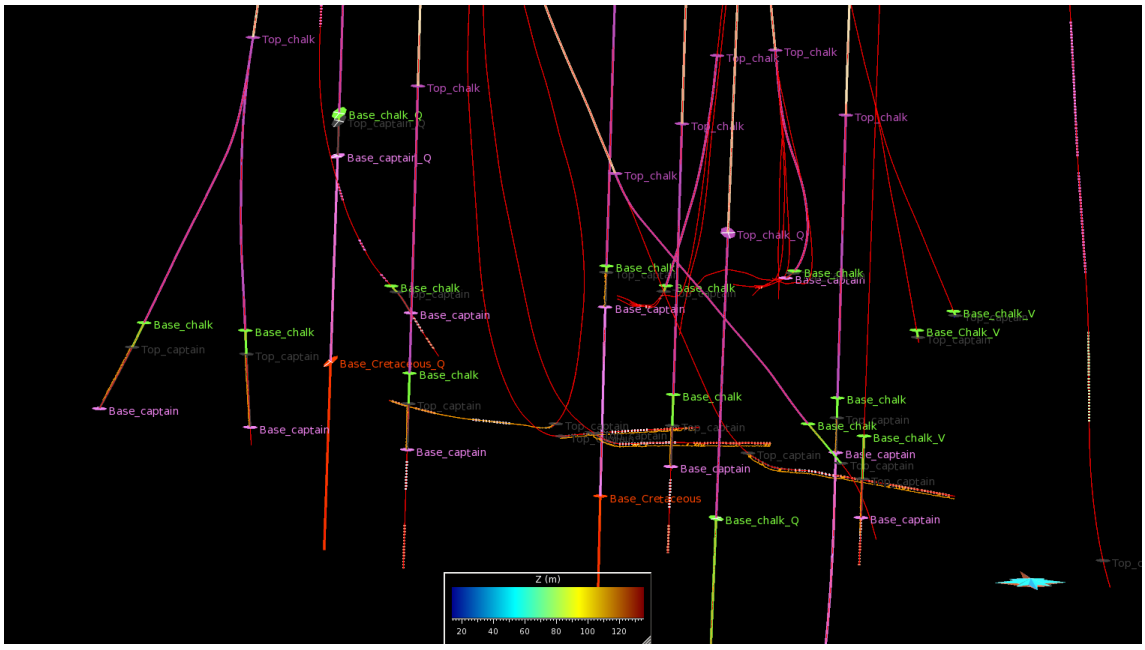


**Figure A3.17. Zoom to Blake Field showing relative high density of wells in this area.**

Some additional wells and associated markers (Table A3.1) have been provided in order to regionally extend the Base Captain surface which was initially restricted to the extent of the Top Captain Sandstone to enable closure of the sandstone volumes within the model.

| | 13 24a-F1 | 13 24a-F1 | 13 24a-F1 | 13 24a-F1 | 13 24a-F2 | 13 24a-F2 | 13 24a-F2 | 13 24a-F2 | 13 24a-F2 | 13 24b-3 | 13 24b-9 | 13 29b-5 | 13 29b-6 | 13 29b-8 | 13 29b-9 |
|---|---|---|---|---|---|---|---|---|---|---|---|---|---|---|---|
| Seabed | N/A | N/A | N/A | N/A | Unpicked | Unpicked | N/A | Unpicked | N/A | | | | Unpicked | | Unpicked |
| Top_chalk | N/A | N/A | N/A | N/A | Unpicked | | N/A | Unpicked | N/A | | Unpicked | | Unpicked | Unpicked | Unpicked |
| Base_chalk | N/A | N/A | N/A | N/A | | | N/A | Unpicked | N/A | | | | | Unpicked | Unpicked |
| Top_captain | N/A | N/A | N/A | N/A | | | N/A | | N/A | | | Eroded | | | |
| Base_captain | N/A | N/A | N/A | N/A | Unpicked | Unpicked | N/A | Unpicked | N/A | | | Eroded | | Unpicked | |
| Base_Cretaceous | N/A | N/A | N/A | N/A | Unpicked | Unpicked | N/A | Unpicked | N/A | | Unpicked | | Unpicked | Unpicked | Unpicked |

**Table A3.1. Well markers status for each well. Surface model must respect these markers.**

To precisely define the extent limit of each horizon, the limit could be optionally associated with an erosion outline. Depending on input data geometry, one erosion phase could affect several horizons. This is typically the case in this study where sea bed erosion affects the westward extension of all the horizons down to the Base Captain.

Table A3.2 below summarizes additional geological features introduced to constrain the structural modelling.

| Horizons | Erosion outline | Deposition outline |
|---|---|---|
| Top Chalk | ☑ | |
| Base Chalk (mudstone seal) | ☑ | |
| Top Captain Sandstone (reservoir) | ☑ | |
| Base Captain | | ☑ |
| Base Cretaceous | | |

**Table A3.2. Summary of additional geological features constraining structural modelling.**

The modelling process began with the creation of the fault network (Figure A3.18) that accommodated all fault relationships present in the area such as branching faults, dying faults, reverse faults and also crossing faults. The initial fault modelling has an impact on final grid quality and must be carried out with care.

The next step consisted of modelling the six interpreted horizons, Sea bed, Top Chalk, Base Chalk, Top Captain Sandstone, Base Captain Sandstone and Base Cretaceous using GOCAD-SKUA - Paradigm™ software (Figures A3.19, A3.20, A3.21, A3.22).

From this surface model, the 3D grids are then generated automatically with very little additional input. The same structural model can be used to generate several customised 3D flow simulation grids at local scale or at regional scale (Section 3.3, Figure 18) using all the layers or a subset of layers around the targeted reservoir.

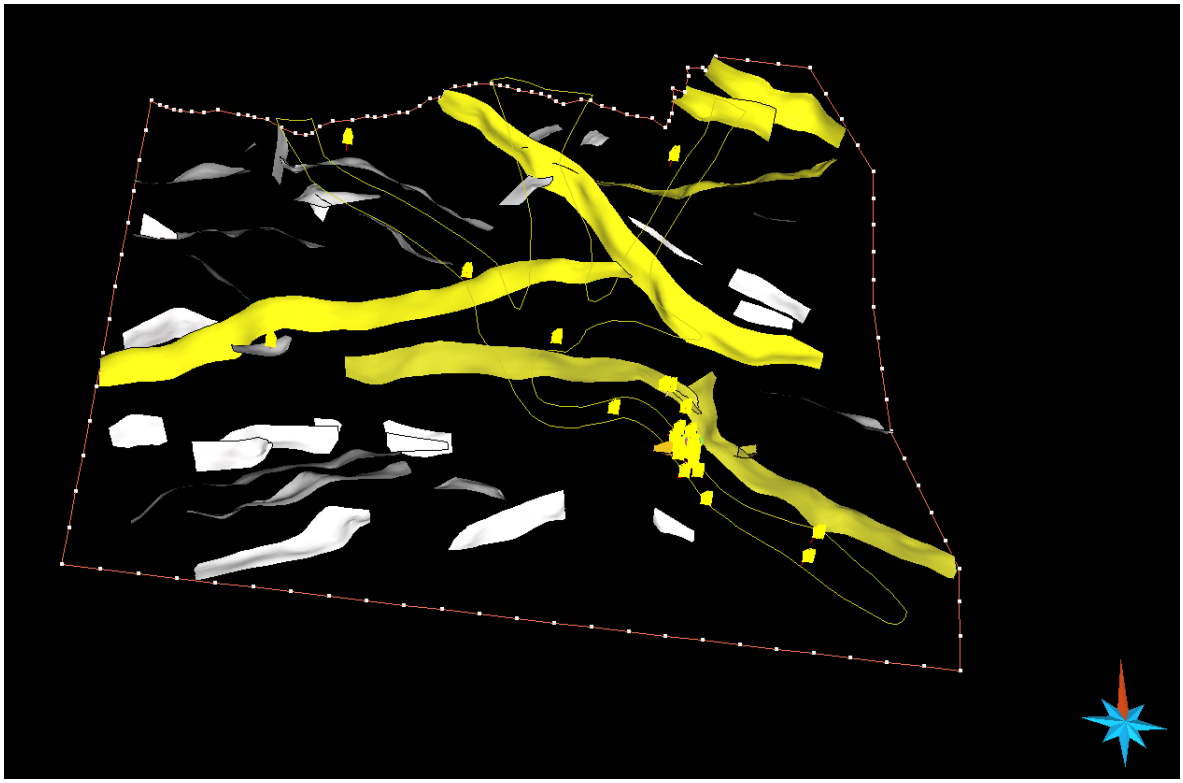

**Figure A3.18. 3D top view of the fault network composed of more than 40 individual faults.**

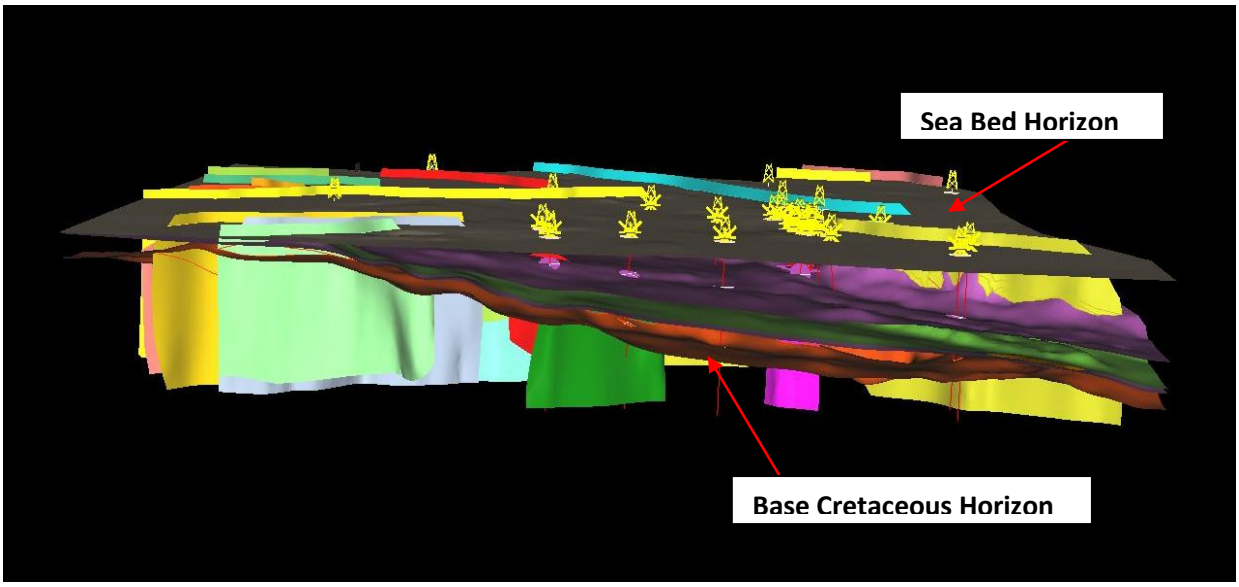


**Figure A3.19. 3D top view of the full surface model at regional scale with all the horizons from Sea bed to base Cretaceous.**

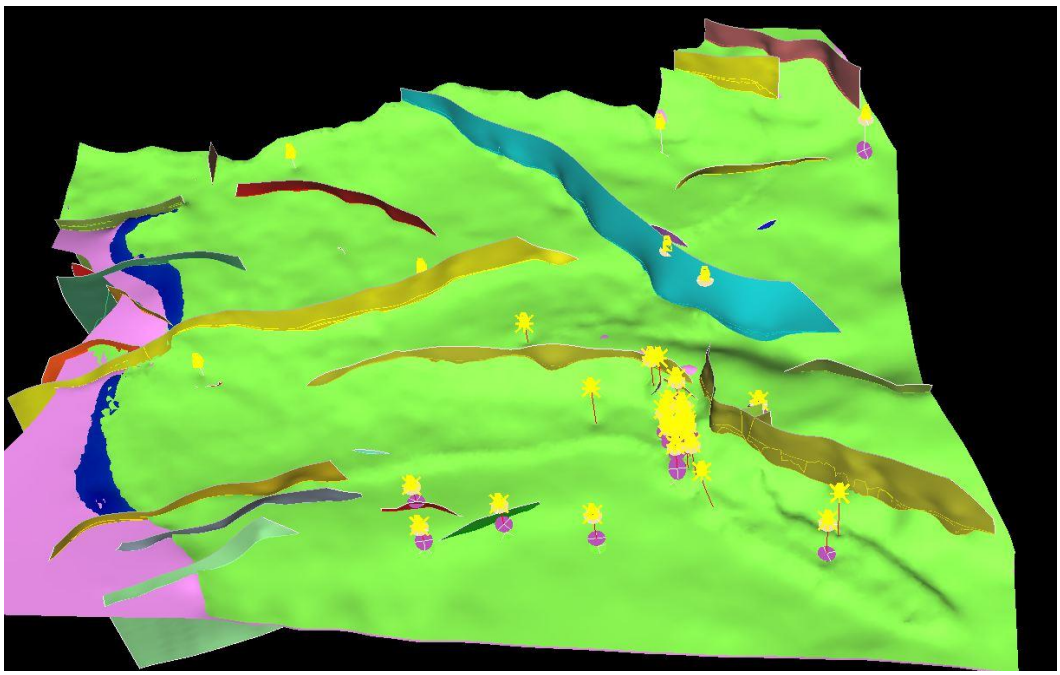

**Figure A3.20. 3D top view showing the top of Base Chalk surface (mudstone seal of reservoir). Note that this layer is present over the basin and is eroded westward where it subcrops at sea bed.**

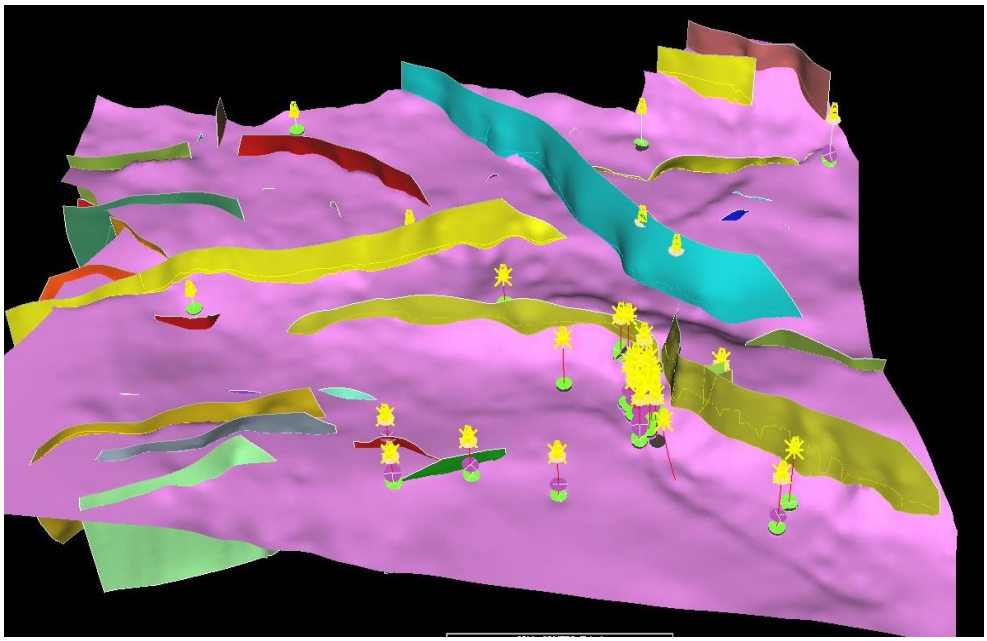

**Figure A3.21. General view of Base Captain horizon. Note that Base Captain horizon (in purple) has been extended over the regional model in accordance with geological knowledge. This allows an accurate modelling of the top Captain Sandstone surface.**

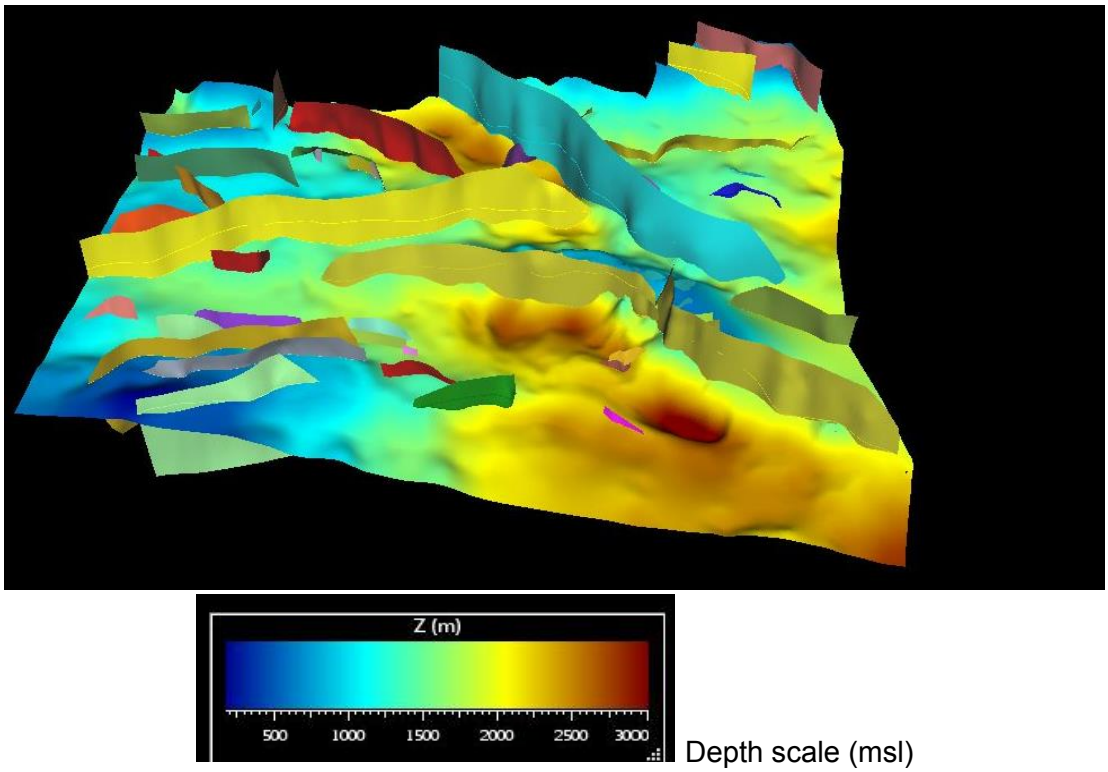


Depth scale (msl)

**Figure A3.22. Base Cretaceous surface top view (contoured in metres below sea level).**

## A3.7 INTERPRETATION OF WELL LOGS FOR ATTRIBUTION

Porosity and lithology data were derived over the Captain Sandstone Member reservoir from wells in and adjacent to the Blake Oil Field and from selected wells in the wider regional 3D model area.

### A3.7.1 Well interpretation for porosity and 'facies'

Lithology and porosity logs were prepared for property input into the geological static models for dynamic modelling. Twenty-three wells with suitable geophysical logs were available over the Captain Sandstone Member within the 'Detailed' geological 3D model boundary (Figure A3.23; Table A3.3). In addition, seven wells also within the Captain Sandstone Member, but outside the 'Detailed' 3D model area were also interpreted to enable attribution of the 'Basin-scale' 3D model (Figure A3.23). The raw digital log *.LAS files were obtained for these wells from well log databases maintained by BGS or CDA. The logs were analysed in 'Interactive Petrophysics' (IP) software (Version 3.6.2010.399, Senergy Software Limited). Core plug porosity and permeability data was also available for some wells and this was used to compare with log interpretation derived porosities and also to inform the population of the model with permeability values.

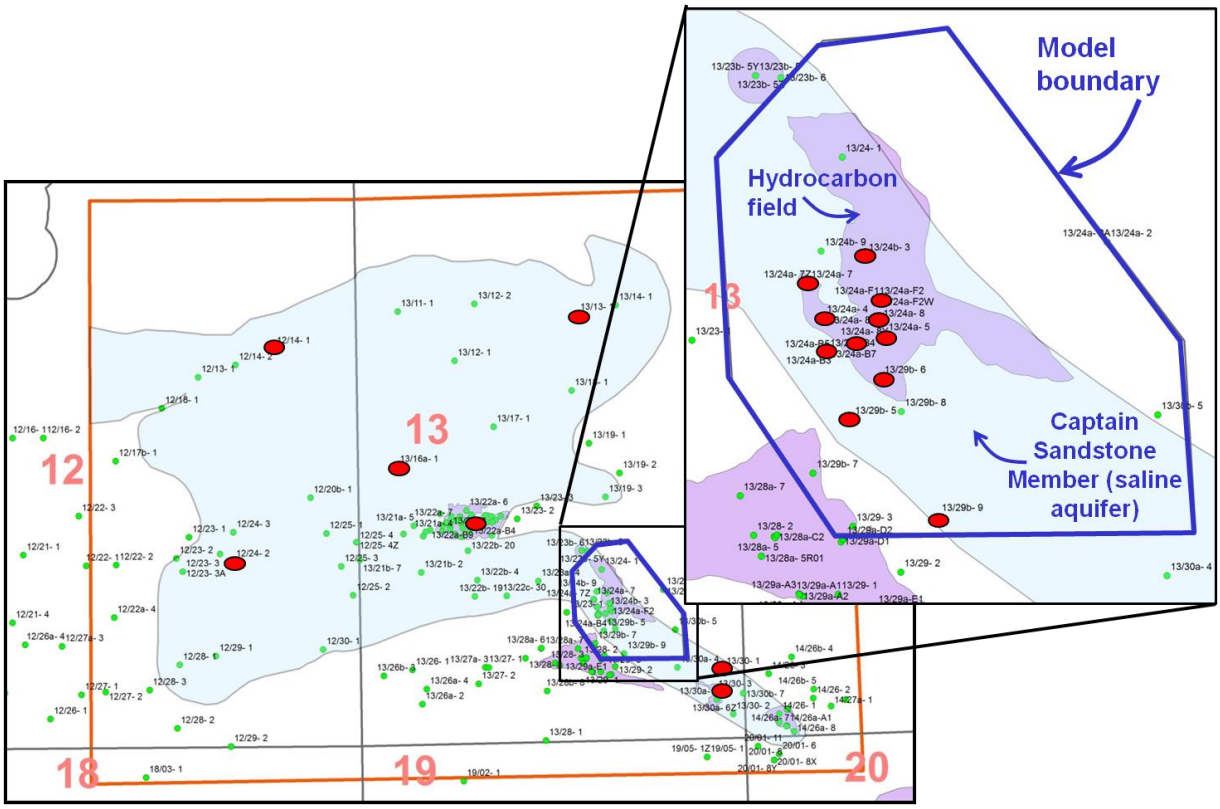


**Figure A3.23: Map showing locations of wells within the project area. Those interpreted are highlighted in red (and listed in Table A3.3). Note that limit of Captain Sandstone Member within detailed model is from regional model and not the new interpretation.**

| Wells with data available | Area | Main log curves available | CORE | Interpretation/ log quality comments | Net to Gross | Main facies | Arithmetic mean porosity PHIE (effective porosity) |
|---|---|---|---|---|---|---|---|
| 13/23a- 4 | Saline aquifer | G, N, D, S, R | | | 0.96 | Channel | 0.26 |
| 13/24a- 4 | HC field | G, N, D, S, R | x | | 1.00 | Channel | 0.27 |
| 13/24a- 5 | HC field | G, N, D, S, R | x | | 0.29 | Flank | 0.11 |
| 13/24a- 6 | HC field | G, N, D, S, R | x | | 0.98 | Channel | 0.25 |
| 13/24a- 7 | HC field | G, N, D, S, R | | | 1.00 | Channel | 0.22 |
| 13/24a- 7Z | HC field | G, N, D, R | | | 1.00 | Channel | 0.19 |
| 13/24a- 8 | HC field | G, N, D, S, R | | | 0.27 | Flank | 0.12 |
| 13/24a- 8y | HC field | G, N, D, R | | | 0.24 | Flank | 0.08 |
| 13/24a-B1 | HC field | G, N, D, R | | | 1.00 | Channel | 0.24 |
| 13/24a-B1Z | HC field | G, N, D, R | | | 0.96 | Channel | 0.26 |
| 13/24a-B2 | HC field | G, N, D, R | | | 0.96 | Channel | 0.26 |
| 13/24a-B2Z | HC field | G, N, D, R | | | 1.00 | Channel | 0.25 |
| 13/24a-B3 | HC field | G, N, D, R | | Suspect log quality curves | 1.00 | Channel | 0.24 |
| 13/24a-B3Z | HC field | G, N, D, R | | Bad log quality over top section of log | 0.94 | Channel | 0.26 |
| 13/24a-B4 | HC field | G, N, D, R | | | 1.00 | Channel | 0.28 |
| 13/24a-B5 | HC field | G, N, D, R | | No curves to derive porosity over formation base | 1.00 | Channel | 0.27 |
| 13/24a-B5Z | HC field | G, N, D, R | | Anomalously high porosity in some areas of spiky neutron-density curves | 1.00 | Channel | 0.25 |
| 13/24a-B6 | HC field | G, N, D, R | | | 1.00 | Channel | 0.27 |
| 13/24a-F2Y | HC field | G, N, D, S, R | | | 0.32 | Flank | 0.26 |

| | | | | | | | |
|---|---|---|---|---|---|---|---|
| 13/24b- 3 | HC field | G, N, D, S, R | x | | 0.56 | Flank | 0.21 |
| 13/29b- 6 | Saline aquifer | G, N, D, S, R | x | Porosity from sonic (bad quality density log) | 0.95 | Channel | 0.18 |
| 13/29b- 9 | Saline aquifer | G, N, R | | Bad log quality over few sections of log | 0.97 | Channel | 0.09 |
| 13/13- 1 | Saline aquifer outside model | G, N, D, S, R | | | 0.93 | Channel | 0.27 |
| 12/14- 1 | Saline aquifer outside model | G, N, D, S, R | | Some areas of poor log quality | 0.56 | Flank | 0.25 |
| 13/16a- 1 | Saline aquifer outside model | G, N, D, S, R | | Anomalously high porosity in some areas of poor data | 0.95 | Channel | 0.29 |
| 12/24- 2 | Saline aquifer outside model | G, S, R | | Some areas of poor log quality | 0.43 | Flank | 0.24 |
| 13/22a- 11 | HC field outside model | G, N, D, S, R | x | Some large hole washouts, but data seems ok | 0.61 | Channel | 0.26 |
| 13/30- 1 | Saline aquifer outside model | G, N, D, S, R | | | 0.81 | Channel | 0.20 |
| 13/30- 3 | HC field outside model | G, N, D, S, R | x | Large hole washout, but other quality curves ok. | 0.93 | Channel | 0.26 |

**Table A3.3. Wells with geophysical logs available used in project. (Curves available: G=Gamma Ray (GR), N=Neutron, D=Density, S=Sonic, R=Resistivity). Coloured cells highlight location of wells either inside (yellow) or outside (orange) 'Detailed' 3D model area.**

### A3.7.2 Log curves, assumptions, quality & corrections

Available well logs include Natural Formation Gamma Ray (GR), sonic transit time, density and neutron logs among others. Different curves were available for different wells and log data was acquired using various tool ages, tool types, conveyance methods and collected at different times. The interpretation methods described here were therefore adapted according to well logs and data quality available. Areas of poor log quality were identified where possible and discarded. For example, poor sections of density – neutron log were identified using the density correction curve and/or calliper curves where available. Across these areas where possible, sonic curves were used to calculate porosity. Assumptions for the log interpretation include a temperature gradient of 34°C/km (with a surface temp of 8°C) within the model area and between 30 and 34°C/km, depending on the well location outside the model area. Where no log metadata was available, assumptions were also made regarding

likely mud type (water based mud assumed) and that suitable environmental corrections were already applied to logs.

### A3.7.3 Interpretation to produce a lithological facies log

A simple, discrete lithological facies log with a two-fold subdivision was produced for each well to help inform the facies modelling. This was based on an interpreted 'Shale Volume ($V_{sh}$)' log. Input curves were the GR or density-neutron curves (where available). Areas interpreted to represent cleanest reservoir sand and the most clayey interval were picked as the end points to create a normalised $V_{sh}$ log scaled from 0 (clean sandstone reservoir) to 1 (shale). A reservoir cut-off of 0.5 was then applied, to separate the formation into 'Reservoir' (where $V_{sh}$<0.5) and 'Non-Reservoir' (where $V_{sh}$>0.5). The thickness of log intervals that fall into those two categories can be used to calculate the formation Net to Gross (NTG) as follows:

$$NTG = \frac{\text{Total thickness of Reservoir}}{\text{Total thickness of Reservoir + Non-Reservoir}}$$

By the same principle the reservoir was split into 'shale' and 'sandstone' lithologies using the $V_{sh}$ cut off of 0.5, illustrated in Figure A3.24. Various cut offs were experimented with (including using porosity cut offs) however it was decided that a $V_{sh}$ cut off of 0.5 adequately subdivided up the reservoir in such a way as to fully represent both end members in the model, and therefore distinguish whether the well penetrated predominantly the Channel or Flank facies.

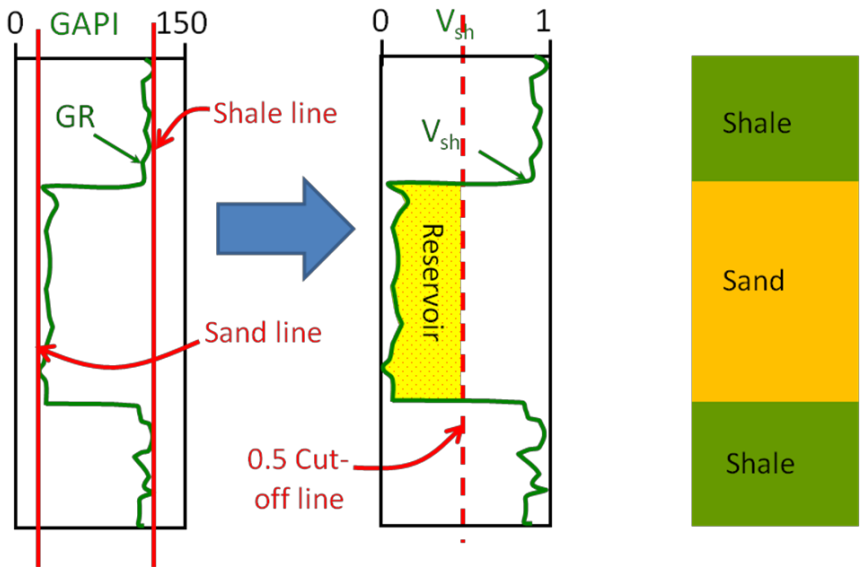


**Figure A3.24: Use of the Gamma Ray (GR) curve to produce a $V_{sh}$ curve. A $V_{sh}$ cut off of 0.5 was used to subdivide the reservoir into 'shale' and sand lithologies. Note that the density - neutron curves were also used to calculate $V_{sh}$ where available.**

These logs were used to help decide on model layer thickness size, to be able to incorporate the necessary level of detail but still keep the total number of cells to the minimum required for the dynamic modelling. The discrete logs were output from IP software as *.LAS files using the lithological codes sand = 1, shale = 0 and imported into GoCad modelling software. The cells can then be up-scaled into the model grid and used to stochastically populate the model honouring the up-scaled lithological facies logs.

### A3.7.4 Porosity

Total and effective porosity curves (PHIT and PHIE respectively) were calculated from the sonic or density-neutron curves. Areas of poor density – neutron log quality were identified using the density correction curves and/or calliper curves. Over log sections where this was the case, the porosity curve was computed from the sonic log. Some wells had no density-neutron log available and in these instances, the porosity was computed using the sonic log.

Equations were used to compute porosity appropriate to the well logs available. These take into account tool measurements; shale volume and assumptions about mud filtrate and mud type properties (in the invaded zone surrounding the borehole wall where most of the tools take their measurements) and also rock matrix properties (where these cannot be determined from other tool measurements) and rock fluids (saline brine or hydrocarbon). The main types of equations used are listed here:

- **Sonic -** Wyllie equation
- **Density -** Standard density porosity equation
- **Density-Neutron** - Standard density – neutron cross plot method

The total porosity curve (PHIT) was provided, to standardise the different measurement types and methods used. This is the total pore volume in the rock i.e. effective plus ineffective porosity. For example, shales have a high total porosity because they have many very small pores which are ineffective (i.e. the fluid in the pores is ‘bound’). The effective porosity (PHIE) is therefore usually less than the PHIT value because it only includes the porosity which contains ‘free fluids’ with connected pores.

The continuous logs were output from IP software as *.LAS files and imported into GoCad modelling software. The cells were then up-scaled into the model grid using the lithological logs to bias the up-scaled values. (This allows the porosity curve to be averaged over the matching lithological interval and assigned to the corresponding up-scaled cell). These were used to stochastically populate the model honouring the up-scaled porosity logs.

### A3.7.5 Permeability

No suitable curves were available to calculate log-derived permeability values. Therefore the relationship between porosity and permeability values from core plug samples was used.

Core data was available for seven wells in the model area. There is a clear exponential relationship between porosity and permeability in the model area (Figure 3.25). This relationship was incorporated into the model by first removing outlying points and then ‘binning’ the porosity values and allowing cells in the model with that range of porosity values

to be assigned the corresponding range of permeabilities (for example, those defined by the orange boxes in Figure A3.25). Note that the method for deriving core plug porosity is naturally different from those derived from down-hole geophysical logs and therefore the values do not necessarily match exactly (Figure A3.26).

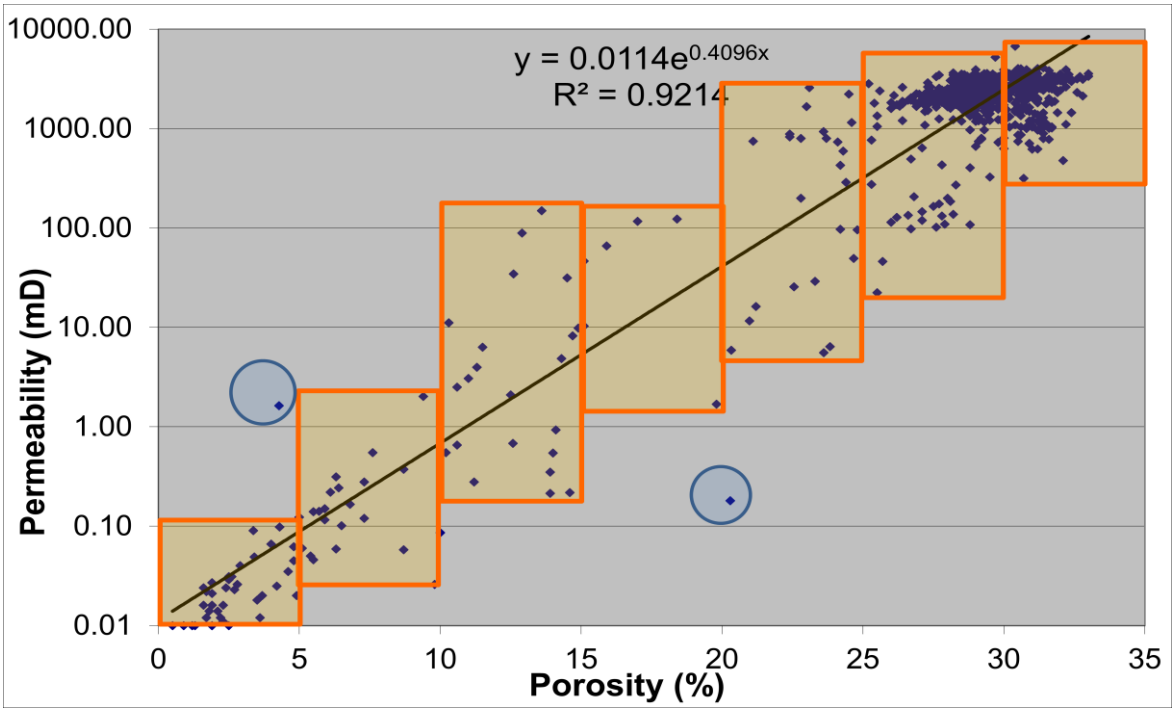


**Figure A3.25: Cross plot of core plug porosity and permeability values for seven wells with available data in the Detailed model area (see Table A3.3).**

## Remaining uncertainties

- Accuracy of interpretation parameters – for the best possible interpretation ideally all borehole and formation conditions should be taken into account or corrected for. However, lack of well metadata or production test data etc means that in many cases 'best guesses' as to parameters had to be made. For example, estimates of hydrocarbon density in wells within the hydrocarbon fields effects porosity calculations.
- Accuracy of raw logs – as mentioned in the log quality section this was approached as rigorously as possible with available data in order to discard areas of poor data quality. However, in some cases where insufficient log curves or associated metadata was available, this is more uncertain.

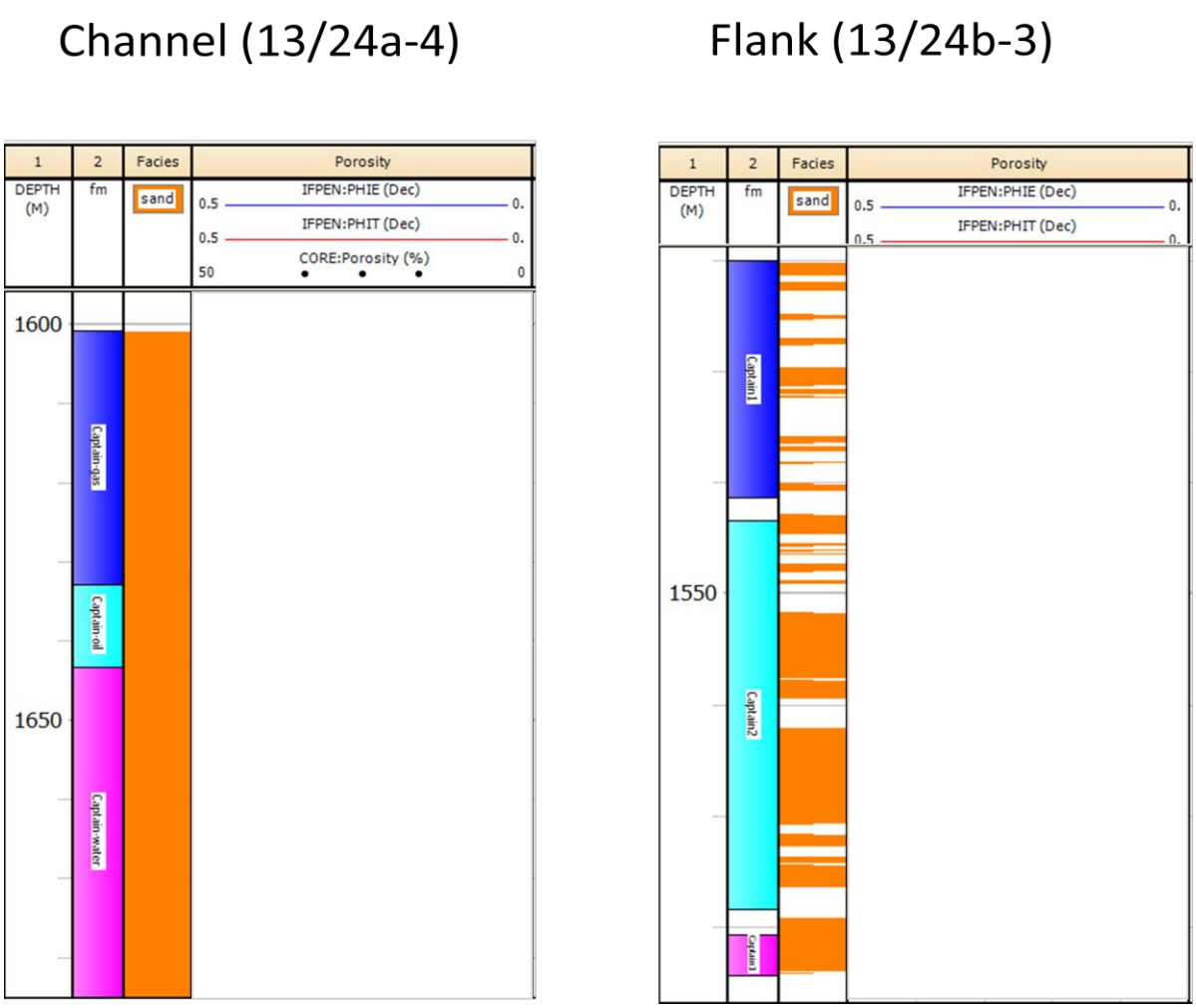


**Figure A3.26: An example well from the Channel and Flank facies areas with the total and effective porosity curves (PHIT red & PHIE blue, respectively). The black dots represent the core plug porosities. The lithological facies log track shows sand as orange and 'shale' as white. Original data used in this interpretation (not shown) was provided under agreement from IHS Global Limited.**

### A3.8 Population of flow simulation grids with petrophysical properties

Facies description from well logs in Channel Area is binary. This unit is mainly composed of one reservoir facies (sandstone) associated with one non reservoir (shaly facies). Without any information on stratigraphic correlations in this reservoir (which is a typical issue associated with a turbiditic depositional environment), a purely stochastic process has been used, respecting as a constraint the core porosity distribution.

This method of populating the grid doesn't give the most realistic result in terms of the geology but gives properties distributions which are statistically representative of existing input data. Identification of Channel and Flank regions leads to a spatial regionalisation

which is directly related to petrophysical values distribution (Figures 28 and 29; also Figures A3.27, A3.28).

**Porosity distribution**

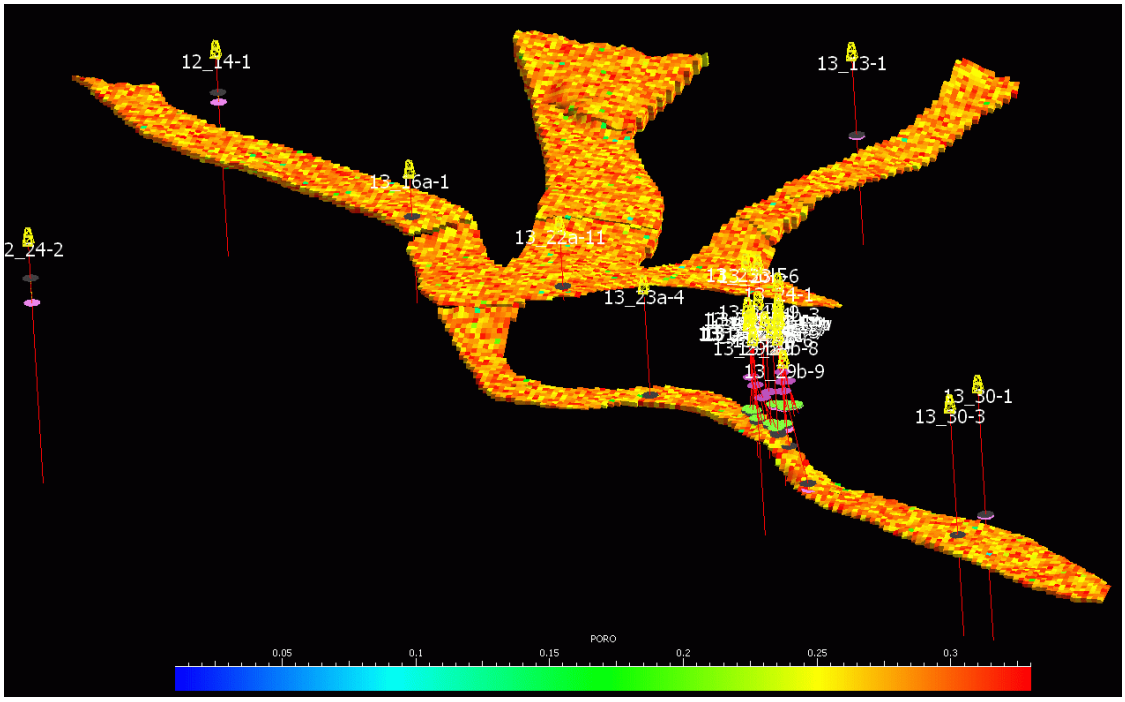


**Figure A3.27. Modelled porosity distribution in Channel areas.**

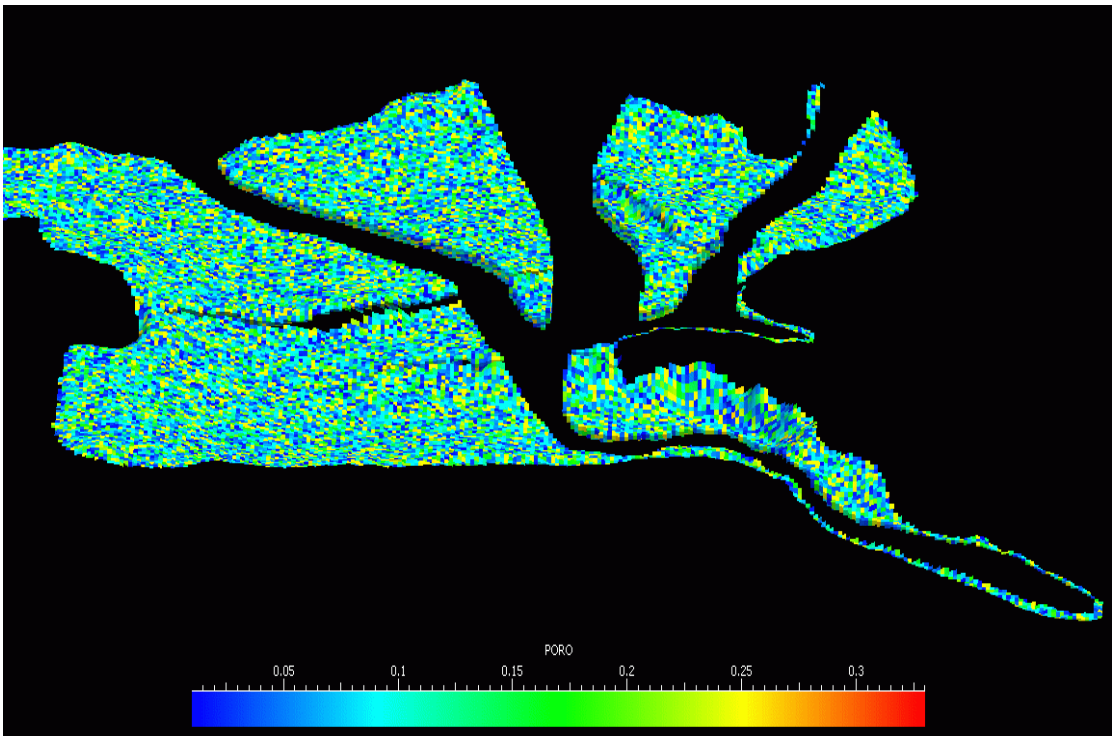


**Figure A3.28. Modelled porosity distribution in Flank areas.**

**Permeability distribution**

To populate a model with permeability attribution, the standard solution is to establish correlations between porosity and permeability with data values from cores analysis. Figure A3.25 shows the empirical relationship of porosity versus permeability derived from core data.

This approach is often used even if there is no causality between porosity and permeability.

Kozeny-Carman derived equations aimed at introducing a causality relationship between porosity and permeability based on laboratory experiments and quantitative physical parameters for rock reservoir composition.

In 1993, Amaefule *et al*. presented an interesting equation for reservoir geology:

$$(K/Phie)^{0.5} = [Phie/(1-Phie)] * [1/(Fs^{0.5} * T * Sgv)]$$

Fs = shape factor, T = tortuosity, Sgv = surface area per unit grain volume,

K = permeability, Phie= effective porosity.

If permeability is expressed in milliDarcy the previous equation becomes:

$$0.0314(K/Phie)^{0.5} = [Phie/(1-Phie)] * [1/(Fs^{0.5} * T * Sgv)]$$

**$RQI = 0.0314(K/Phie)^{0.5}$ Reservoir Quality Index**

**Phiz =Phie/(1-Phie) Normalized effective porosity**

**FUI = 1/(Fs $^{0.5}$ * T * Sgv) Flow Unit Indicator (or FZI Flow Zone Indicator depending of authors)**

**RQI = Phiz * FUI**

$$\log RQI = \log FUI + \log Phiz$$

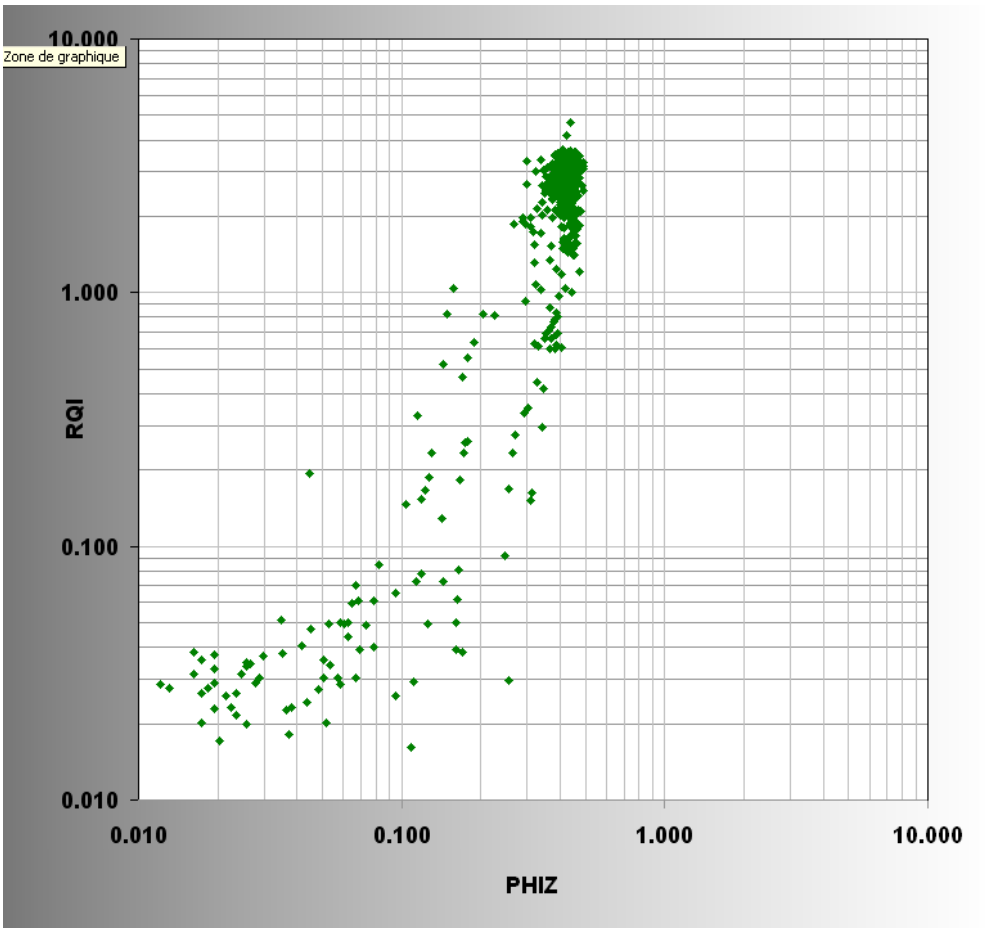


**Figure A3.29. Log/log scale plot of PHIZ versus RQI.**

This cross-plot RQI versus PHIZ (Figure A3.29) based on Kozeny-Carman theoretical causality can thus be easily established even without any information on the values of the physical parameters regrouped in the term FUI. Knowing PHIZ and RQI, FUI values could be inferred and classified.

In practise, log FUI values were ordered and classed and a cumulative probability was assigned to each class. This approach allows us to compute Z, the inverse function of the standard normal cumulative distribution (CDF) function. The way to compute the function Z for normal laws is described in the ***Handbook of mathematical functions*** (Abramovitch and

Stegun. 1965, p.933). The number of straight lines (drawn manually) approximating this law determines the number of Flow Units.

The Z function can be plotted versus FUI and this plot allows us to determine how many Flow Units are present in this core dataset (Figure A3.30). The number of straight lines used to approximate this cross-plot identifies and gives the number of flow units.

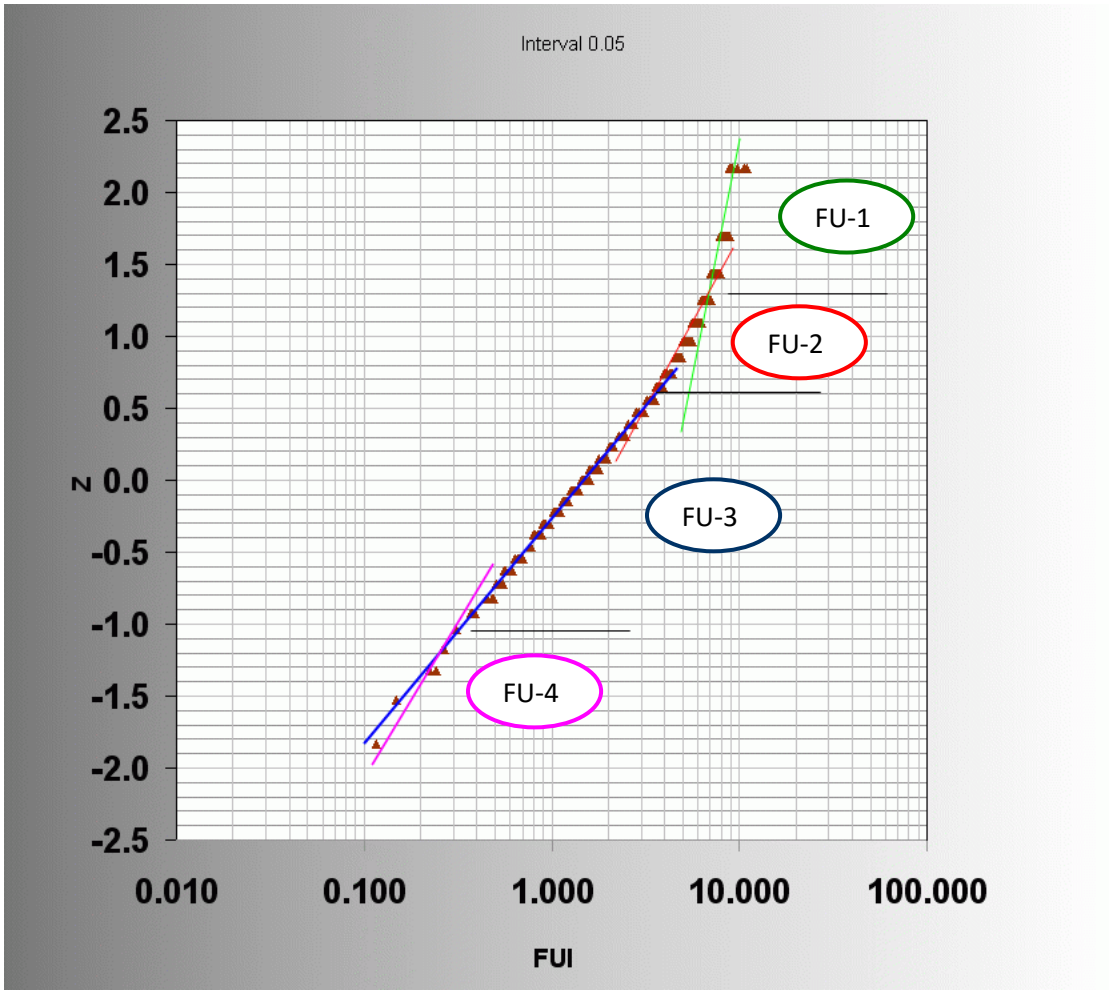


**Figure A3.30. Determination of Flow Units on log probability paper.**

As a result, at least three causal relationships between porosity and permeability were identified on this dataset as shown in Figure A3.31, FU-1 to FU-3. FU-4 is questionable since it relies on few samples. Flow Unit FU-4 is thus considered as non representative.

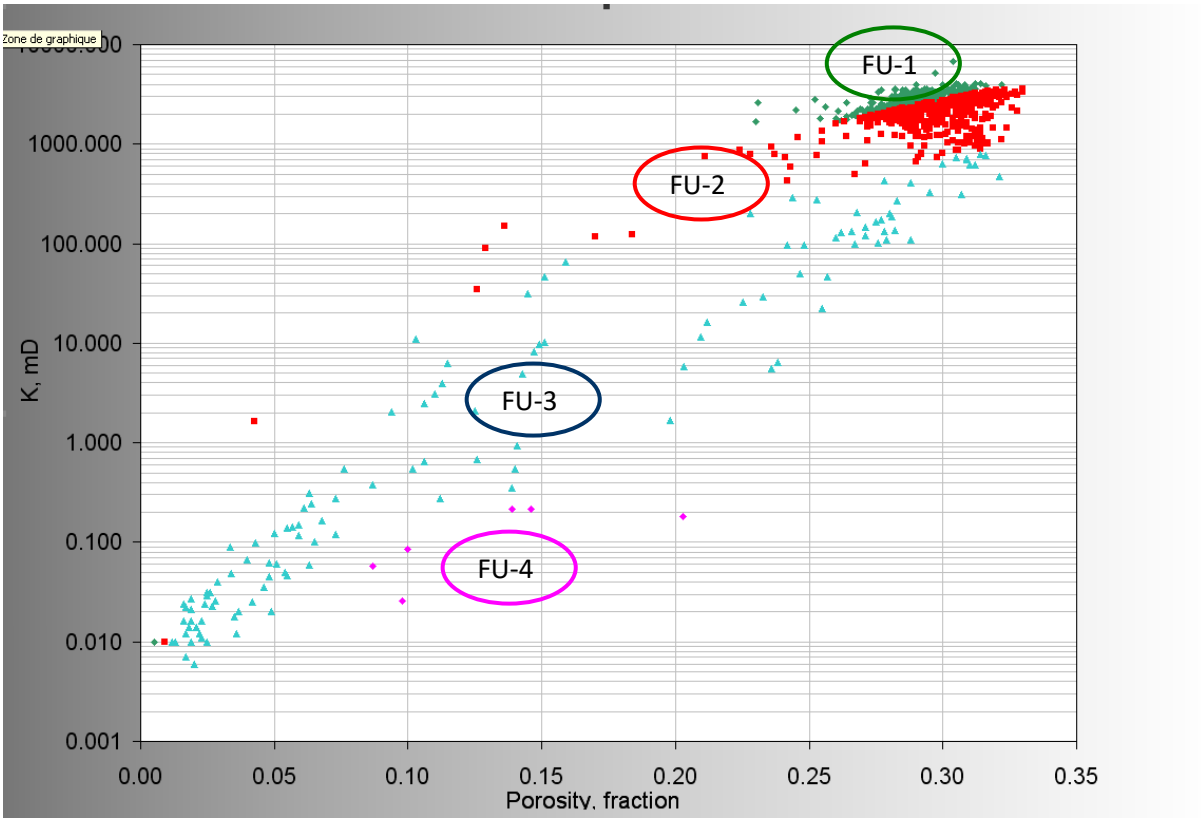


**Figure A3.31. Underlining determined Flow Units on classical porosity versus permeability plot.**

Figure 30 (Section 3) shows, for each Flow Unit the causal relationship between porosity and permeability and its approximation by a power law:

Flow Unit 1 (FU-1) $K = 133015 \times PHIE^{3.0943}$

Flow Unit 2 (FU-2) $K = 147237 \times PHIE^{3.5726}$

Flow Unit 3 (FU-3) $K = 9292.8 \times PHIE^{3.5982}$

These laws are then finally used to populate grids cells in permeability knowing porosity values. Additional laws (Section 3, Figure 31) have been added in order to limit the variations of the flow units and consequently to derive a quantitative evaluation of the range of variations of the permeability for a given porosity for each flow unit or set of flow units.

Below is an example of script for permeability attribution in channel area knowing porosity distribution: (*cf.* detailed explanations in Section A3.10 below).

```
{
KINIT=147237 * pow(PORO,3.5726);        Red curve = base law for channel region
KMAX=173298*pow(PORO,2.9878);     Upper black curve (max values)
KMIN=66501*pow(PORO,3.7304);       Middle black curve (min values)
```

```
#
DKMAX=(KMAX - KINIT);          upper variation of Perm
DKMIN=(KINIT - KMIN);                  lower variation of Perm
#
ALEA=urand(0,1);               term for random attribution
TRESH=0.5;                     default value for weighting factor (sampling correction)
#                              modify with care
if (ALEA>TRESH) {PERM=KINIT+((1-((1-ALEA)/(1-TRESH)))*DKMAX);} else
{PERM=KINIT-(((1-ALEA)/(1-TRESH)-1)*DKMIN);}
}
```

These few lines of script allows rapid population of a 3D grid with permeability values according to our simple model.

The same process has been applied to populate the Flank region with permeability values (*cf.* detailed explanations in A3.10 below).

```
{
KINIT=147237 * pow(PORO,3.5726);       Red curve = base law for channel region
KMAX=173298*pow(PORO,2.9878);    Upper black curve (max values)
KMIN=66501*pow(PORO,3.7304);      Middle black curve (min values)
#
DKMAX=(KMAX - KINIT);          upper variation of Perm
DKMIN=(KINIT - KMIN);                  lower variation of Perm
#
ALEA=urand(0,1);               term for random attribution
TRESH=0.5;                     default value for weighting factor (sampling correction)
#                              modify with care
if (ALEA>TRESH) {PERM=KINIT+((1-((1-ALEA)/(1-TRESH)))*DKMAX);} else
{PERM=KINIT-(((1-ALEA)/(1-TRESH)-1)*DKMIN);}
}
```

### A3.9 Exporting fluid simulation grids

The most popular format for flow simulation grids is the Eclipse TM format (SLB software) since it can be read by most of the fluid flow simulators.

The file has an extension ".grdecl "and it is associated with a file which described faults in the grids; this last file having an extension ".faults".

As the structural model and the grids have been built in SKUA, the complete study could only be visualised with it. Nevertheless, grids could be visualised in most up-to-date geomodelling software.

A flow simulation grid is in fact composed by several sub-grids (fault blocks) due to the existence of faults. The decomposition in several fault blocks induces different indexation of K (vertical indexation) for each fault block. This index is not related to initial layering and geological description. To overcome this drawback, two indexes have been added during the export of the flow simulation to an Eclipse grid. The first one is called Unit and allows in Gocad to create a specific region around a stratigraphical unit; the second one called GeologicK is related to geological layering in the grid and allows creation of regions with a customised number of cell layers.

### A3.10 Scripts

This section provides short explanations about the scripts used to populate the grids with petrophysical properties.

Porosity script:

The function 'nrand' is related to a random normal law and is defined by two parameters which are average and standard deviation.

With this kind of law, it is possible to generate negative numbers. In order to bound porosity values between a maximum and a minimum value, two lines have been added in the script.

The function 'urand' is related to random uniform law and is defined by a minimum and a maximum values.

This method is very flexible and allows a fit to most measured distributions.

Script for permeability (same as in chapter V.2):

```
{
KINIT=147237 * pow(PORO,3.5726);        Red curve = base law for channel region (fig.32)
KMAX=173298*pow(PORO,2.9878);     Upper black curve (max values) (fig.33)
KMIN=66501*pow(PORO,3.7304);       Middle black curve (min values) (fig.33)
#
DKMAX=(KMAX - KINIT);           upper variation of Perm
DKMIN=(KINIT - KMIN);                    lower variation of Perm
```

```
#
ALEA=urand(0,1);            term for random attribution
TRESH=0.5;                  default value for weighting factor (sampling bias correction)
#                           modify with care
if (ALEA>TRESH) {PERM=KINIT+((1-((1-ALEA)/(1-TRESH)))*DKMAX);} else {PERM=KINIT-(((1-ALEA)/(1-TRESH)-1)*DKMIN);}
}
```

The function pow is related to power function and is defined by the name of the variable and the value of its exponent.

KINIT=147237 * pow(PORO,3.5726) means KINIT=147237 * PORO $^{3.5726}$

The function ALEA generates a random number between zero and one.

TRESH is just a weighting variable defined to improve the script when the distribution from core data is biased. With a recommended default value of 0.5, this has no impact on the results.

## Appendix 4 - SUMMARY OF KEY UNCERTAINTIES SURROUNDING INTEGRITY OF THE MORAY FIRTH MULTI-STORE SITE

Following the mapping and building of the 'Detailed' geological 3D model, examination of the Blake Oil Field development history and definition of the Containment model in Task 3.1, some uncertainties have been identified that might present increased risk to the integrity of the proposed store. These uncertainties, their impact, probability, severity and possible mitigating activities within the SiteChar project are presented in Tables A4.1, A4.2, A4.3 and A4.4 below and will inform the Risk Assessment (Deliverable 3.3) and preliminary and final licence application (Milestones 7 and 8).

**Table A4.1. 'DETAILED' GEOLOGICAL 3D MODEL.**

| Uncert-ainty | Detailed uncertainty description | Impact/consequence prior to mitigation | PROBABILITY L-Low; M-Medium; H-High | SEVERITY Impact is L-Low; M-Medium; H-High | MITIGATION |
|---|---|---|---|---|---|
| 1 | Incorrect interpretation of surfaces for 3D model | Potential to effect dynamic modelling results. | H – there are errors inherent in interpretation | L– Errors are judged to be within acceptable limits. | Not required |
| 2 | Incorrect interpretation of faults imaged on the seismic data for the 3D model. Presence of faults/fractures below seismic resolution. | Migration of $CO_2$ out of Storage Site and into Storage Complex and possible leakage to water column and atmosphere. | M- This may not impact on containment risk as sandstone reservoir was interpreted not to reach these faults. However, see risk above. | H - $CO_2$ has potential to migrate into Storage Complex and possibly leak to water column and atmosphere. | Model as possible scenario. Locate injection wells to avoid migration to faults. |
| 3 | Incorrect depth conversion | Potential to effect dynamic modelling results. | H – There are errors inherent in depth conversion process | L – Errors are relatively well known and are judged to be within acceptable limits. | Not required |
| 4 | Building the 3D model. Specifically smoothing and interpolation algorithms for both horizon surfaces and fault surfaces; likely greater with latter. | It is not expected this uncertainty will have much impact on the model | H – there are errors inherent in these processes | L – Errors judged to be within acceptable limits. | Not required |
| 5 | Building 3D model. Junction between fault and horizon requires a degree of interpretation to facilitate a geologically realistic fit. | This may not impact on containment risk as Sst. reservoir interpreted not to reach these faults. But see risk above. | H – there are errors inherent in these processes | H – $CO_2$ has potential to migrate into Storage Complex and possibly leak to water column and atmosphere. | Model as possible scenario. |
| 6 | Uncertainty over integrity of well penetrations. | Migration of $CO_2$ out of Storage Site and into Storage Complex and possible leakage to water column and atmosphere. | M – Probability will be assessed in Task 3.4 of WP3 | H – $CO_2$ has potential to migrate into Storage Complex and possibly leak to water column and atmosphere. | Assess all wells and carry out remedial action and focussed monitoring of these well locations |

**Table A4.2. STORAGE SITE.**

| Uncert -ainty | Detailed uncertainty description | Impact/consequence prior to mitigation | PROBABILITY L-Low; M-Medium; H-High | SEVERITY Impact is L-Low; M-Medium; H-High | MITIGATION |
|---|---|---|---|---|---|
| 1 | Regional and detailed understanding of the distribution of Lower Cretaceous submarine fan sandstones may be incorrect | Potential to effect dynamic modelling results. | L– The Lower Cretaceous. Sandstones of the storage site are complex but their general distribution and classification is fairly well constrained | L– Errors judged to be within acceptable limits. | Not required |
| 2 | Incorrect interpretation of the extent of the reservoir sandstone | Migration of $CO_2$ out of Storage Site and into Storage Complex | M – Insufficient well data to fully constrain seismic data. In some areas interpretation of seismic data is equivocal | M – $CO_2$ will migrate into Storage Complex and be contained. | Model as possible scenario |
| 3 | Limited connectivity within Captain Sandstone Member | May cause pressure increase as injection of $CO_2$ progresses | H – Within Flank Area<br>L – Within Channel Area | M – Injectors are located in Channel Area | Ensure injectors are placed within Channel Area. |
| 4 | The degree of connectivity between the different members of the Wick Sandstone Formation unknown. | May cause pressure increase as injection of $CO_2$ progresses | H – Within Flank Area<br>L – Within Channel Area | M – Injection planned to take place within Captain Sandstone in Channel Area, but this may be juxtaposed with older sandstones. | Model as possible scenario |
| **5** | Uncertainty over exact position of fluid contacts | May effect dynamic modelling | L – variation in position of contacts quite small | L – Low impact | Model as possible scenario |
| **6** | Uncertainty over nature of trap in north-west corner of the Blake Oil Field | Possible migration for $CO_2$ out of Storage Site and eventual leakage to sea bed and atmosphere | M –All wells with data show good thickness of potential sealing rocks | H – $CO_2$ has potential to leak out of Storage Complex and possibly leak to water column and atmosphere. | Model as possible scenario |
| **7** | Uncertainty over present day reservoir pressure as this will have to be modelled | May effect dynamic modelling | M – Modelling of pressure change in reservoir will be dependent on many assumptions | M –May affect storage capacity estimates and modelled injection rates | Model as possible scenario |
| 8 | Mapped sandstone reservoir thickness is uncertain . | Potential to effect storage capacity estimates and injectivity. | H – There are errors inherent in interpretation | Low – Errors judged to be within acceptable limits. | Not required |

**Table A4.2. STORAGE SITE.**

| Uncert-ainty | Detailed uncertainty description | Impact/consequence prior to mitigation | PROBABILITY L-Low; M-Medium; H-High | SEVERITY Impact is L-Low; M-Medium; H-High | MITIGATION |
|---|---|---|---|---|---|
| 9 | Attribution of reservoir: Accuracy of interpretation parameters | Potential to effect dynamic modelling results. | H – There are errors inherent in interpretation | L – Errors judged to be within acceptable limits. | Not required |
| 10 | Attribution of model; Accuracy of raw logs | Potential to effect dynamic modelling results. | H – There are errors inherent in interpretation | L – Errors judged to be within acceptable limits. | Not required |

**Table A4.3. STORAGE COMPLEX – PRIMARY SEAL.**

| Uncert-ainty | Detailed uncertainty description | Impact/consequence prior to mitigation | PROBABILITY L-Low; M-Medium; H-High | SEVERITY Impact is L-Low; M-Medium; H-High | MITIGATION |
|---|---|---|---|---|---|
| 1 | Regional and detailed understanding of the distribution of Lower Cretaceous argillaceous rocks is incorrect | Migration of $CO_2$ out of Storage site and into Storage Complex. | L – Well data and seismic mapping suggest good thickness of low permeability seal rocks to storage site. | M – $CO_2$ will migrate into Storage Complex and be contained. | Model as possible scenario |
| 2 | Limits and thickness of Lower Cretaceous seal rocks subject to uncertainties | Migration of $CO_2$ out of Storage site and into Storage Complex. | L – Well data and seismic mapping suggest good thickness of low permeability cap rocks to storage site. | M – $CO_2$ will migrate into Storage Complex and be contained. | Model as possible scenario |
| **3** | Presence of faults/fractures below seismic resolution. | Migration of $CO_2$ out of Storage Site and into Storage Complex and possible leakage to water column and atmosphere. | M- The Lower Cretaceous seal is proven to be effective in the Blake Oil Field | H - $CO_2$ has potential to migrate into Storage Complex and possibly leak to water column and atmosphere. | Model as possible scenario. |
| **4** | Potential seal is not as effective as expected | Migration of $CO_2$ out of Storage Site and into Storage Complex | L – Well data and seismic mapping suggest good thickness of low permeability seal rocks to storage site. | M – $CO_2$ will migrate into Storage Complex and be contained. | Model as possible scenario |

**Table A4.4. STORAGE COMPLEX – SECONDARY CONTAINMENT, RESERVOIR AND SEAL.**

| Uncert-ainty | Detailed uncertainty description | Impact/consequence prior to mitigation | PROBABILITY L-Low; M-Medium; H-High | SEVERITY Impact is L-Low; M-Medium; H-High | MITIGATION |
|---|---|---|---|---|---|
| 1 | Regional and detailed understanding of the distribution of geological formations with reservoir potential is incorrect | Delineation and assessment of reservoir rocks difficult leading to reduced storage capacity if reservoirs underestimated | L – Palaeogene succession very sand-prone | L– Less pore space than anticipated means better sealing of Storage Complex | Not required |
| 2 | Potential pore space not available in Storage Complex | Reduced storage capacity | L – Palaeogene succession very sand-prone | L – Less pore space than anticipated means better sealing of Storage Complex | Not required |
| 3 | Regional and detailed understanding of the distribution of geological formations with sealing potential is incorrect | Delineation and assessment of seal rocks difficult leading to potential leakage if seal presence is underestimated | M – Continuity and thickness of Palaeogene argillaceous rocks difficult to delineate. | H– If our uncertainty results in sealing rocks being too thin or absent then $CO_2$ could leak out of Storage Complex | Model as possible scenario |

## REFERENCES

ABRAMOVITCH, M., AND STEGUN, I. A. 1965. ***Handbook of mathematical functions***. Dover.

AHMADI, Z.M., SAWYERS, M., KENYON-ROBERTS, S., STANWORTH, C.W., KUGLER, K.A., KRISTENSEN, J. AND FUGELLI, E.M.G. 2003. Paleocene. 235-259 In: Evans, D., Graham, C., Armour, A. and Bathurst, P (editors and co-ordinators) *The Millennium Atlas: petroleum geology of the Central and Northern North Sea*. London: The Geological Society.

AMAEFULE, J. AND ALTUNBAY, M. 1993. Enhanced Reservoir description: Using Core and Log Data to Identify Hydraulic (Flow) Units and Predict Permeability in Uncored Intervals/Wells, SPE 26436, 68th Annual SPE Conference and Exhibition, Houston, TX.

ARGENT, J D, STEWART, S A, AND UNDERHILL J R. 2000. Controls on the Lower Cretaceous Punt Sandstone Member, a massive deep-water clastic deposystem, Inner Moray Firth, UK North Sea.Petroleum Geoscience, Vol. 6, 275–285.

ARGENT, J.D., STEWART, S.A., GREEN, P.F. AND UNDERHILL, J.R. 2002. Heterogeneous exhumation in the Inner Moray Firth, UK North Sea: constraints from new AFTA® and seismic data. *Journal of the Geological Society*, *London,* **Vol. 159**, pp. 715-729.

CHADWICK, R.A., ARTS, R., BERNSTONE, C., MAY, F., THIBEAU, S. AND ZWEIGEL, P. 2008. Best practice for the storage of $CO_2$ in saline aquifers. Keyworth, Nottingham: British Geological Survey Occasional Publication No. 14.

DEEGAN, C.E. AND SCULL, B.J. 1977. A standard lithostratigraphic nomenclature for the Central and Northern North Sea. Institute of Geological Sciences Report **77/25**; NPD-Bulletin **No.1**.

DU, E.K. 2002. Blake Flank Well 13/24a- 8, Test Analysis Report. BG Group, Petroleum Engineering.

HILTON, V.C. AND MORRIS, S. 2002. An integrated interpretation of core and borehole image data. Report for BG Group, Blake Flank, Wells 13/24a- 8, 8z & 8y. Baker Atlas GEOScience.

HILTON, V.C. 1999. Structural and sedimentological interpretation of STAR image data, core sedimentology and petrography. Report for BG Exploration and Production, Blake Field, Well 13/24a-6. Baker Atlas GEOScience.

HOSA, A., ESENTIA, M., STEWART, J. AND HASZELDINE, S. 2010. Benchmarking worldwide $CO_2$ saline aquifer injections. www.erp.ac.uk/sccs

JOHNSON, H. AND LOTT, G.K.. 1993. 2. Cretaceous of the Central and Northern North Sea. In: Knox, R. W. O'B. and Cordey, W.G. (eds) *Lithostratigraphic nomenclature of the UK North Sea.* British Geological Survey, Nottingham.

KNOX, R.W. O'B. AND HOLLOWAY, S. 1992. 1. Palaeogene of the Central and Northern North Sea. In: Knox, R. W. O'B. and Cordey, W.G. (eds) *Lithostratigraphic nomenclature of the UK North Sea.* British Geological Survey, Nottingham.

LAW, A., RAYMOND, R., WHITE, G., ATKINSON, A., CLIFTON, M., ATHERTON, T., DAWES, I., ROBERTSON, E., MELVIN, A. AND BRAYLEY, S. 2000. The Kopervik fairway, Moray Firth, UK. Petroleum Geoscience, 6, pp 265-274.

LOWE, D., AND GUY, M. 2000. Slurry-flow deposits in the Britannia Formation (Lower Cretaceous), North Sea: a new perspective on the turbidity current and debris flow problem. Sedimentology, 47, 31.70.

MACKERTICH, D.S. AND GOULDING, D.R.G. 1999. Exploration and appraisal of the South Arne Field, Danish North Sea. *In: Fleet, A.J. & Boldy, S.A.R. (eds) Petroleum Geology of Northwest Europe: Proceedings of the 5th Conference,* 959-974. Geological Society, London.

MAYALL, M., JONES, E. AND CASEY, M. 2006. Turbidite channel reservoirs – Key elements in facies prediction and effective development. Marine and Petroleum Geology, V 23, pp. 821-841.

MEGSON, J. AND HARDMAN, R. 2001. Exploration for and development of hydrocarbons in the Chalk of the North Sea: a low permeability system. *Petroleum Geoscience,* Vol**. 7**, pp.3-12.

MIN JIN, MACKAY, E., QUINN M.F., HITCHEN K. AND AKHURST M. 2012. Evaluation of the $CO_2$ Storage Capacity of the Captain Sandstone Formation. Paper prepared for presentation at EAGE incorporating SPE Europe, Copenhagen.

MUNRO, G.J. 2010. Pressure and Temperature Distribution in the Captain Saline Aquifer, UK North Sea, for $CO_2$ Storage. University of Edinburgh, School of Geoscience. Dissertation for the Degree of Master of Science in Carbon Capture and Storage.

OAKMAN, C.D. 2005. The Lower Cretaceous plays of the Central and Northern North Sea: Atlantean drainage models and enhanced hydrocarbon potential *In:* DORE, A.G. & VINING, B.A. (eds) *Petroleum Geology: North-West Europe and Global Perspectives - Proceedings of the 6th Petroleum Geology Conference*, 187-198. London: The Geological Society.

OLARIU, M.I, AIKEN, C.L.V, BHATTACHARYA, J.P., AND XU, X. 2011. Interpretation of channelized architecture using three-dimensional photo real models, Pennsylvanian deep-water deposits at Big Rock Quarry, Arkansas Original Marine and Petroleum Geology, Volume 28, Issue 6, June 2011, Pages 1157-1170.

PINNOCK, S.P. AND CLITHEROE, A.R.J. 1997. The Captain Field, UK North Sea: appraisal and development of a viscous oil accumulation. Petroleum Geoscience, **Vol. 3**, 305-312.

POSAMENTIER, H., WALKER, R. 2006. Deep-water turbidites and submarine fans. In: H.W. Posamentier and R.G. Walker, Editors, Facies Models Revisited, SEPM (Society for Sedimentary Geology) Special Publication, 84, 399–520.

RICHARDS, P.C., LOTT, G.K., JOHNSON, H., KNOX, R.W.O'B. AND RIDING, J.B. 1993. Jurassic of the Central and Northern North Sea. In: Knox, R. W. O'B. and Cordey, W.G. (eds) *Lithostratigraphic nomenclature of the UK North Sea.* British Geological Survey, Nottingham.

RICHARDS, M., BOWMAN, B., AND READING, H. 1998, Submarine fan systems I: characterization and stratigraphic prediction. Marine and Petroleum Geology, v. 15, p. 578–606.

ROSE, P.T.S. 1999. Reservoir characterization in the Captain Field: integration of horizontal and vertical well data. *In:* FLEET, A.J. & BOLDY, S.A.R. (eds) *Petroleum Geology of Northwest Europe: Proceedings of the 5th Conference*, 1101-1113. London: The Geological Society.

ROSE, P., MANIGHETTI, A., REGAN, K., AND SMITH, T. 2000, Sand body geometry, constrained and predicted during a horizontal drilling campaign in a Lower Cretaceous turbidite sand system, Captain Field, UKCS Block 13/22a. Petroleum Geoscience, 6, 255-263.

SCOTTISH CENTRE FOR CARBON STORAGE. 2009. Opportunities for $CO_2$ Storage around Scotland — an integrated strategic research study, 56pp. Available at: http://www.erp.ac.uk/sccs, Accessed: September 2009.

SCOTTISH CARBON CAPTURE & STORAGE. 2011. Progressing Scotland's $CO_2$ Storage opportunities, 60pp. Available at: http://www.sccs.org.uk/progress-to-co2-storage-scotland Accessed: March 2010.

SINCLAIR, H., AND TOMASSO, M. 2002. Depositional evolution of confined turbidite basins. Journal of Sedimentary Research, 72, 451–456.

SKURTVEIT, E, AKER, E, SOLDAL, M, ANGELI, M AND WANG, ZHONG. 2012. Experimental investigation of $CO_2$ breakthrough and flow mechanisms in shale. Petroleum Geoscience, Vol.**18**, pp. 3-15.

STOW AND JOHANSSON. 2000. Deep-water massive sands: nature, origin and hydrocarbon implications. Marine and Petroleum Geology, 17, 145-174.

THOMSON, K. AND UNDERHILL, J.R. 1993. Controls on the development and evolution of structural styles in the Inner Moray Firth Basin. *In:* PARKER, J.R. (ed) *Petroleum Geology of Northwest Europe: Proceedings of the 4th Conference*, 1167-1178. London: The Geological Society.